CHEMICAL STUDIES IN SHOCK WAVES

Thesis by

Garry Lee Schott

In Partial Fulfillment of the Requirements

for the Degree of

Doctor of Philosophy

California Institute of Technology

Pasadena, California

1956

ACKNOWLEDGMENTS

Professor Norman Davidson has directed both my research and teaching experience at the Institute. I am very grateful for his stimulating and considerate guidance.

Dr. Doyle Britton was responsible for the construction of much of the shock tube equipment. His close co-operation in the work on iodine is also acknowledged.

I should like to thank Dr. Oliver R. Wulf and Professor Harold S. Johnston for their encouraging and helpful discussions of the work on nitrogen pentoxide, and for permission to include material from their papers in this thesis.

The Office of Naval Research has supported this work and has provided the author with research assistantships during the summers of 1953 and 1954 and the academic year 1955-56. The National Science Foundation has contributed a predoctoral fellowship (1954-55) and the California Institute has contributed teaching assistantships (1952-53 and 1953-54) to the author's graduate training. The financial assistance of these agencies is gratefully acknowledged.

ABSTRACT

Shock waves in argon bearing about one percent nitrogen pentoxide vapor have been used to initiate the rapid decomposition of N_2O_5 between 450° and 1100°K. The important intermediate in the reaction is the nitrate radical, NO_3, whose characteristic absorption bands in the green and red are known. These bands have been identified in flash absorption spectrograms, and quantitative photoelectric measurements of absorption by NO_3 have followed its appearance and disappearance in the reaction mixture. Simultaneous measurements with violet light have recorded the production of NO_2.

The first step in N_2O_5 decomposition is: $N_2O_5 \longrightarrow NO_2 + NO_3$. Near 500°K, the forward rate and the equilibrium in this reaction have been measured. Above 600°K, the dissociation is rapid and complete, and the rates of the bimolecular decomposition reactions $NO_2 + NO_3 \longrightarrow NO + O_2 + NO_2$ and $2NO_3 \longrightarrow 2NO_2 + O_2$ have been measured. The contributions of these steps have been established by experiments in the presence of excess NO_2. The reaction $NO_3 + NO \longrightarrow 2NO_2$ is fast, and although NO_2 is unstable with respect to NO and O_2 above about 600°K, the stoichiometric reaction $N_2O_5 \longrightarrow 2NO_2 + \frac{1}{2}O_2$ has been observed in the short times of these experiments. The rate equations and the constants and energies measured agree very well with predictions based on mechanisms known at room temperature.

Two papers on the rate of dissociation of molecular iodine, by the present author and others, are included. The abstracts accompanying these papers are on pages 118 and 131.

TABLE OF CONTENTS

I. THE DECOMPOSITION OF NITROGEN PENTOXIDE AT HIGH TEMPERATURES

A. INTRODUCTION

1. The Problem.

Many reactions of nitrogen pentoxide gas depend upon the dissociation of N_2O_5 into the molecular radicals NO_2 and NO_3 and the subsequent reactions that result in the reduction of NO_3.[1] The rate of oxidation of nitric oxide[2][3] and the rate of equilibration with isotopically labelled NO_2[4][5][6] are controlled by the rate of dissociation of N_2O_5.

$$(1) \qquad O_2NONO_2 \underset{\text{recombination}}{\overset{\text{dissociation}}{\rightleftharpoons}} NO_2 + NO_3$$

In the well known first order decomposition of pure N_2O_5, the rate determining step is the bimolecular decomposition reaction between NO_2 and NO_3:[7]

$$(2) \qquad NO_2 + NO_3 \longrightarrow NO + O_2 + NO_2$$

In mixtures of N_2O_5 and excess ozone, NO_2 is oxidized rapidly to NO_3, and the rate of destruction of ozone is controlled by the bimolecular decomposition reaction:[8]

$$(3) \qquad NO_3 + NO_3 \longrightarrow NO_2 + O_2 + NO_2$$

Near room temperature, the equilibrium in reaction (1) lies far to the left, and the rates of reactions (2) and (3) are controlled by the small equilibrium concentrations of NO_2 and NO_3. For this reason, the rate constants of reactions (2) and (3) have not been separated from the equilibrium constant in reaction (1). The research described here is an

investigation of the decomposition of N_2O_5 between 450° and 1200°K. The rate of dissociation of N_2O_5 and the equilibrium in reaction (1) have been observed directly between 450° and 550°K, and the rate constants of reactions (2) and (3) have been measured between 600° and 1100°K under conditions where N_2O_5 is completely dissociated.

The experiments have been designed to take advantage of several properties of this system. The most important of these is the strong, characteristic absorption of visible light by NO_3. This absorption spectrum readily identifies NO_3 qualitatively in the reaction mixture. The strong absorption in the red has been used to measure spectrophotometrically the appearance and disappearance of NO_3 in the course of the decomposition of N_2O_5 into NO_2 and oxygen. The simultaneous formation of NO_2 has also been determined, with the use of violet light. Values of the absorption coefficients of NO_2 and NO_3 at several wave lengths and temperatures have been recorded as part of the kinetics investigation.

Under the concentration conditions of the present experiments, the dissociation of N_2O_5 requires several seconds at room temperature. Near 500°K, complete dissociation has been measured in about 10^{-5} seconds, and at higher temperatures, the dissociation is still faster. The activation energies of reactions (2) and (3) are much lower than that of reaction (1). However, the rates of these bimolecular reactions are kept small by the use of low concentrations of

the reactants, and the decomposition of NO_3 requires between 10^{-3} and 10^{-4} seconds in these experiments between 450° and 1000°K. These times are short enough that no significant decomposition of NO_2 occurs, and yet they are long enough that equilibrium in reaction (1) is established relatively quickly.

These reaction times between 10^{-3} and 10^{-5} seconds are in the range that can be examined conveniently by the shock wave methods developed recently in this laboratory.(9) Since the system N_2O_5-NO_2-NO_3 contains two differently colored substances, it is very well suited for study with the present shock tube equipment. The analysis of the kinetics of decomposition of N_2O_5 represents an extension of the shock wave method to a more complicated reaction than those previously analyzed.(9)(10)(11)(12)

The results that have been obtained agree very well with the predictions made by extrapolation of the room temperature results. They add to the information derivable from room temperature experiments by providing directly measured values and temperature coefficients of the equilibrium constant in reaction (1) and the rate constants in reactions (2) and (3). The most significant contribution of this investigation is the preparation and direct study of known concentrations of the intermediate, NO_3, whose importance in several reactions has been deduced kinetically, but whose concentration and absolute reaction rates have not previously been measurable directly.

2. The Method.

A direct method of studying rapid chemical processes has three important characteristics.[13] First, a macroscopic sample is uniformly displaced from equilibrium in a period of time that is short compared to the time available for observation. The shock wave method does this by suddenly compressing and heating a homogeneous sample of gas to a temperature at which reaction proceeds. It is a fact of hydrodynamics[14] that a finite sustained compression is propagated into a gas as a shock wave, which has a steep front and a velocity that is supersonic with respect to the unshocked gas. A cylindrical shock tube is used to generate a plane shock wave that travels the length of the tube with a constant velocity. In the absence of induced chemical processes, the temperature, density, and flow velocity of the shocked gas are constant behind a shock wave of constant velocity. The values of these shock wave parameters are calculated from the shock wave velocity and the properties of the gas.

The second feature of a rapidly reacting system is that it cannot be kept at constant temperature by external means. Instead, the conditions in the reaction mixture are at the mercy of the heat and the composition change of the reaction. (The times involved in shock wave experiments are so short that thermal contact between the walls of the tube and the hot flowing gas in the shock wave is practically negligible.) In general, a chemical reaction occurring in a shock wave

situation is neither isothermal nor adiabatic. Nor does the reaction occur at constant volume. This is because the thermal state of the gas and the parameters of the flow are rigidly related. In order to maintain nearly constant temperature and density throughout the course of the reaction, one uses an internal thermal buffer in the form of a large excess of inert gas. In all the present work, this gas is argon, whose behavior is simple and well known. This carrier gas determines the conditions of the shock wave, which, to a first approximation, are constant and independent of the reacting material. The effect of the presence of up to one percent of the reacting component is easily treated as a linear perturbation on the conditions determined by the inert carrier gas.

The third characteristic of an experiment to follow a fast reaction is a fast method of detecting and recording the progress of the reaction. The methods of detection used in most shock wave experiments are optical. The methods of recording are electronically operated and generally provide a photographic record of the data. The present experiments have used both spectrophotography and photoelectric spectrophotometry. A spectrogram made with an electronically operated flash lamp has recorded the absorption spectrum of NO_3 during its brief presence in the shock tube. Rate measurements are made by following the appearance or disappearance of a colored substance as the reaction proceeds. An appropriate wave length band is selected and the transmission of the system is measured photoelectrically and recorded continuously over the experiment

by an oscilloscope. A camera records the oscilloscope trace during the experiment and auxiliary calibration traces. Measurements at two wave lengths have been made in each experiment in order to determine NO_2 and NO_3 simultaneously. Two photoelectric observation stations and oscilloscopes make this possible.

B. RESULTS, INTERPRETATIONS, AND CONCLUSIONS

1. Background from Experiments near Room Temperature.

The background for this investigation lies in three reaction systems whose kinetics have been studied and correlated at room temperature.(1)

The oxidation of nitric oxide by nitrogen pentoxide,

(4) $N_2O_5 + NO \longrightarrow 3NO_2$,

is a reaction which occurs in two steps.(2) The first step is the dissociation of N_2O_5 into two fragments.

(5) $N_2O_5 \xrightarrow{A(M)} NO_2 + NO_3$ (dissociation)*

The second step is the oxidation of nitric oxide by the very reactive nitrate radical, NO_3.

(6) $NO_3 + NO \xrightarrow{f} 2NO_2$ (reaction (f))

The recombination of NO_3 with NO_2,

(7) $NO_2 + NO_3 \xrightarrow{B(M)} N_2O_5$ (recombination),

competes with reaction (f) for the available NO_3. The exact rate equation derived from these steps is:

(8) $$\frac{d[NO_2]}{d\,t} = \frac{3\,A(M)\,[N_2O_5]}{1 + \dfrac{B(M)\,[NO_2]}{f\,[NO]}}$$

---

*The scheme of denoting reaction rate constants is taken from reference (1).

In most of the studies of the reaction of N_2O_5 with NO, reaction (f) is much faster than the recombination reaction, and the rate determining step is the dissociation of N_2O_5. This makes the denominator in equation (8) nearly unity and the overall rate of NO_2 production practically independent of the NO concentration. Thus:

$$(9) \qquad \frac{d\left[NO_2\right]}{d\,\underline{t}} = 3\,A(M)\left[N_2O_5\right]$$

Recently,[15] the oxidation of NO by N_2O_5 has been studied in the presence of excess NO_2 and the ratio $B(M)/\underline{f}$ has been evaluated.

This reaction system has been used to obtain extensive information about the unimolecular dissociation of nitrogen pentoxide.[3] The dependence of its rate and activation energy on the composition and amount of inert gas, M, that is present will be considered more fully later. In general, both A(M) and B(M) depend on pressure, but their ratio, K, is the equilibrium constant and is independent of pressure. At low total pressures, the dissociation rate constant, A(M), is nearly linear in pressure and at high pressures it is independent of pressure. The activation energy of the high pressure rate is the critical energy of splitting the N_2O_5 molecule, about 21 kcal/mole, and the activation energy at low pressures is a few kilocalories lower than that.

Nitrogen pentoxide gas by itself is unstable at room temperature and decomposes according to the equation:

$$(10) \qquad N_2O_5 \longrightarrow 2NO_2 + \tfrac{1}{2}O_2$$

The kinetics of the reaction puzzled chemists for many years. The reaction is of the first order in $[N_2O_5]$ and independent of $[NO_2]$, but the rate constant does not exhibit the pressure dependence which is characteristic of a unimolecular decomposition process.[16] The mechanism that explains the observed kinetics[7] involves the dissociation of N_2O_5, the recombination of NO_2 with NO_3, and in addition, the decomposition reaction between NO_2 and NO_3:

(11) $NO_2 + NO_3 \xrightarrow{e} NO + O_2 + NO_3$ (reaction (e))

The nitric oxide produced in this reaction is an intermediate which is quickly removed by reaction (f). The rate equations:

$$(12)\quad \frac{-d[N_2O_5]}{dt} = +\frac{\frac{1}{2}d[NO_2]}{dt} = +\frac{2d[O_2]}{dt} = \frac{2\ e\ K\ [N_2O_5]}{1 + \frac{B(M)}{2\ e}}$$

with the definition:

$$(13)\quad K = \frac{A(M)}{B(M)}$$

are valid provided that $f \gg e$, so that the steady state concentration of NO is very small. Except at very low pressures, B(M) is also very much greater than e, and the reaction rate is simply proportional to the N_2O_5 concentration. Under these circumstances, the activation energy observed for the decomposition process is the sum of the activation energy of step (e) and the internal energy change which accompanies the dissociation reaction, (5). Its value is 24.7 kcal/mole. Since the equilibrium energy of dissociation is approximately equal to the critical energy, 21 kcal/mole, the activation

energy of reaction (e) is only about 4 kcal/mole. These facts are important in the qualitative understanding of the kinetics of decomposition of N_2O_5 at higher temperatures.

The third reaction system that provides pertinent information about the reactions of NO_3 is the decomposition of ozone catalyzed by nitrogen pentoxide. By the reaction between ozone and NO_2, this system generates appreciable concentrations of NO_3, which can be readily observed spectroscopically. Unfortunately, the NO_3 concentrations obtained in mixtures of O_3 and N_2O_5 cannot be measured or calculated directly, so that absolute values of the absorption coefficients of NO_3 are not known. The key reaction is the decomposition of NO_3 into NO_2 and the product, oxygen, according to:

(14) $NO_3 + NO_3 \xrightarrow{g} NO_2 + O_2 + NO_2$ (reaction (g))

The estimated activation energy of this process is 8 kcal/mole. It is never important in the decomposition of N_2O_5 at room temperature because of the ever present excess of NO_2, but it will be seen that the high temperature decomposition mechanism includes step (g).

In the first order decomposition of nitrogen pentoxide, the macroscopic rate of appearance of the irreversible decomposition product, oxygen, follows directly the disappearance of N_2O_5 with no time lag. This comes about because the equilibrium dissociation of N_2O_5, reactions (5) and (7), is very small. Equilibrium is maintained by virtue of the fact that NO_2 and NO_3 recombine to form N_2O_5 much faster than

they decompose to liberate oxygen. Let us consider what happens to this mechanism when the temperature is raised to a point where equilibrium in the dissociation process calls for appreciable dissociation. Two limiting cases are possible for the rates of dissociation and decomposition of an initially pure sample of N_2O_5. First, the dissociation equilibrium may be achieved rapidly and maintained throughout the course of the slower decomposition reactions, (e) and (g). Under such circumstances, the initial reaction is the dissociation of N_2O_5, and the rate equation is:

$$(15) \qquad \frac{-d[N_2O_5]}{dt} = \frac{d[NO_2]}{dt} = \frac{d[NO_3]}{dt} = A(M)[N_2O_5]$$

The second reaction that becomes important is the recombination, so that the rate equation becomes:

$$(16) \qquad \frac{-d[N_2O_5]}{dt} = \frac{d[NO_2]}{dt} = \frac{d[NO_3]}{dt} = A(M)[N_2O_5] - B(M)[NO_2][NO_3]$$

When the steady state of virtual equilibrium is reached, this rate expression becomes substantially zero. The equilibrium conditions determine the rates of whatever subsequent steps, such as (e) and (g), occur, and equilibrium keeps pace with the changes resulting from the liberation of O_2.

The other limiting case is that in which the recombination reaction is slow compared to the formation of oxygen. Equilibrium is not maintained, and the stoichiometric decomposition, equation (10), keeps pace with the disappearance of N_2O_5. This case is realized at extremely low pressures near 50°C.

The equilibrium controlled case is the one that can be most nearly achieved in shock wave experiments, where one works with a low concentration of N_2O_5 in a large excess of inert carrier gas. The carrier gas enhances the rates of dissociation and recombination while the rates of such bimolecular reactions as (e) and (g) are kept low by the small concentrations of reactable species that are produced. Moreover, the activation energies are such that the dissociation rate constant A(M) increases with temperature very much faster than the rate constants $\underline{e}$ and $\underline{g}$. This means that at very high temperatures the dissociation reaction proceeds to completion before significant decomposition of NO_3 occurs. On the other hand, reactions (e) and (g) have significant energies of activation, whereas the recombination of NO_2 and NO_3 requires virtually no energy. Thus at temperatures near 500°K and inert gas pressures near one atmosphere the rate constants $\underline{e}$ and $\underline{g}$ are much smaller than B(M), so that equilibrium between NO_2, NO_3, and N_2O_5 is practically maintained even under conditions where N_2O_5 is over half dissociated.

The rate equations under conditions of comparable concentrations of NO_2, NO_3, and N_2O_5 are much more complicated than the simple equation, (12), which holds at the low temperature limit of the equilibrium controlled decomposition of N_2O_5. However, it is possible for shock wave experiments to achieve another simple kinetic system as the high temperature limit of the equilibrium controlled decomposition. The dissociation is rapid and quantitative, and is completely separated in time

from the production of oxygen.

2. Spectral Properties of NO_2 and NO_3.

Both NO_2 and NO_3 absorb light strongly in the visible spectrum. NO_2 absorbs strongest in the blue and near ultraviolet regions; NO_3 absorbs strongest in the red. The concentration measurements in the several experiments reported here make use of the absorption spectra of both of these oxides.

The absorption spectrum of gaseous NO_3 has been photographed in the visible region under low dispersion and at room temperature by Jones and Wulf.[17] The strongest absorption bands are centered near 662 mμ and 624 mμ. Weaker bands fill the region between 610 mμ and 500 mμ, becoming progressively weaker at the shorter wave lengths. In a series of photographs of a decomposing mixture of ozone and nitrogen pentoxide, these bands appear and then disappear before the absorption by NO_2 below 500 mμ becomes evident.

Figure 1 shows a flash spectrogram of a decomposing N_2O_5 sample in a shock wave experiment. The flash, which lasted for about fifty microseconds, was triggered 12 microseconds after the shock wave passed the segment of the shock tube between the lamp and the spectrograph slit. The timing of this exposure was arranged so that the dissociation of N_2O_5 was virtually complete when the flash was started but the decomposition of NO_3 was less than half over when the flash ended. The presence of NO_3 in the shock tube is undeniable.

The quantitative analysis of NO_2 in gas mixtures is often done spectrophotometrically using blue light. The absorption

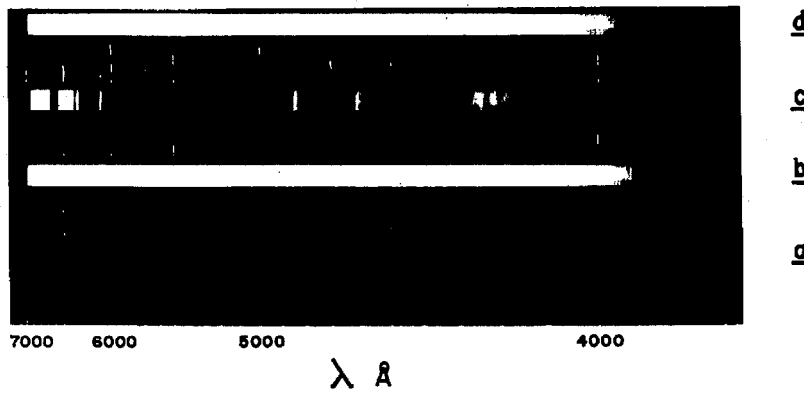

Figure 1. Flash absorption spectrogram of NO_3. The characteristic bands of NO_3, together with absorption by NO_2, are shown in exposure c. The source, a xenon flash lamp, is shown through the empty 15 cm shock tube in b and through the unshocked mixture of N_2O_5 and argon in d. The difference between b and d is the slight irreproducibility of the source. a is a two minute exposure to the other lights that were used in the experiment. When this page is held to the light, the 5461 Å and 4358 Å lines of mercury and some continuous exposure in the red are faintly visible. The plate is an Eastman Kodak Co. type 103-F. The formal N_2O_5 concentration was 23 x 10^{-5} m/l, the shock temperature was about 530°K, and dissociation was at least 90% complete before the fifty microsecond flash was started.

The print below is copied from that published by Jones and Wulf. (17)

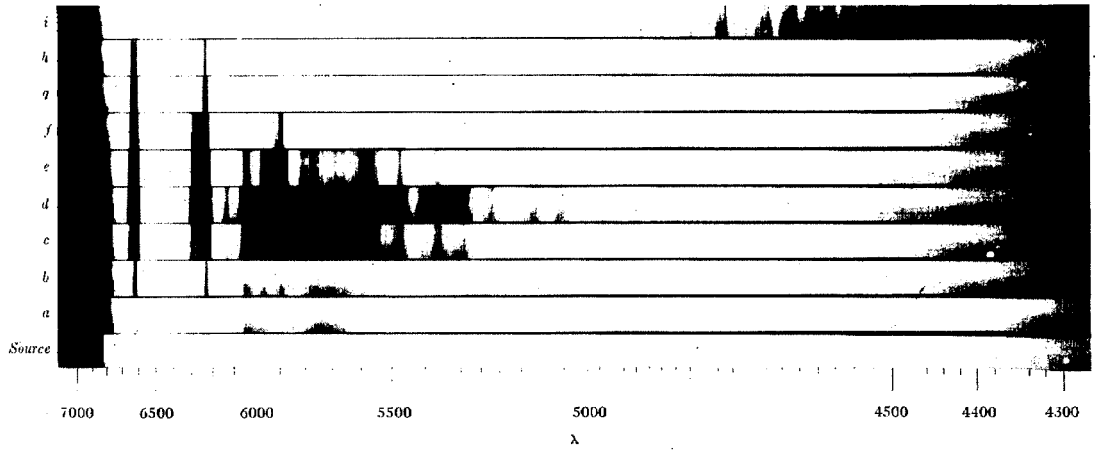

FIG. 1. The absorption of NO_3, overlain with weak ozone absorption in *a*, *b*, *c*. The absorption of NO_2 shows in *i*. The apparent relative intensity differences within the NO_3 spectrum between different strips is probably to be accounted for by the diffuse ozone absorption overlying certain of these. The wave-length, λ, is given in angstroms. Maximum N_2O_5 pressure roughly 80 mm Hg; maximum O_3 pressure roughly 50 mm Hg.

coefficients have been measured repeatedly[18][19][20] for a number of selected wave length bands at temperatures near 300°K. Beer's law has been found to be generally applicable, and the absorption coefficients are satisfactorily independent of the total pressure in the system. The determination of NO_2 in the decomposition of N_2O_5 at high temperatures requires knowledge of the extinction coefficients for a particular wave length band over the entire range of temperature of the experiments. To provide this information, a number of shock wave experiments have been done in which mixtures of NO_2 and argon were compressed and heated to temperatures between 500° and 1000°K. The extinction coefficients of NO_2 at the shock wave temperatures have been calculated from the initial conditions and the measurements of light transmission after the passage of the shock wave.

Let i_o represent the intensity of the incident light beam, i_r the light that is transmitted to the photomultiplier through the NO_2 sample before it is shocked, and i_1 the light transmitted after the shock wave passes the observation station. In the unshocked gas, the concentration of NO_2 is $C_o\phi$, where C_o is the total concentration of gas and ϕ is the mole fraction of NO_2. The concentration of NO_2 that is present in the shocked gas is given by $C_o\phi\Delta$, where Δ is the density compression ratio across the shock front. The optical densities $D_1 = \log_{10}(i_o/i_1)$, $D_o = \log_{10}(i_o/i_r)$, and $D' = \log_{10}(i_r/i_1)$ are defined. These are related by:

$$(17) \quad \epsilon_{(\lambda,T_2)}C_o\phi\Delta L = D_1 = D_o + D' = \epsilon_{(\lambda,\ 300^oK)}C_o\phi L + D'$$

The length of the light path is L. The initial optical density, D_o, is calculated from the measured concentration and path length and the extinction coefficient quoted from other measurements. D' is the increment in optical density observed in the experiment. The value of the high temperature extinction coefficient, $\epsilon(\lambda, T_2)$, is calculated from these data and the particular T_2 and Δ of the shock wave. Correction of D_o for the small amount of transparent N_2O_4 is straightforward. The results of these measurements at several wave lengths are presented in table 1. The results at 366 mμ, 546 mμ, and 650 mμ are included in figure 2.

The significant qualitative conclusion that can be drawn from these measurements is that near the maximum in the NO_2 absorption spectrum, the absorption coefficient decreases with temperature, while in the green and red regions the weaker absorption has a positive temperature coefficient. This behavior is typical of molecular electronic absorption spectra. The maximum in the absorption curve represents absorption from low vibrational states, while the edges of the absorption region correspond to transitions from higher vibrational states. At low temperatures, only the lower states have significant populations, and the absorption is confined to the spectral region in which they absorb. At higher temperatures, the higher vibrational states are populated at the expense of the lower ones, and the absorption spectrum is broader and flatter.

The analysis of shock wave mixtures for NO_3 has been carried out with light in the green and red regions of the

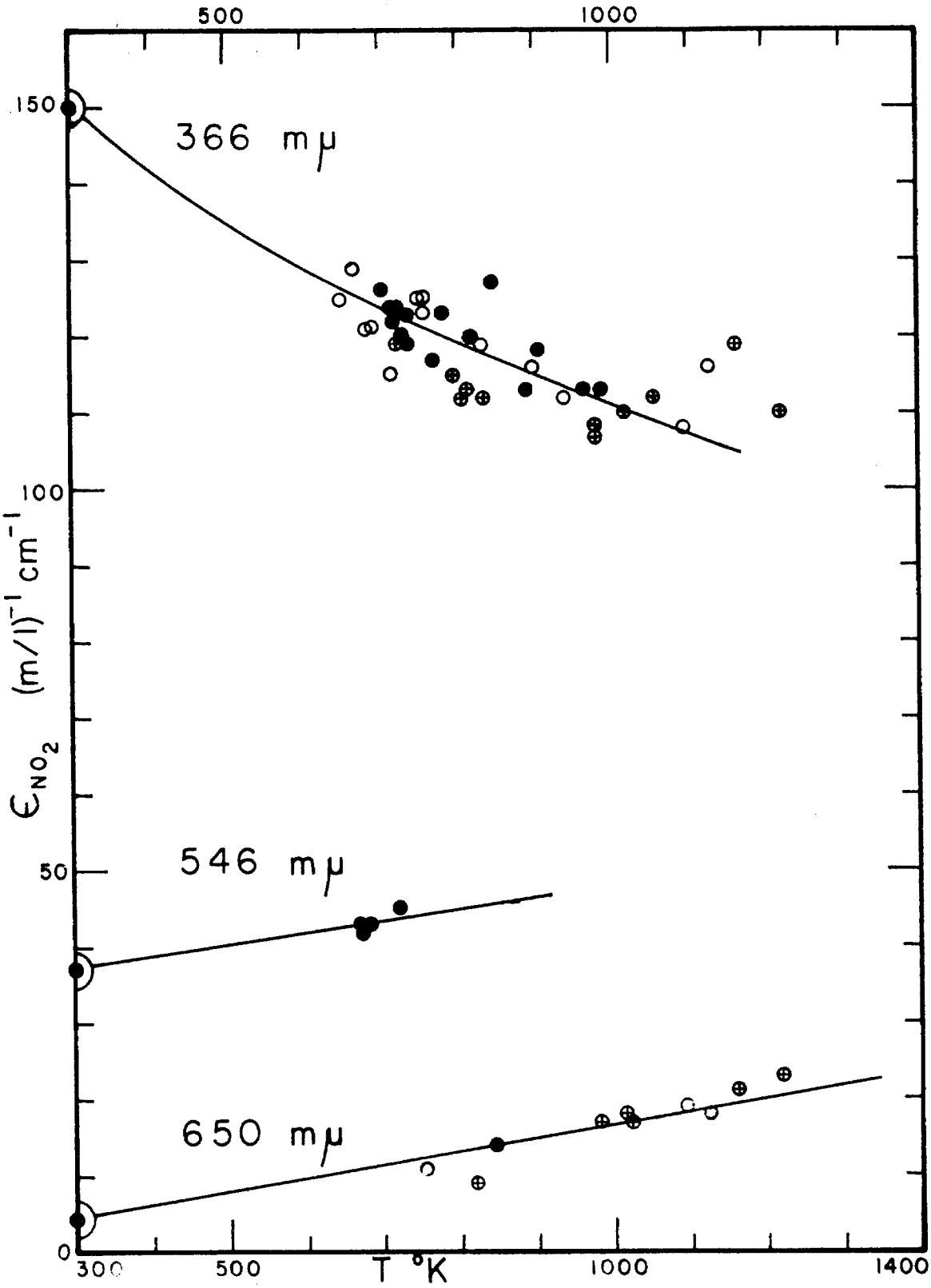

Figure 2. Extinction coefficients of NO_2. (●), in NO_2 - argon mixtures; (⊕), in final decomposition products of N_2O_5; (○), in mixtures containing N_2O_5 and NO_2, after decomposition.

spectrum. The absorption by NO_3 in the red is very much stronger than any visible absorption by NO_2, so that the small absorption by NO_2 in the red introduces little difficulty in the simultaneous determination of comparable amounts of NO_2 and NO_3.

To a greater degree than the NO_2 spectrum, the NO_3 spectrum is marked by a number of strong bands separated by sharp minima. From the standpoint of qualitative analysis, this is ideal, but for quantitative spectrophotometry in the gas phase, it presents several complications. Beer's law is strictly valid only for a line source of light, and its applicability to band sources depends on the constancy of the absorption coefficient over the interval of the spectrum that is used. The choice of a suitable wave length interval for use in the analysis of NO_3 is severely restricted by the large changes in extinction coefficient between successive maxima and minima. Even when one works with a monochromatic source, the effect of pressure on the absorption intensity in an absorption band may be annoyingly large. The general effect of temperature noted in NO_2 likewise may be expected to be present in the NO_3 spectrum. In addition to these fundamental difficulties, there is the practical problem of obtaining a rapidly responding photocathode with adequate sensitivity in the red end of the visible spectrum.

Most of the experiments have been done using a tungsten lamp as source and a wave length band of 3.6 mμ half width centered at 652 mμ. This wave length is near an absorption

minimum between the two strongest absorption bands, 624 mμ and 662 mμ, and it also excludes two fairly pronounced bands near 634 mμ and 640 mμ. The extinction coefficients recorded in table 2 have been measured in mixtures of NO_2 and NO_3 produced immediately after the dissociation of N_2O_5 behind a shock wave. They have been calculated from equation (17) with the substitution of zero for D_o and the mole fraction of N_2O_5 in the unshocked gas for ϕ. The latter substitution is based on the hypothesis that at the instant when D_1 is measured, N_2O_5 has been quantitatively converted to an equimolar mixture of NO_2 and NO_3. The data are confined to temperatures above 600°K, where the evidence presented in the next section indicates that the dissociation is complete. The values listed have been corrected for the absorption by NO_2 using the curve shown in figure 2. They show more scatter than the absorption coefficients measured in NO_2 because the conditions of the measurement of D_1 are only present momentarily before the decomposition of NO_3 becomes significant. (See figure 3a.) Accordingly, the scatter is greatest at the highest temperatures and the highest concentrations of nitrogen oxides.

These extinction coefficients describe the absorption by NO_3 in an environment of about 10^{-2}m/l of argon. The extreme values of the NO_3 concentration are 2.5×10^{-5}m/l and 12.5×10^{-5}m/l. No systematic deviation from Beer's law is evident over this range of concentrations. (See experiments 91-96 in table 2.) There is, however, some indication of a positive effect of total pressure on the absorption coefficients.

(See experiments 81-85.) The magnitude of this effect cannot be reliably estimated, but probably it does not exceed fifteen percent per atmosphere of argon.

Experiments were carried out to test the dependence of the extinction coefficients of NO_3 on wave length near 650 mμ. These experiments were done near 825°K using wave length bands centered at 648, 650, and 652 mμ. (See experiments 72-78.) The results can be expressed as $d \ln \epsilon / d\lambda = +3 \pm 2\%$ per mμ, and they confirm the hypothesis that a 4 mμ half width is tolerable.

The results contained in table 2 can be summarized as follows:

T (°K)	$\epsilon_{(652\ m\mu,\ T)}$ $(m/l)^{-1}cm^{-1}$	Estimated Uncertainty
300	220 (extrapolated)	30
650	260	15
825	282	15
1050	305	25

A few experiments were done with 546 mμ light isolated from a high pressure mercury arc. Around 650°K in 0.008 m/l argon, $\epsilon_{NO_3} = 530 \pm 50\ (m/l)^{-1}cm^{-1}$, and it appears that ϵ_{NO_3} is rather pressure dependent. (546 mμ is in the edge of one of the stronger absorption bands.)

One exploratory experiment was done with a 4 mμ wave length band centered near 615 mμ. The measured extinction coefficient was 1250 $(m/l)^{-1}cm^{-1}$ at 520°K. This result indicates considerable inclusion of the 624 mμ band, which is the

broader of the two very strong absorption maxima shown in figure 1. Another such experiment was done in the band at 589 mμ, and the extinction coefficient is about 1000.

From these measured extinction coefficients and visual examination of the flash spectrograms like figure 1, one can estimate the maximum absorption coefficients of NO_3 in the strong bands at 662 and 624 mμ as $3000 \pm 1000(m/l)^{-1}cm^{-1}$.

The absorption by NO_3 in the blue and violet regions is not nearly so strong as in the strong bands in the green and red. Nevertheless, there is considerable absorption by NO_3 throughout the blue and into the near ultraviolet. This absorption is not obvious in the flash spectrogram of the mixture of NO_2 and NO_3 because it is masked by the NO_2 absorption. In the published spectrogram[17] of an ozone and nitrogen pentoxide mixture it is less striking than the characteristic bands. There is, however, unmistakable general darkening (of the positive print) in the 440 mμ region. This darkening is not due to absorption by ozone or by NO_2, because its time history exactly parallels that of the NO_3 bands. However, the sign of $d\epsilon_{NO_3}/d\lambda$ in the blue is not determined by the room temperature plate, even though the darkening clearly increases toward the blue end of the spectrum. This is because the illumination of the plate decreases strongly toward the blue end of the spectrogram and much less absorption is required to produce noticeable darkening of the print.

The following data on the absorption coefficients of NO_3 were obtained as a by-product in photoelectric measurements

whose principal function was to record the appearance of NO_2 in the decomposition of N_2O_5.

$\lambda_{(m\mu)}$	$T_{av.}$ °K	$\epsilon_{(\lambda, T)}$	Uncertainty	Number of Experiments
436	650	130	20	6
405	650	90	20	2
366	600	25	15	4
366	825	40	15	12

These values represent the averages of several individual experiments in which the optical density was measured after the rapid increase produced by the dissociation of N_2O_5 but before the decomposition of NO_3 was appreciable. (See figure 3b.) The equimolar composition in NO_2 and NO_3 corresponding to complete dissociation of the N_2O_5 was assumed. The absorption by NO_3 was computed as the difference between the observed absorption and that calculated for one equivalent of NO_2 on the basis of the independent extinction coefficient data presented in table 1. The individual data are badly scattered because they are obtained by difference. At 366 mμ, where data are most plentiful, the differences are smallest and the scatter is greatest. Alternative interpretations of these experiments and the evidence in favor of this one will be presented in the next section.

Two qualitative conclusions can be drawn about the NO_3 absorption in the blue. First, the absorption decreases toward the violet. The lowest values recorded are at 366 mμ, and these have a positive temperature coefficient. The minimum

that must occur someplace is not located, but it seems certain that no strong maxima are present in the near (pyrex) ultraviolet. Second, the absolute strength of absorption by NO_3 at elevated temperatures is comparable to that of NO_2 in the blue region, and even at 366 mμ, NO_3 interferes considerably in the analysis of NO_2.

3. Stoichiometry of Dissociation and Decomposition of N_2O_5.

At 300°K, the decomposition of nitrogen pentoxide is described by the equation:

(18) $N_2O_5 \longrightarrow 2NO_2 + \frac{1}{2}O_2$

At equilibrium, the reaction is complete and the products, NO_2 and O_2, are stable with respect to further reduction of NO_2. The only side reaction is the removal of NO_2 to satisfy the equilibrium:

(19) $N_2O_4 \rightleftharpoons 2NO_2$

At high concentrations, this process complicates colorimetric or manometric determination of the extent of the decomposition reaction. However, at the high temperatures of the present experiments, it is unimportant.

It was proposed at the outset of this work to separate the decomposition of N_2O_5 into two stoichiometric steps, first the dissociation of N_2O_5,

(20) $N_2O_5 \longrightarrow NO_2 + NO_3$,

and second the decomposition of NO_3,

(21) $NO_2 + NO_3 \longrightarrow 2NO_2 + \frac{1}{2}O_2$

Quantitative establishment of these steps has been a significant part of this investigation.

Proof of both of these steps would be straightforward if one could analyze the mixture specifically for NO_2. Attempts to do this spectrophotometrically using light in the blue and near ultraviolet regions have not been wholly successful. Figures 3 and 4 are typical of the records of optical

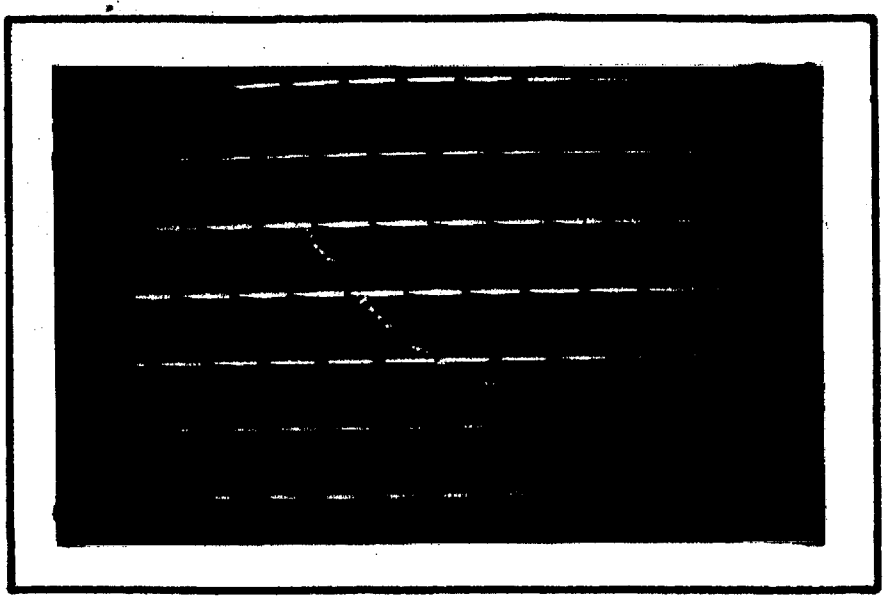

Figure 3a. Photoelectric record at $\lambda = 652$ mμ showing initially no absorption, sudden rise in absorption as N_2O_5 dissociates into NO_2 and NO_3, and finally constant small absorption by the product, NO_2. $T_2 = 801^\circ$ after dissociation, $811^\circ K$ after decomposition. Timing blanks are every 30 μsec.

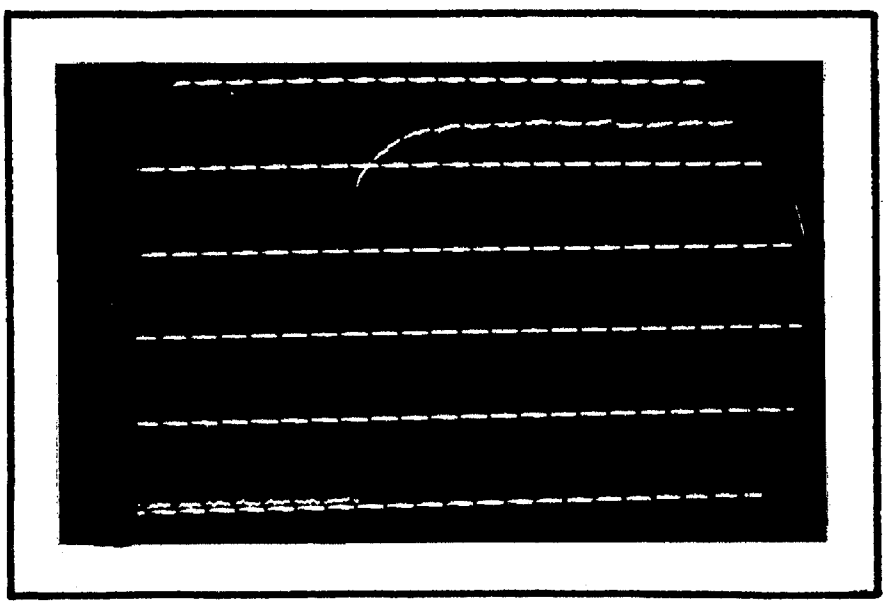

Figure 3b. Photoelectric record at $\lambda = 366$ mμ showing incident light, absorption by equimolar NO_2 and NO_3, and finally somewhat greater absorption after NO_3 becomes NO_2 and O_2. Same experiment as above. Sweep only half as fast. Calibration spacings are about 15% of incident light. $[NO_3]_{max} = 12.5 \times 10^{-5}$ m/l; $[NO_2]_{final} = 23.6 \times 10^{-5}$ m/l.

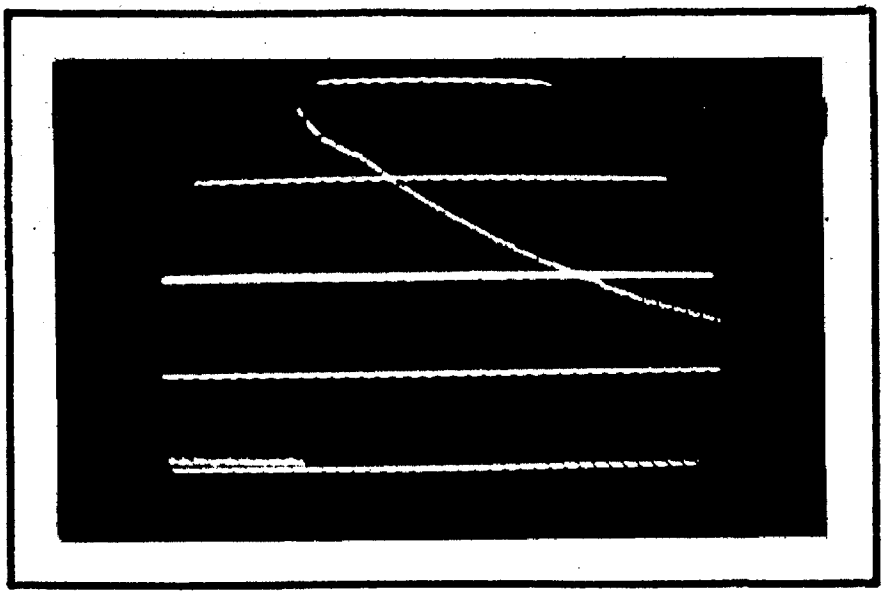

Figure 4a. Photoelectric record at $\lambda = 546$ mμ showing initially no absorption, sudden rise in absorption as N_2O_5 dissociates in the shock wave, and then the decrease in absorption as NO_3 disappears. $T_2 = 627^oK$ after dissociation. $[NO_3]_{max} = 3.66 \times 10^{-5}$ m/l. Timing blanks are every 30 μsec.

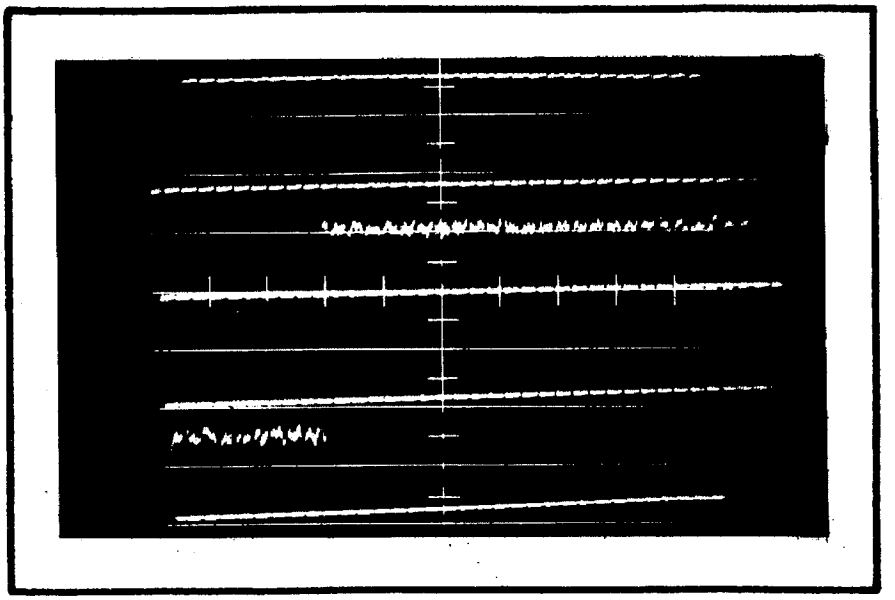

Figure 4b. Photoelectric record at $\lambda = 436$ mμ in the same experiment as that shown above. The absorption remains constant as NO_3 is converted to NO_2. As the decomposition occurs in this mixture containing 0.44% N_2O_5, the density decreases by 1%, and the temperature increases by 6^oK.

absorption versus time in the experiments between 600° and 1100°K. In all these experiments, the absorption by the N_2O_5 and argon mixture before the arrival of the shock wave is nil. Immediately after the shock wave passes the observation station, light absorption commences and rises nearly as a step function in time to a definite level. Further changes in the absorption occur much more slowly, and finally a condition of constant absorption is reached. In the green and red, the initial surge of absorption is mostly due to the production of NO_3, and the absorption decreases with the subsequent decomposition of NO_3. (Figures 3a and 4a) The records at 366 mμ are qualitatively consistent with the expected course of absorption by NO_2. (Figure 3b) The initial surge is followed by a slow further increase to the final constant value. At 436 mμ (Figure 4b) almost no change in absorption occurs after the initial fast rise, although the simultaneous record at 546 mμ clearly shows that NO_3 is disappearing.

Quantitative measurements of the initial absorption increments at each of the wave lengths shows that the amount of absorbing material is proportional to the formal N_2O_5 concentration at any given temperature. Moreover, the variation in absorption per mole of N_2O_5 originally present increases only slightly with temperature between 600° and 1100°K at 652 mμ and indetectably at 366 mμ.

At 366 and 436 mμ the initial absorption is consistently higher than corresponds to one mole of NO_2 from each mole of N_2O_5 by a factor that is independent of the amount of N_2O_5

present. This factor at 366 mμ is about 1.3, and it increases somewhat with temperature. At 436 mμ near 650°K it is about 2.0. Exploratory experiments have also been done at 405 mμ and 487 mμ. The behavior at 405 mμ is intermediate between the phenomena at 366 and 436 mμ, while at 487 mμ the absorption by NO_3 is dominant and the total absorption decreases after the initial rise.

All these data are consistent with the hypothesis that the dissociation of N_2O_5 is rapid and complete and that appreciable NO_3 absorption exists throughout the blue and violet regions, increasing toward the red and having a positive temperature coefficient. Quite apart from the predictions made by extrapolation of room temperature experiments, this interpretation is the most reasonable one on the basis of the high temperature data alone. Let us consider briefly some alternative interpretations.

Suppose that the dissociation of N_2O_5 were incomplete. This would mean that the initial absorption would not be linear in the formal N_2O_5 concentration. Also, the absorption would increase markedly with temperature, since the equilibrium dissociation energy is about 21 kcal/mole. Further, the absorption in the blue would be expected to be less than instead of greater than that calculated for the amount of NO_2 produced by complete dissociation. Such behavior has of course been observed between 450 and 550°K. The dissociation rate and equilibrium data are presented later. Suppose, on the other hand, that the initial destruction of N_2O_5 is complete

but is somehow more complicated than the simple dissociation reaction, (20). Suppose specifically that NO_3 does not absorb at 366 mμ at all, and that NO_2 is produced in excess of the formal N_2O_5 concentration, while NO_3 makes up the balance of the dissociation products. This could come about if there were some other mode of decomposition of N_2O_5 which yields two NO_2 molecules and whose rate is comparable to the simple dissociation rate. The data between 600° and 1100°K require that any such process have a rate that remains comparable to that of reaction (20) over this entire temperature range. This means that its activation energy must be near 20 kcal/mole. Any bimolecular process, such as

(22) $N_2O_5 + NO_3 \longrightarrow 3NO_2 + O_2 \qquad \Delta H_{298} = -3\text{kcal/mole}$

could not keep pace with the unimolecular dissociation, (20), unless its activation energy were substantially less than 5 kcal/mole. Any process involving oxygen atoms is endothermic by at least 50 kcal/mole, and need not be considered. Nor can any process be considered which involves NO_3 but not N_2O_5. Such a process would be required to destroy one portion of the NO_3 immediately and the remainder rather slowly.

The analysis of the final state of constant absorption is free of complications. With NO_3 destroyed, NO_2 is the only possible oxide in the system, including NO, which can absorb visible light significantly. The results of all the experiments in which the final state was observed show, within experimental error, that N_2O_5 has been converted quantitatively to NO_2 and O_2. This statement applies to

measurements at several wave lengths and to the highest temperature of this investigation, 1216°K. The results are presented in table 3 as extinction coefficients calculated from the final optical densities observed and the assumption that two moles of NO_2 appear in place of every one of N_2O_5. They may be compared with the extinction coefficients of NO_2 measured in independent experiments. (See figure 2.) The complete results are recorded in table 3, and the data at 366 mμ and 652 mμ are included in figure 2. Incomplete conversion to NO_2 would have given values of ϵ that were too low. Measurements made when there was still some NO_3 in the system would have given high results in the red and low results in the violet.

This conclusion that in the shock wave experiments N_2O_5 has decomposed stoichiometrically into NO_2 and O_2 is an important one, because at temperatures of 600°K and higher, NO_2 is unstable with respect to NO and oxygen. The thermal decomposition of 10^{-4} m/l NO_2 at 1000°K is known to require about two seconds.[21] Hence it is too slow to be significant in the present experiments, which are of much shorter duration. However, the present conclusion also excludes the possibility that NO is accumulated in the system by other reactions, particularly those involved in the decomposition of NO_3.

4. Kinetics of Decomposition of NO_3.

In the previous section, the stoichiometric steps in the high temperature decomposition of N_2O_5 were established. In the experiments between 600° and 1100°K the dissociation step is too fast for its rate to be measured with present techniques. The decomposition step, however, occurs at a rate that is convenient for studying. The useful part of the photoelectric record begins somewhat after the shock wave has passed the observation slit. N_2O_5 is completely dissociated and the optical density, $D = \log_{10}(i_o/i)$, has the value D_1. The continuous record of transmission follows the changing optical density as it approaches its final constant value, D_∞. In general D in this system is composed of two terms, representing absorption by NO_2 and by NO_3.

$$(23) \qquad D = \epsilon_{NO_2} [NO_2] L + \epsilon_{NO_3} [NO_3] L$$

In the shock wave notation, the formal concentration of N_2O_5 at any point behind the shock wave is $C_o \phi \Delta$, where $C_o \phi$ is the N_2O_5 concentration before the shock arrives, and Δ is the density compression ratio.

In the shock wave situation, chemical reactions do not take place at constant volume. For this reason, it is convenient to use the degree of decomposition of NO_3, β, in developing and using the rate equation. β is defined by:

$$(24) \qquad [NO_3] = C_o \phi \Delta (1 - \beta)$$

When no added NO_2 is present, it follows from the stoichiometry that:

(25) $[NO_2] = C_o \phi \Delta (1 + \beta)$

To relate β to D, it is necessary to consider the effect on D of the change in the density of the reaction mixture with the progress of the reaction. In experiments in an excess of inert gas, this change is small and can be treated as a linear correction. Accordingly:

(26) $\Delta = \Delta_1 (1 + \beta \, d \ln\Delta/d\beta) = \Delta_1 (1 - \beta \, d \ln\Delta/d\beta)^{-1}$

With these substitutions, equation (23) becomes:

(27)

$$D = C_o \phi L \Delta_1 (1 + \beta \, d \ln\Delta/d\beta) \{\epsilon_{NO_3}(1-\beta) + \epsilon_{NO_2}(1+\beta)\}$$

$$= C_o \phi L \Delta_1 (1 + \beta \, d \ln\Delta/d\beta) \{(\epsilon_{NO_2} + \epsilon_{NO_3})(1-\beta) + 2\epsilon_{NO_2}\beta\}$$

Substitution of the end conditions, D_1 and D_∞ and the definition

(28) $D^* = D \, (1 - \beta \, d \ln\Delta/d\beta)$

$$D_1^* = D_1 \qquad D^* = D_\infty \, (1 - d \ln\Delta/d\beta)$$

yields

(29) $D^* = D_1 (1 - \beta) + D_\infty^* \beta$

from which

(30) $$\beta = \frac{D_1 - D^*}{D_1 - D_\infty^*} \qquad (1 - \beta) = \frac{D^* - D_\infty^*}{D_1 - D_\infty^*}$$

Possible variation of the extinction coefficients with the temperature changes accompanying reaction has been ignored.

The special case in which both extinction coefficients have the same logarithmic temperature coefficient can be easily incorporated into the above treatment by replacing $(d \ln\Delta/d\beta)$ by the sum $(d \ln\Delta/d\beta + d \ln\epsilon/d\beta)$. In the present experiments the temperature changes are only a few degrees, and corrections for changing extinction coefficients are negligible.

The differential rate equation can be deduced from the kinetics of the processes believed to be important in the transformation of NO_3 into NO_2 and oxygen. These are:

(31) $NO_3 + NO_3 \xrightarrow{g} NO_2 + O_2 + NO_2$

and the combination:

(32) $NO_2 + NO_3 \xrightarrow{e} NO + O_2 + NO_2$

followed rapidly by:

(33) $NO_3 + NO \xrightarrow{f} NO_2 + NO_2$

The rate constants describe the reactions at constant volume. When $f \gg e$, the total rate can be expressed as:

(34) $(-d[NO_3]/d\,t)_v = \text{Rate} = 2\,e\,[NO_2][NO_3] + 2\,g\,[NO_3]^2$,

from which:

(35) $$\frac{\text{Rate}}{2[NO_2][NO_3]} = e + g\,\frac{[NO_3]}{[NO_2]}$$

In the shock tube situation, differentiation of (24) at constant volume gives:

(36) $$(-d[NO_3]/d\,\underline{t})_v = \text{Rate} = C_0 \phi \Delta\, d\beta/d\,\underline{t}$$

$\underline{t}$ is the time since the shock wave heated the particular element of flowing gas under observation. τ is the time since the shock wave was observed at the fixed observation station. The transformation is:

(37) $$d\,\underline{t} = \Delta\, d\,\tau$$

With this substitution and division by (24) and (25), (36) becomes:

(38) $$\frac{\text{Rate}}{[NO_2][NO_3]} = \frac{d\beta/d\tau}{C_0 \phi \Delta^2 (1-\beta^2)}$$

and the rate equation, (35) is:

(39) $$\underline{e} + g\frac{(1-\beta)}{(1+\beta)} = \frac{d\beta/d\tau}{2\,C_0 \phi \Delta^2 (1-\beta^2)}$$

In the event that NO_2 is added to the initial mixture, (39) becomes:

(40) $$\underline{e} + g\frac{(1-\beta)}{(1+\beta+\eta)} = \frac{d\beta/d\tau}{2\,C_0 \phi \Delta^2 (1-\beta)(1+\beta+\eta)}$$

where η is the formal ratio of NO_2 to N_2O_5 in the unshocked gas.

Two limiting cases are of interest. If $g \gg \underline{e}$, all but the last part of the reaction is just the simple bimolecular decomposition of NO_3, and the rate decreases as $(1-\beta)^2$.

Sooner or later, as NO_3 is depleted and NO_2 is built up, reaction (e) becomes significant. If $\underline{e} \gg \underline{g}$, reaction (e) is dominant from the start, and the rate decreases only as $(1 - \beta^2)$.

If by coincidence $\underline{e} = \underline{g}$, the reaction rate is pseudo first order, decreasing as $(1 - \beta)$. The effective rate constant is $C_0 \phi \Delta (\underline{e} + \underline{g})$. In this case NO_3 reacts equally rapidly with NO_2 and NO_3, the sum of whose concentrations is constant. It will be seen that this last situation is closely approximated near 600°K, and that $\underline{e}$ and $\underline{g}$ are of comparable magnitude throughout the temperature range of this investigation.

In any event, the rate predicted by this mechanism is controlled exclusively by bimolecular processes, and the initial rate of reaction is proportional to the square of the formal N_2O_5 concentration and independent of the inert gas pressure. This seems to be the case.

If one or the other of the two reaction paths were dominant, an integrated rate equation would be useful in treating the data. In general, however, the ratio $\underline{e}/\underline{g}$ is not known <u>a priori</u>, so the following point by point procedure has been used. D is evaluated from the optical transmission record at selected values of τ. An approximate value of β is deduced, and D* is evaluated by equation (28). In the experiments where D_∞ is not observed, it is calculated using the extinction coefficients of NO_2 measured in other experiments. Most of the points have been taken from measurements

at 652 mμ and 546 mμ. The measurements at 366 mμ are less precise because of the significant interference of the NO_3 absorption. This interference renders measurements at 436 mμ useless. From the measured sequence of β versus τ, the average value of $d\beta/d\tau$ is evaluated between successive points and assigned to the mean values of β and τ. The reduced rate function, which is the right side of equation (39) or (40), is tabulated and plotted against $[NO_3]/[NO_2]$. In the absence of added NO_2, the abscissae in such a plot are $(1-\beta)/(1+\beta)$, and cover the interval between zero and unity. The mechanism predicts that the plot is linear with positive slope equal to g and positive left intercept equal to e. In practice, the points are scattered, but in all but one case, the most plausible curve is a straight line with positive slope and intercept. This exception is a very fast reaction at 1127°K, and a negative slope is indicated.

The intercept of these plots at $[NO_3]/[NO_2] = 1$ (the right intercept) is the apparent bimolecular rate constant at the beginning of the reaction, which is the sum, (e + g). This is the quantity that is most accurately deduced from the experiments by this plotting procedure. The data measured early in the reaction are inherently more reliable, and the later data are included as a guide in extrapolating to the beginning of the reaction. In calculating the ordinates for these points, the initial value, Δ_1, has been used in equation (39) throughout each experiment. This does not affect the right intercept, and the corrected left intercept

can be obtained merely by multiplication by

$$(\triangle_1/\triangle_\infty)^2 = (1 - 2\ d\ \ln\triangle/d\beta).$$

The decomposition of NO_3 is exothermic, and the temperature at the end of the reaction is higher than that at the beginning. Adjustment of the left intercept, e, to the initial temperature, $T_{(\beta = 0)}$, involves a negative correction that nearly cancels the positive correction for the density change. This cancellation is a consequence of the peculiar combination of the activation energy of reaction (e), the exothermicity of reaction (21), and the heat capacity of argon. It is independent of ϕ because the changes in $\triangle$ and T are both proportional to ϕ.

The resulting values of (e + g) in the several experiments are plotted on logarithmic scale against reciprocal temperature in figure 5. The nearly linear form of this plot indicates that e and g have not very different temperature coefficients. The line has been calculated by the least squares method. It gives the average activation energy as 6.42 $\pm$ 0.3 kcal/mole. The equation of the line is:

$$(41) \qquad \log_{10}(e + g) = -(1403 \pm 60)/T + 9.340$$

The two rate constants have been separated in two ways. The most reliable of these uses the initial rate data in a series of experiments in which NO_2 was added to the initial mixture so that at the beginning of the decomposition, $[NO_3]/[NO_2]$ was between 0.3 and 0.1. These values of $(e + g\ [NO_3]\ /\ [NO_2]\ )$ were combined with the values of

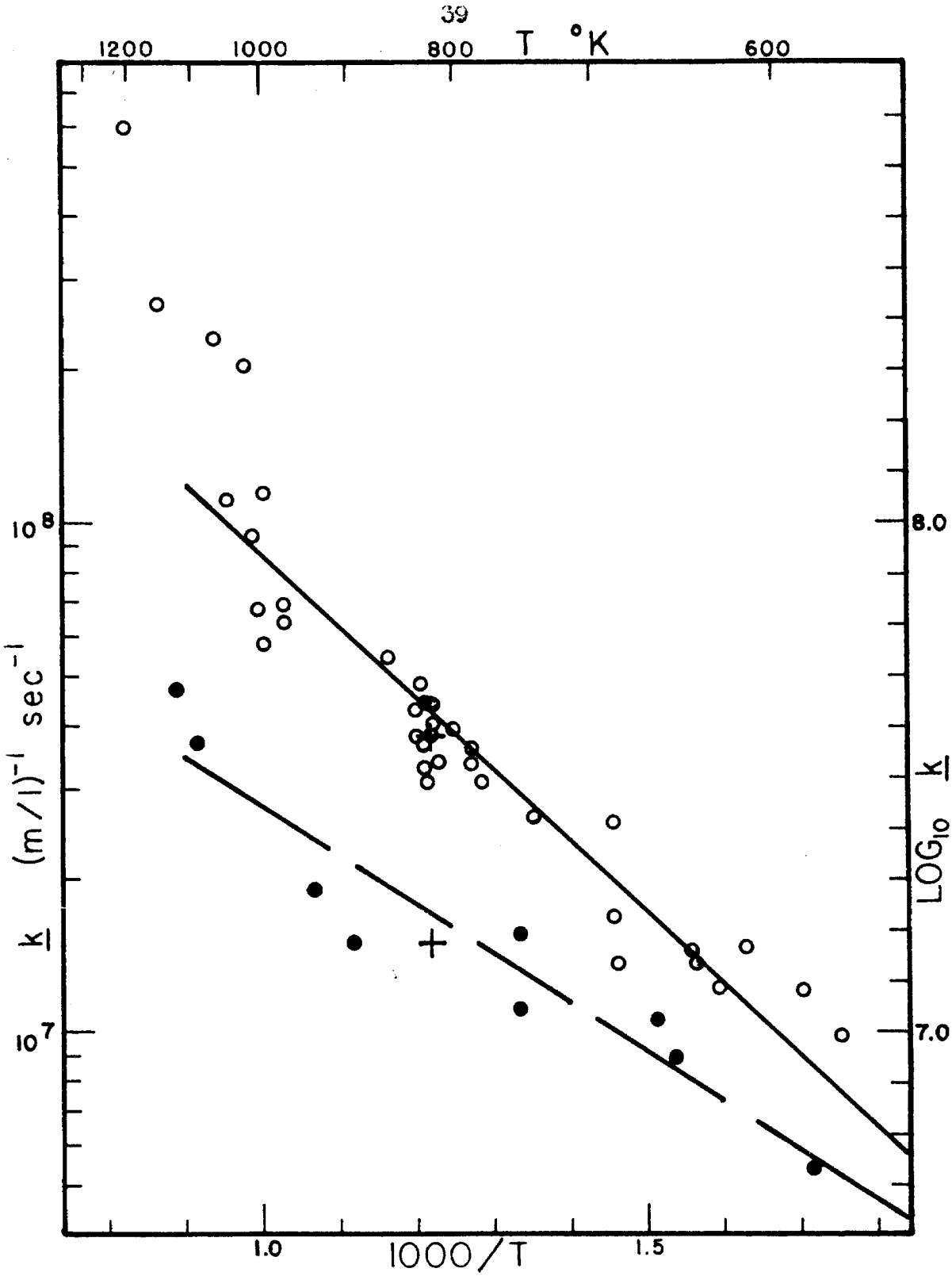

Figure 5. Bimolecular rate constants from the initial rate of decomposition of NO_3. (○), $\underline{k} = (\underline{e} + \underline{f})$; solid line, equation (41); (●), $\underline{k} = \underline{e}$; broken line, equation (42); (+), equation (44).

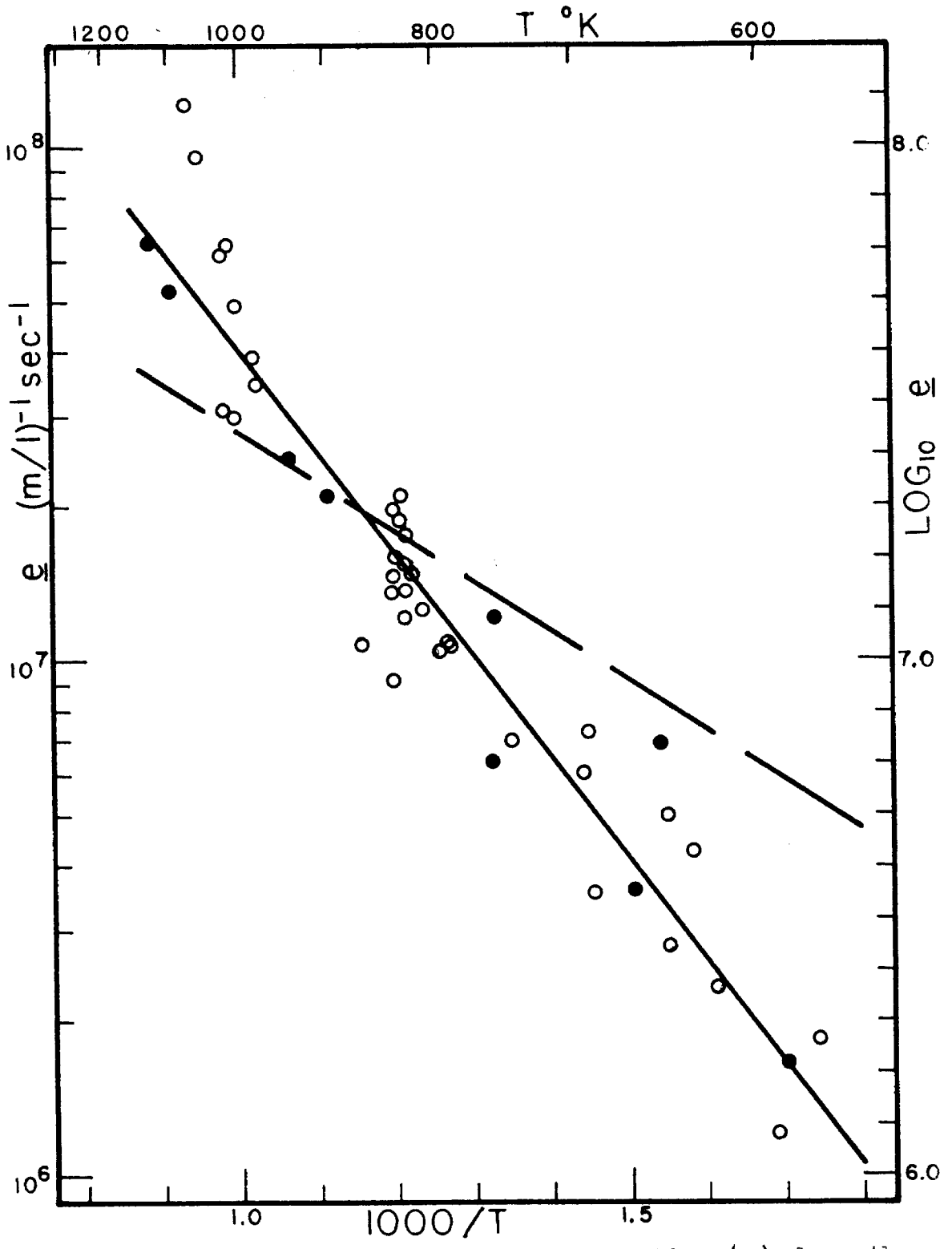

Figure 6. Apparent rate constants in reaction (e) from the final rate of decomposition of NO_2. (○), experiments with pure N_2O_5; (●), experiments with NO_2 added; solid line, equation (43); broken line, equation (42).

($\underline{e}$ + $\underline{g}$) at the same temperatures given by equation (41). The values of $\underline{e}$ obtained in this way are plotted in the lower part of figure 5. The equation of the line through them is:

$$(42) \quad \log_{10}(\underline{e}) = -(965 \pm 150)/T + 8.41$$

and the activation energy is 4.42 $\pm$ 0.7 kcal/mole.

The other set of values of $\underline{e}$ are obtained as the left intercepts of the plots of equation (39). These data are shown in figure 6. The calculated line is

$$(43) \quad \log_{10}(\underline{e}) = -(1981 \pm 60)/T + 9.590$$

and the activation energy is indicated as 9.1 $\pm$ 0.3 kcal/mole. The dashed curve in figure 6 is equation (42). This strong disagreement between the values of the activation energy of reaction (e) calculated by the two procedures arises largely from the data at the low end of the temperature range. Here the reaction is not followed past about $\beta = 0.5$, and the extrapolation to $[NO_3]/[NO_2] = 0$ is long and uncertain. The plots always yielded positive intercepts, but the values of $\underline{e}$ indicated were substantially lower than those measured by the method of adding NO_2 to the original mixture.

Near 820°K, the center of the temperature range, the two methods of separating $\underline{e}$ and $\underline{g}$ agree with each other. Data from twenty-one experiments between 750° and 934°K have been adjusted to 820°K using the temperature coefficient of equation (41). These include data from experiments with the initial N_2O_5 concentrations differing by a factor of five

and from experiments with NO_2 added to the mixture. The plot of these data according to equation (40) is shown in figure 7. The general validity of the kinetic interpretation, equation (34), is supported. The best values of the individual rate constants afforded by this investigation are derived from this plot. The parameters determined from this treatment by the least squares method are:

$$(44) \qquad \underline{e} = (1.50 \pm 0.09) \times 10^7 (m/l)^{-1} sec^{-1} \text{ at } 820^\circ K$$

$$\underline{g} = (2.34 \pm 0.17) \times 10^7 (m/l)^{-1} sec^{-1} \text{ at } 820^\circ K$$

$$(\underline{e} + \underline{g}) = (3.84 \pm 0.10) \times 10^7 (m/l)^{-1} sec^{-1} \text{ at } 820^\circ K$$

The activation energy of reaction (g) is calculated from the temperature coefficients of $\underline{e}$ and $(\underline{e} + \underline{g})$ as follows. Consider the formulation: $\underline{k} = (\underline{e} + \underline{g})$. The activation energy, $-R \, d \ln(\underline{k})/d(1/T)$, is the weighted average of the individual activation energies:

$$(45) \qquad E_{av} = \frac{\underline{e} E_e + \underline{g} E_g}{(\underline{e} + \underline{g})}$$

Substituting $E_{av} = 6.4$ kcal/mole and the preferred value of E_e, 4.4 kcal/mole, together with the values of $\underline{e}$ and $\underline{g}$ at $820^\circ K$, gives the result: $E_g = 7.7$ kcal/mole.

Above about $1000^\circ K$, investigation of the kinetics of decomposition of NO_3 in the presence of NO_2 is complicated by several factors. First, there is the experimental difficulty of measuring the very fast disappearance of NO_3 at higher temperatures. In the fastest of the present experi-

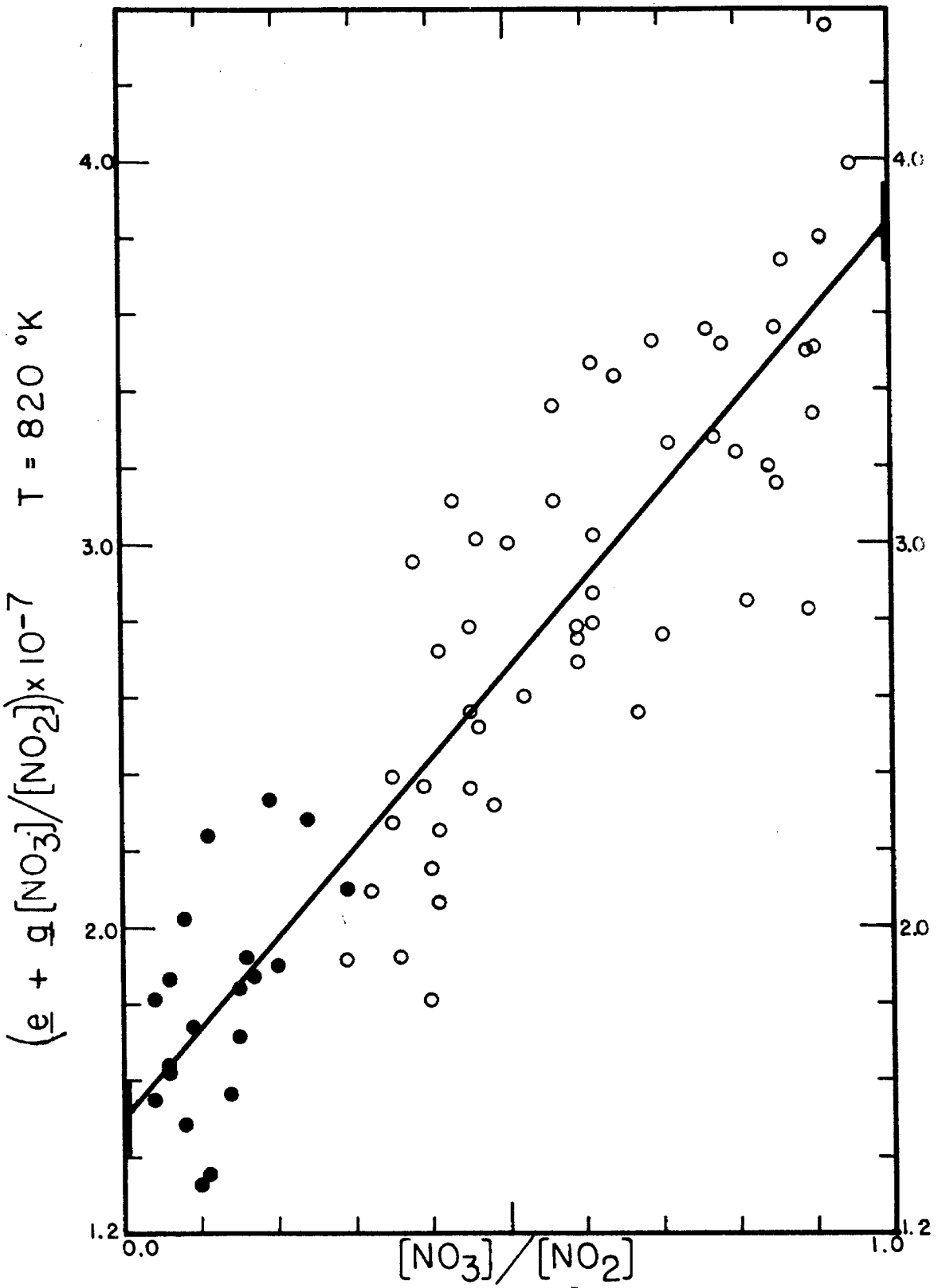

Figure 7. Evaluation of $\underline{e}$ and $\underline{g}$ at 820°K using data from 21 experiments between 750° and 934°K. See equation (44). (○), experiments with pure N_2O_5; (●), experiments with NO_2 added.

ments, the decomposition was followed virtually to completion in about 20 μsec. The minimum resolution time of the apparatus is about two μsec. The bimolecular reactions (e) and (g) can be slowed down by working with lower concentrations of reactants, but the spectrophotometric analysis is then less accurate.

Of more interest than the experimental problems are the complications that may occur in the reaction mechanism itself at higher temperatures. The rate equation that describes the decomposition of NO_3 between 600° and 1000°K involves only two reactions, (e) and (g). As in the low temperature decomposition of N_2O_5, reaction (f) is so fast that its inclusion in the mechanism of decomposition of NO_3 does not affect the rate equation. The concentration of NO remains small so long as NO_3 is still present. The analysis of the decomposition products after NO_3 has disappeared shows that all of the original N_2O_5 has been converted to NO_2. The uncertainty in this analysis is about ten percent. This sets an upper limit of 0.1 on the ratio $[NO]/[NO_2]$ at the end of the decomposition of NO_3. The net rate of production of NO in the system is given by:

$$\frac{d\,[NO]}{d\,\underline{t}} = [NO_3]\left\{\underline{e}\ [NO_2] - \underline{f}\,[NO]\right\} \tag{46}$$

In the steady state approximation, this expression is zero, and:

$$[NO]/[NO_2] = \underline{e}/\underline{f} \ll 1 \tag{47}$$

This relationship and the observed maximum value of $[NO]/[NO_2]$ of 0.1 lead to the conclusion that $\underline{f} \geq 10\ \underline{e}$ throughout the temperature range of these experiments.

Because 0.1 is really not negligible with respect to unity and because a large fraction of the NO_3 is converted directly to NO_2 by reaction (g), the steady state approximation, equation (47), may not be justified. If in fact the net rate of production of NO is not negligible compared to the rate of reaction (e), then the steady state is not reached before the NO_3 is all gone, and $[NO]/[NO_2]$ is always less than $\underline{e}/\underline{f}$. This means that the estimated maximum value of $\underline{e}/\underline{f}$, 0.1, may be too small. An upper limit can be placed on $\underline{e}/\underline{f}$, however. Consideration of the values of $\underline{e}$ and $\underline{g}$ near 1000°K indicates that about half of the NO_3 undergoes reaction (g), so that only the other half can undergo reaction (e). At least 90% conversion of N_2O_5 to NO_2 means that not more than 50% of all the NO produced by reaction (e) remains at the end of the reaction. This fact can be expressed as:

$$(48)\quad \int_{\text{reaction}} \underline{e}\,[NO_2][NO_3] - \underline{f}\,[NO]\,[NO_3]\,d\,\underline{t} \leq 0.5 \int_{\text{reaction}} \underline{e}\,[NO_2][NO_3]\,d\,\underline{t}$$

Rearrangement yields:

$$(49)\quad \underline{f} \int_{\text{reaction}} [NO_2][NO_3] \left\{0.5\ \underline{e}/\underline{f} - [NO]/[NO_2]\right\} d\,\underline{t} \leq 0$$

This says that on the average, $[NO]/[NO_2])_{av} \geq 0.5\ \underline{e}/\underline{f}$. The approach to the steady state from the initial condition

of $[NO]/[NO_2] = 0$ means that:

$$(50) \qquad 0.1 \geqq [NO]/[NO_2])_{final} \geqq [NO]/[NO_2])_{av} \geqq 0.5\ \underline{e}/\underline{f}\ ,$$

from which: $\underline{f} \geqq 5\ \underline{e}$.

The rate equation for the room temperature oxidation of NO by N_2O_5 depends on the fact that $\underline{f}$ is greater than B(M), the rate constant for recombination of NO_2 with NO_3. It will be shown in the next section that near 500°K and at moderate pressures, B(M) is about one hundred times the value of $\underline{e}$ at 1000°K. The conclusion that $\underline{f} \geqq 5\ \underline{e}$ is really a very weak one, and serves only to show that $\underline{f}$ does not have a large negative temperature coefficient.

No other decomposition reactions are fast enough to be of any consequence in the times of the present experiments, at least in those below about 1000°K. Below 1200°K, the bimolecular decomposition of NO_2,

$$(51) \qquad NO_2 + NO_2 \longrightarrow NO + O_2 + NO$$

is insignificant in 10^{-4} m/l NO_2 in times shorter than a milisecond.[21] However, the rate of NO_2 decomposition has been measured at temperatures as low as 1450°K in the shock tube,[22] and the instability of NO_2 must be considered in the decomposition of NO_3 above about 1500°K.

Probably the most serious complication in the kinetics of NO_3 decomposition above 1000°K comes from unimolecular dissociation of NO_3. The present experiments between 1000°

and 1200°K indicate that some reaction with a high activation energy is competing with reactions (e) and (g). In Figure 5 the computed values of ($\underline{e}$ + $\underline{g}$) break sharply upward from the linear plot at the high temperature limit of the investigation. In the two experiments above 1100°K, the deviation is unmistakable. Near 1000°K, the dependence of the initial decomposition rate on the formal N_2O_5 concentration shows slight deviations from the bimolecular rate law, equation (34). The experiments with the largest NO_2 and NO_3 concentrations give lower values of ($\underline{e}$ + $\underline{g}$) than the experiments with one fifth as much N_2O_5 in the initial reaction mixture. The differences in the apparent rate constants are much smaller than the fivefold variation in concentrations, but they are in the direction of less than second power dependence on the formal N_2O_5 concentration. Among the data at lower N_2O_5 concentrations, the highest apparent rate constants are measured in the experiments with the highest argon concentrations. This dependence on total gas concentration is characteristic of a unimolecular decomposition reaction of a simple molecule at low total pressures.

In the experiment at 1216°K, the initial rate of decomposition gives a computed bimolecular rate constant that is four times the value of ($\underline{e}$ + $\underline{g}$) indicated by equation (41). In this one experiment, the value of the apparent unimolecular decomposition rate has been computed. The bimolecular contribution to the initial rate,

$2\ (\underline{e} + g)[NO_2][NO_3]$, has been calculated and subtracted from the observed rate. The remainder of the decomposition rate can be described by:

$$(52) \qquad \frac{-d[NO_3]}{d\ \underline{t}} = 2.3 \times 10^4 [NO_3]$$

or

$$(53) \qquad \frac{-d[NO_3]}{d\ \underline{t}} = 2.5 \times 10^6 [NO_3][\text{argon}]$$

Time is in seconds; concentrations are in moles per liter. The interpretation of these rate constants is not clear. It is clear that they describe the rate of initiation of some process by which NO_3 is converted to NO_2 without the production of appreciable quantities of NO. In the experiment at 1216°K, this path is the dominant one, and the analysis indicates virtually complete conversion of N_2O_5 to NO_2.

The most reasonable dissociation of NO_3 is:

$$(54) \qquad NO_3 \longrightarrow NO_2 + O \qquad \triangle E = +\ 50 \text{ kcal/mole.}$$

The rates of the many possible secondary reactions of oxygen atoms in this system are not known, and the rate equation might be very complicated indeed. The order of magnitude of the rate of decomposition of NO_3 initiated by unimolecular dissociation of NO_3 is not inconsistent with the known

energy of reaction (54) and simple unimolecular reaction rate theory. If one supposes that the rate of recombination of oxygen atoms with NO_2 (the reverse of reaction (54)) is small and that the principal reactions of oxygen atoms are:

(55) $NO_3 + O \longrightarrow NO_2 + O_2$

and

(56) $NO_2 + O \longrightarrow NO + O_2$

followed rapidly by reaction (f), then the total rate of disappearance of NO_3 by this path is twice the rate of reaction (54). The rate given by equation (53) can be approximately computed by the expression:[23]

$$(57) \qquad \frac{-d\,[NO_3]}{d\,\underline{t}} = 2\,Z\,(E/RT)^{(\underline{s}-1)}(\underline{s}-1)!^{-1}\,e^{-E/RT}[\text{argon}][NO_3]$$

when Z is the kinetic theory collision number, E is taken as 50 kcal/mole, and $\underline{s}$ is taken as 5.

Another possible reaction is:

(58) $NO_3 \longrightarrow O_2 + NO \qquad \triangle E = +4$ kcal/mole,

which may proceed unimolecularly through isomerization of NO_3 to the much less stable peroxy compound,[24] O - O - N = O. This process is stoichiometrically equivalent to reaction (e), but kinetically, it is very different. Its activation energy may be as low as 45 kcal/mole. If

reaction (58), and not reaction (54), is in fact the important one, then it may be possible to measure the rate of reaction (f) in experiments with low concentrations of NO_3 and NO_2 at temperatures between 1100° and 1300°K.

The specific effect of molecular oxygen in catalyzing reaction (54) through the intermediate production of ozone can be examined. The activation energy of the bimolecular reaction:

(59) $$NO_3 + O_2 \longrightarrow NO_2 + O_3$$

can be estimated at high temperatures from the heat of the reaction and the known activation energy of the reverse reaction near room temperature.[25] The sum of these energies is 32 kcal/mole. Under conditions where reaction (59) is fast enough to be significant in the decomposition of NO_3, the mean life of ozone molecules is very short indeed.

5. Kinetics and Equilibrium in the Dissociation of N_2O_5.

At temperatures between 450° and 550°K, shock wave experiments in one percent mixtures of N_2O_5 and argon give photoelectric records like those in figure 8. These differ from the experiments at higher temperatures in two respects. First, the fast increase in absorption after the passage of the shock wave is slow enough that its rate can be measured. Second, the magnitude of the initial rise, which determines the maximum in the NO_3 absorption record at 650 mμ (figure 8a), is less than that calculated for complete dissociation of the N_2O_5. The decrease after the maximum and the corresponding slow increase in absorption at 366 mμ are generally too slow for accurate measurement. They are also so slow that they do not interfere seriously with measurement and interpretation of the initial increases.

From the initial rates of appearance of NO_2 and NO_3 after the passage of the shock wave, the rate constants for the dissociation of N_2O_5, A(M), have been obtained. A(M) has been studied as a function of argon concentration near 520°K, and as a function of temperature near $[A] = 0.0076$ m/l. Equilibrium constants for the reaction

(60) $$N_2O_5 \rightleftharpoons NO_2 + NO_3$$

(61) $$K_c = \frac{[NO_2][NO_3]}{[N_2O_5]} \text{ (m/l)} = \frac{A(M)}{B(M)}$$

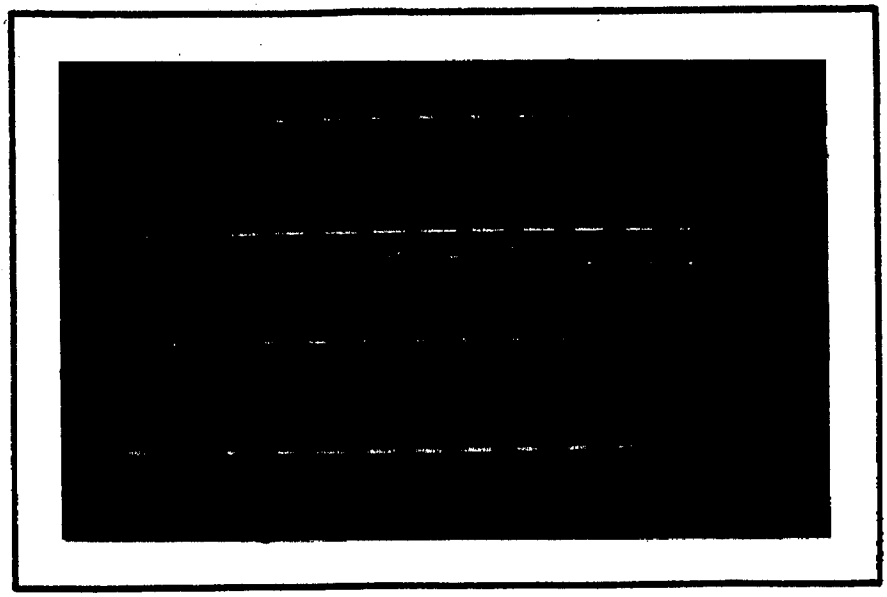

Figure 8a. Photoelectric record at $\lambda = 650$ mμ showing slow, incomplete dissociation of N_2O_5 at 480°K. In about 100 μsec after the shock, the absorption rises to a maximum and then decreases slowly as NO_3 decomposes. In this mixture, $\phi = 0.36$ %, and $T_2 = 483^\circ$ before dissociation, 475°K afterward.

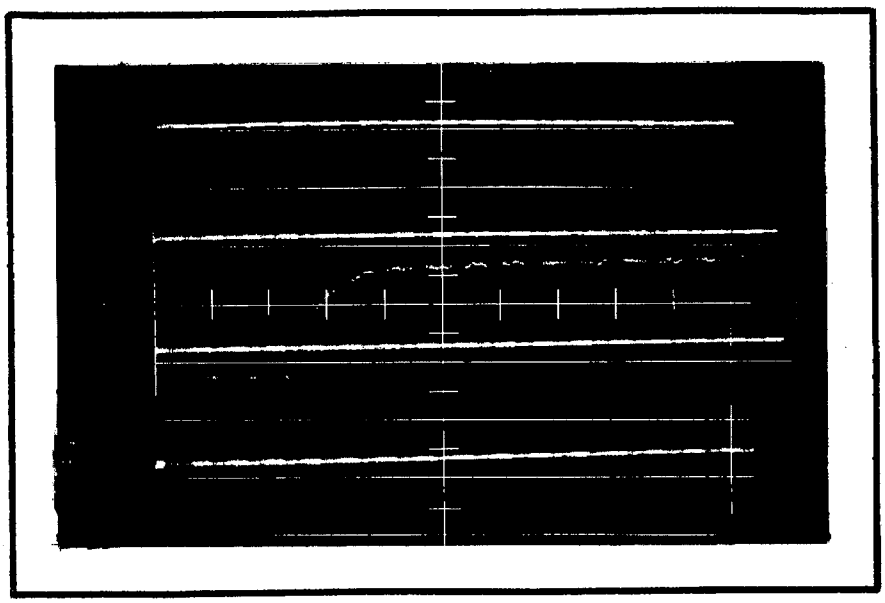

Figure 8b. Photoelectric record at $\lambda = 366$ mμ in the same experiment as that shown above. After the fast rise, there is a slow further increase in absorption as NO_3 is converted to NO_2. In this experiment, $[N_2O_5]_{formal} = 3.2 \times 10^{-5}$ m/l and $[A] = 8.8 \times 10^{-3}$ m/l. At equilibrium, $\alpha = 0.79$.

have been calculated between 450° and 550°K from the state of near equilibrium that obtains at the time of the maximum in the 650 mμ absorption record. All these measurements depend on values of the extinction coefficients of NO_2 and NO_3 extrapolated from the work at higher temperatures.

The reactions whose rates are important are:

(62) $$N_2O_5 \xrightarrow{A(M)} NO_2 + NO_3$$

(63) $$NO_2 + NO_3 \xrightarrow{B(M)} N_2O_5$$

(64) $$NO_2 + NO_3 \xrightarrow{e} NO + O_2 + NO_2$$

(65) $$NO_3 + NO \xrightarrow{f} 2NO_2$$

(66) $$NO_3 + NO_3 \xrightarrow{g} 2NO_2 + O_2$$

The concentration of N_2O_5 is given in the shock wave situation in terms of the degree of dissociation, α , by:

(67) $$[N_2O_5] = C_0 \phi \Delta (1 - \alpha)$$

Equations (24) and (25) can be extended to describe the NO_2 and NO_3 concentrations for the case when α is less than unity.

(68) $[NO_2] = C_o \phi \Delta (\alpha + \beta)$

(69) $[NO_3] = C_o \phi \Delta (\alpha - \beta)$

For completeness:

(70) $[O_2] = \frac{1}{2} C_o \phi \beta$

(71) $[A] = C_o \Delta (1 - \phi)$

Early in the dissociation reaction, β is substantially zero, and $[NO_2] = [NO_3] = C_o \phi \Delta \alpha$. This is the portion of the experiments in which the rate of dissociation of N_2O_5 is studied. The optical density, by equation (23), is:

(72) $D = C_o \phi \Delta L \alpha (\epsilon_{NO_2} + \epsilon_{NO_3})$

Differentiation of (72) with respect to time and substitution of the time transformation, equation (37), yields:

(73)

$$\frac{d D}{d \tau} = C_o \phi L (\epsilon_{NO_2} + \epsilon_{NO_3}) \left\{ 1 + \left(\frac{d \ln \Delta}{d \alpha} + \frac{d \ln \epsilon}{d \alpha} \right) \right\} \frac{d \alpha}{d \underline{t}}$$

Partial differentiation of equation (67) at constant volume gives the rate equation:

(74)

$$(-d[N_2O_5]/d\,\underline{t})_v = \text{Rate} = C_o \phi \Delta\, d\alpha/d\,\underline{t}$$

From the mechanism, equations (62) and (63), the rate equation is:

(75)

$$(-d[N_2O_5]/d\,\underline{t})_v = \text{Rate} = A(M)[N_2O_5] - B(M)[NO_2][NO_3]$$

$$= A(M)\, C_o \phi \Delta(1-\alpha) - B(M)\,(C_o \phi \Delta \alpha)^2$$

Combination of equations (73), (74), and (75) yields a useful expression for A(M) at $\alpha = 0$.

(76)

$$A(M) = \frac{(d\,D/d\,\tau)_o}{C_o \phi L\, \Delta_o^2\, (\epsilon_{NO_2} + \epsilon_{NO_3})} \text{ sec}^{-1}$$

A(M) is the first order dissociation rate constant, which depends on the nature and amount of each of the gases present. Properly, M is the weighted sum of the concentrations of all the gases in the system. The weighting factor for each gas is its efficiency, relative to some standard gas, in exchanging energy with the internal motions of

N_2O_5. In this work, the standard gas is argon, and for the present considerations, the differences between M and $[A]+[N_2O_5] \approx 1.01\,[A]$ are ignored. These experiments have been performed in a region of argon concentration where A(M) is nearly linear in M. Accordingly, it is of interest to compute the ratio of A(M) to the total gas concentration, $C_o\Delta$. Calling this ratio A', the apparent second order dissociation rate constant, we have:

$$(77) \qquad A' = \frac{(d\,D/d\,\tau)_o}{c_o^2\,\phi L \Delta_o^3 (\epsilon_{NO_2} + \epsilon_{NO_3})} \ (m/l)^{-1} sec^{-1}$$

A(M) and A' have been calculated from the initial slopes of smoothed plots of D versus τ in twenty experiments. The results are recorded in table 4. The values of the logarithm of A' at M = 0.0076 m/l are plotted against reciprocal temperature in figure 9. The line fitted to these points by the least squares method is:

$$(78) \qquad \log_{10}(A'_{0.0076\ m/l}) = -(3607 \pm 150)/T + 13.681$$

The activation energy given by this equation is 16.5 ± 0.7 kcal/mole.

Figure 9 also contains measured values of A' near 0.003 m/l. It can be seen that these experiments yield values of A' that are larger than the average values at 0.0076 m/l. This trend is to be expected, since at any

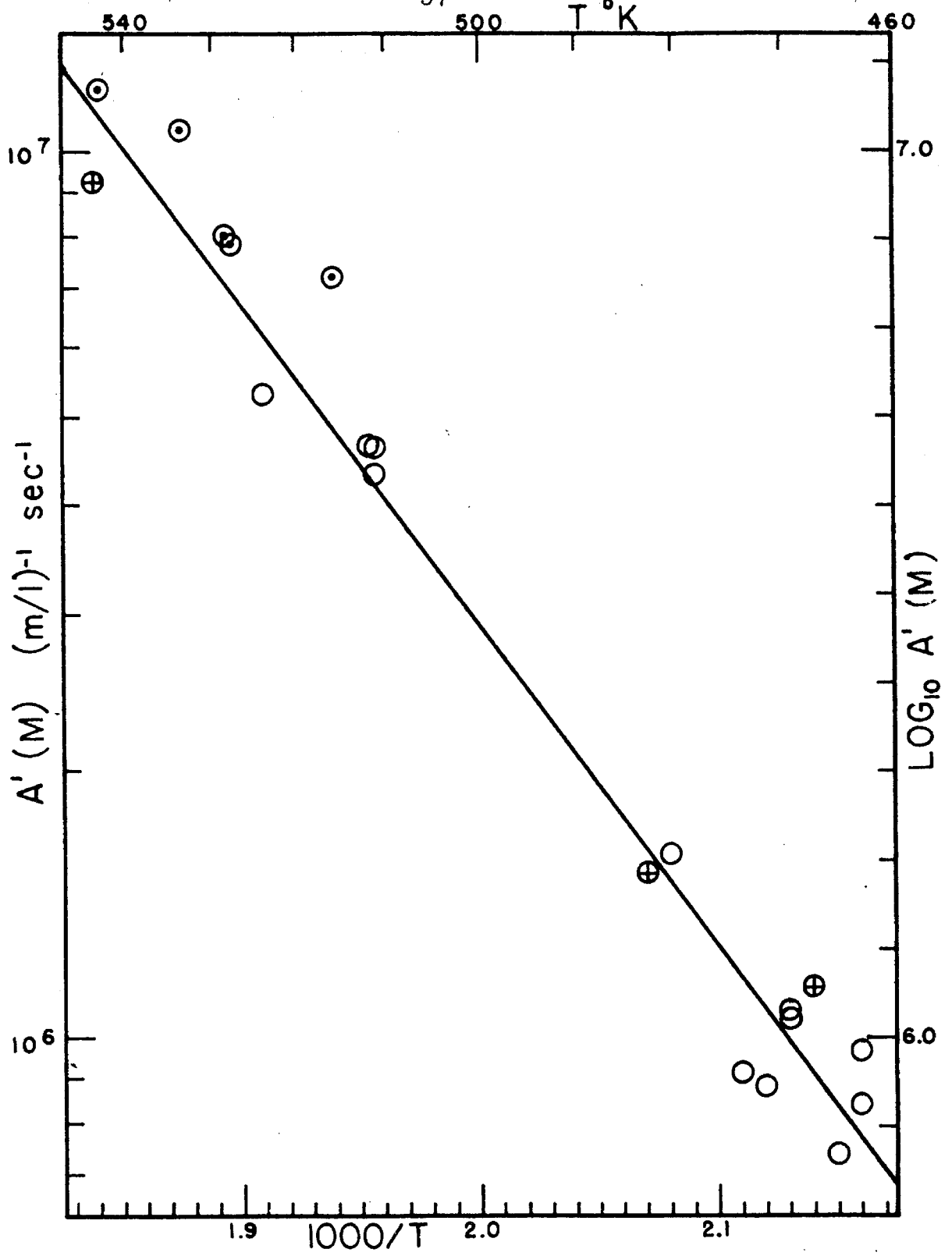

Figure 9. Dissociation rate constants of N_2O_5 in argon near the low pressure limit. (○), [A] = 0.0076 m/l; line, equation (78); (⊙), [A] = 0.003 m/l; (⊕), [A] = 0.009 m/l.

finite pressure, $A' \leq A'_0$, the low pressure limit of A(M)/M. The average deviation of the 0.003 m/l points from the line, equation (78), is 22 $\pm$ 14%. Crude extrapolation to M = 0 indicates that A'_0 is about 30% greater than $A'_{0.0076\ m/l}$, as given by equation (78), within the temperature range of these experiments. On this basis, A'_0 at 500°K is estimated as $3.84 \times 10^6 (m/l)^{-1} sec^{-1}$.

These data include measurements of photoelectric records at 366 mμ and at 650 mμ. The data at 366 mμ have consistently given values of $D/(\epsilon_{NO_2} + \epsilon_{NO_3})$ at particular values of τ that are from zero to fifteen percent higher than those given by the 650 mμ data. Some excess absorption at 366 mμ is to be expected, since as β becomes significant, $[NO_2] > [NO_3]$. However, the values of β indicated in several of the experiments are somewhat too large too early in the reaction. It is not known which of the measurements are more reliable, so the averages have been used. Two sources of error are known which can account for this type of discrepancy. Extrapolated extinction coefficient data are used at both wave lengths, and either of the extrapolations may be wrong by a few percent. The other possibility is that more than the estimated one percent of the N_2O_5 in the unshocked mixture is decomposed. If this were so, the compression of the excess NO_2 would add a noticeable amount to the absorption at 366 mμ. This would produce an erroneously high ratio of the absorption at 366 mμ to that at 650 mμ,

especially at the beginning of the dissociation. It is not possible to decide between these explanations from the data.

As the dissociation of N_2O_5 becomes appreciable, the recombination reaction, (63), and the decomposition reactions, (64) through (66), become important. The expression for zero net formation of NO_3, derived from the known reactions, can be written in a constant volume situation as:

$$(79)\quad \frac{[NO_2]\ [NO_3]}{[N_2O_5]} = \frac{K_c}{1 + \dfrac{2\,(\underline{e} + \underline{g}\,[NO_3]/[NO_2])}{B(M)}}$$

This equation is formally equivalent to the steady state approximation which determines the small NO_3 concentration in the room temperature first order decomposition of N_2O_5. It is invoked here not as an approximation but as the condition for the observed maximum in the NO_3 concentration. It is adapted to describe the condition of maximum absorption at 650 mμ through equation (23). This introduces the parasitic effects of the small amount of absorption by NO_2 and the change in density with reaction, and the result is:

(80)

$$\frac{[NO_2][NO_3]}{[N_2O_5]} = \frac{K_c}{1 + \frac{2(\underline{e}+\underline{g}\frac{[NO_3]}{[NO_2]})(1 - \frac{\epsilon_{NO_2}}{\epsilon_{NO_3}} - \frac{D_{total}}{D_{NO_3}}\frac{d\ \ln\Delta}{d\beta})}{B(M)\ \ (1 + \frac{\epsilon_{NO_2}}{\epsilon_{NO_3}} + \frac{D_{total}}{D_{NO_3}}\frac{d\ \ln\Delta}{d\alpha})}}$$

The data from the pairs of photoelectric records have been analyzed for the values of the NO_2, NO_3, and N_2O_5 concentrations at the time of the maximum in the absorption at 650 mμ. The equilibrium constants, K_c, have been calculated in those experiments where $\alpha < 0.9$ at that time. The results are recorded in table 5 together with the measured values of α and β and other essential data. The range of temperature of these determinations has been extended from 520° to 550°K by experiments in which excess NO_2 was added to suppress the extent of dissociation. Figure 10 is a plot of $\log_{10}K_c$ versus reciprocal temperature. It shows rather large scatter in the results at the higher temperatures. The most reliable data have been obtained near 460°K, where 5 x 10^{-5}m/l N_2O_5 is only about half dissociated at equilibrium. The average value of K_c at 460°K is 2.75 x 10^{-5} m/l. The best linear relationship, shown in figure 10, is:

(81) $$\log_{10}(K_c) = -(4383 \pm 232)/T + 4.967$$

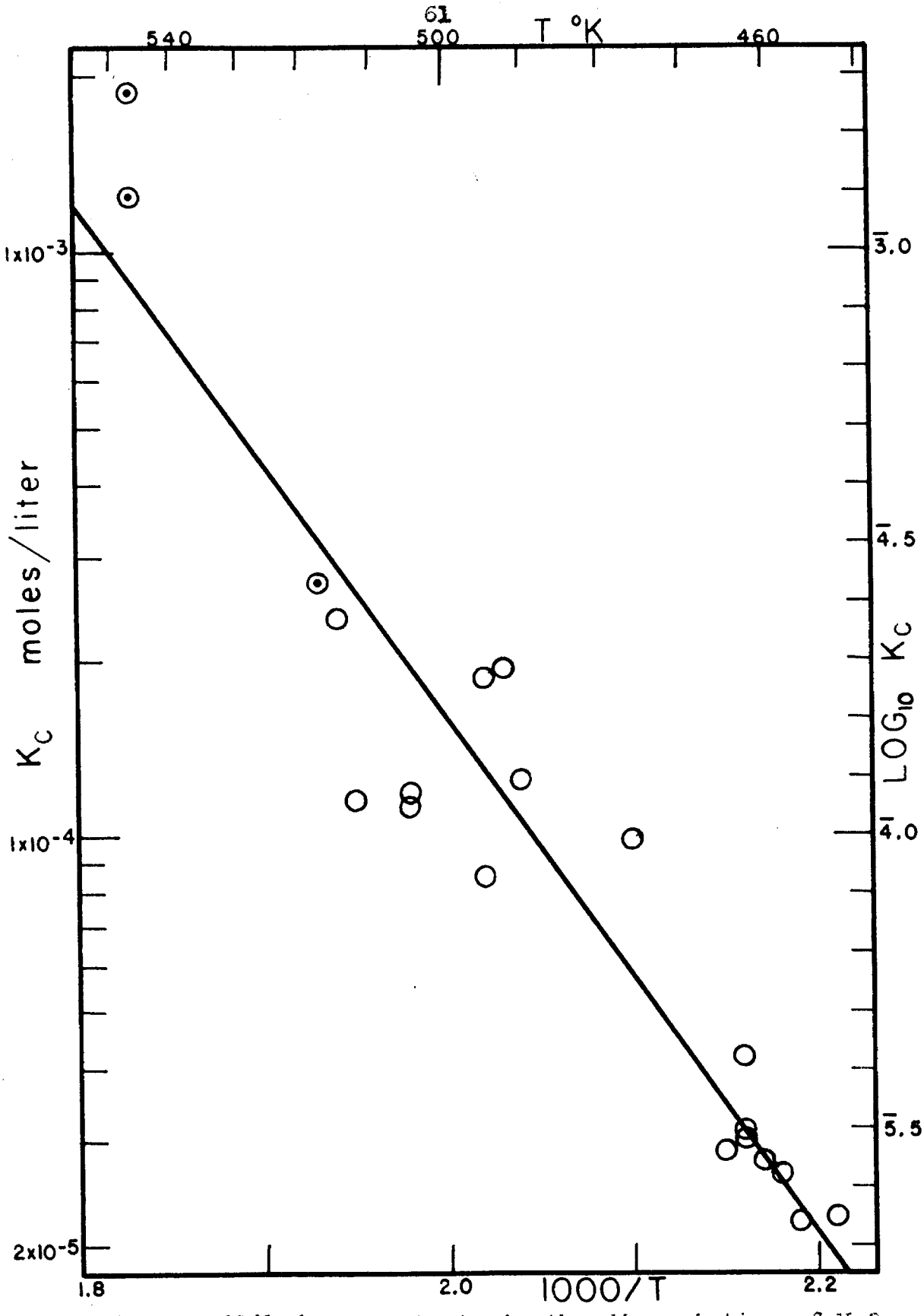

Figure 10. Equilibrium constants in the dissociation of N_2O_5. (○), in pure N_2O_5; (⊙), with NO_2 added; line, equation (81).

The energy change, $\triangle E$, for the dissociation of N_2O_5 is calculated to be 20.1 ± 1.1 kcal/mole. The fact that this reasonable temperature coefficient is measured indicates that there is no great error in the extrapolated extinction coefficients and other data used in interpreting the results. For it can be seen that a small error in the extinction coefficient of NO_2 or NO_3 produces a large percentage error in the calculated value of the N_2O_5 concentration in the experiments above $500^{\circ}K$, where the degree of dissociation is large.

In the calculation of K_c by equation (80), the cumbersome correction term is negligibly small under the conditions of high inert gas concentration used in these experiments. This does not imply that the extent of NO_3 decomposition, β, is negligible in the time before the NO_3 concentration reaches its maximum value, but merely that the rate of turnover in the NO_3 population is high at the maximum and thereafter.

6. Correlation with Room Temperature Results.

The state of our knowledge of the kinetics of gas phase reactions of the nitrate radical was reviewed in 1951 by Johnston.[1] In the high temperature decomposition of N_2O_5 we have been concerned with the elementary processes of that paper. These are:

(82a) $N_2O_5 + M \xrightarrow{a_i} N_2O_5^*_i + M$

(82b) $N_2O_5^*_i + M \xrightarrow{b_i} N_2O_5 + M$

(82c) $N_2O_5^*_i \xrightarrow{c_i} NO_2 + NO_3$

(82d) $NO_2 + NO_3 \xrightarrow{d_i} N_2O_5^*_i$

(82e) $NO_2 + NO_3 \xrightarrow{e} NO + O_2 + NO_2$

(82f) $NO_3 + NO \xrightarrow{f} 2NO_2$

(82g) $NO_3 + NO_3 \xrightarrow{g} 2NO_2 + O_2$

(82h) $NO_2 + O_3 \xrightarrow{h} NO_3 + O_2$

This formulation of the kinetics of dissociation and recombination of N_2O_5 considers the rates of dissociation and recombination of the critically excited states of N_2O_5 individually in steps (c) and (d). Steps (a) and (b) include the dependence of the excitation and deexcitation rates of each of the activated states, i, on the nature and concentration of specific molecules as M. The special cases that are of particular interest involve limiting concentration conditions. These are:

$$(83a) \qquad \lim_{[M]\to 0} A(M)/[M] = \sum_i \underline{a}_i = A'_0(M)$$

$$(83b) \qquad \lim_{[M]\to \infty} A(M) = \sum_i \underline{a}_i \underline{c}_i / \underline{b}_i = A_\infty$$

$$(83c) \qquad \lim_{[M]\to \infty} B(M) = \sum_i \underline{d}_i = B_\infty$$

Measurements of the rate of oxidation of NO by N_2O_5 have given considerable information on the unimolecular dissociation constants, A(M).[3] The best data near the low pressure limit, $A'_0(M)$, are in a temperature range about 50^oC, while the high pressure data have been measured at lower temperatures. Additional data at the low pressure limit have been derived from experiments on the decomposition of pure N_2O_5 at such low pressures (10^{-3}mm) that equilibrium in the dissociation reaction is not maintained.[26] Selected data from reference (1) and other

recent sources are:

Quantity	T °K	Value $(m/l)^{-1}sec^{-1}$	E_{act} kcal/mole	System	Source
$A'_o(N_2O_5)$	323.7	2250.	-	N_2O_5-NO	(3a, 3b)
$A'_o(N_2O_5)$	323.7	3500.	$18.3 \pm 2.$	N_2O_5, M=0	(26) (27)
$A'_o(N_2O_5+NO)$	323.3	$1130. \pm 30.$	19.3 ± 0.6	N_2O_5-NO	(3c)
A'_o(argon)	323.7	$304. \pm 24.$	-	N_2O_5-NO	(3a, 3b)
A'(argon) 0.0076 m/l	500.	2.9×10^6	16.5 ± 0.7	N_2O_5	shock waves
A'_o(argon)	500.	3.8×10^6		extra-polated	shock waves
A_∞	300.	0.29 sec^{-1}	$21. \pm 2.$	N_2O_5-NO	(3d)

One basis for comparison of the results near 500°K obtained in the present investigation with those near room temperature is the Rice-Ramsperger-Kassel formulation of the unimolecular dissociation rate.[28] This theory allows definite values of A(M) to be calculated at any value of [M] and T by specifying the form of $\underline{a}_i$, $\underline{b}_i$, and $\underline{c}_i$ in terms of four parameters which may be adjusted, within certain limits, to fit the available experimental data. The model of the reacting molecule is a system of $\underline{s}$ lightly coupled harmonic oscillators all having the frequency $\nu = E_c/h\underline{m}$. The frequency factor, J, measures the rate at which energy is exchanged among the oscillators. Dissociation occurs when the critical energy, E_c, ($\underline{m}$ quanta) is present in a particular one of the oscillators. The theory has the important qualitative feature that the specific dissociation

rates of the excited states, $\underline{c}_i$, increase with the energy, $\underline{i}h\nu$, in excess of the critical energy. This is in agreement with the usual observation that the activation energy is less at low pressures than at the high pressure limit. The great simplifying approximation is that the deactivation rate constants, $\underline{b}_{i,M}$, are independent of the degree of activation, $\underline{i}$. In the simplest RRK formulas, $\underline{b}$ is equated to the kinetic theory collision number. The collision number contains some dependence on the nature of M, but additional dependence of $\underline{b}$ on M, independent of $\underline{i}$, can be easily incorporated as a slight refinement. The frequency factor and the critical energy alone determine the high pressure limit.

$$(84) \qquad A_\infty = J\ e^{-E_c/RT}\ \text{sec}^{-1}$$

In these terms,

$$(85a) \qquad \underline{a}_i = \underline{b}\begin{pmatrix} \underline{m}+\underline{i}+\underline{s}-1 \\ \underline{s}-1 \end{pmatrix}(1 - e^{-h\nu/kT})^{\underline{s}}\ e^{-(\underline{m}+\underline{i})h\nu/kT}$$

$$(85b) \qquad \underline{b} = \underline{f}_M\ (8\pi kT/\mu)^{\frac{1}{2}}\ \sigma^2\ \text{Nx}10^{-3}(\text{m/l})^{-1}\text{sec}^{-1}$$

$$(85c) \qquad \underline{c}_i = J\begin{pmatrix} \underline{i}+\underline{s}-1 \\ \underline{s}-1 \end{pmatrix}\begin{pmatrix} \underline{m}+\underline{i}+\underline{s}-1 \\ \underline{s}-1 \end{pmatrix}^{-1} \text{sec}^{-1}$$

and

$$(86) \qquad A(M) = \sum_i \frac{a_i c_i [M]}{b[M] + c_i}$$

The calculations made here have used the fixed values of J and E_c indicated by the high pressure limiting results, $A_\infty = 6.85 \times 10^{15} e^{-21.0/RT}$, in spite of the uncertainty in these values. Various values of s and m have been selected to fit the low pressure limit, $A_0'(N_2O_5) = 2250$ at 323.7°K. The maximum allowed value is s is taken as fifteen, the number of vibrational modes of the N_2O_5 molecule. The minimum value of s, seven, is the one that is needed to fit $A_0'(N_2O_5)$ in the classical limit of the RRK summation as $\gamma \to 0$. Though it is known that the collisional excitation efficiency, f_M is substantially less than unity for several monatomic and diatomic gases,[3a] the approximation $f_{N_2O_5} \approx 1$ is believed to be more nearly correct. For definiteness, it has been used, and f_{argon} is taken as 0.154,[3a] independent of i and of temperature. In performing the computations of the low pressure limits, the approximate summation formulas, equations (12) and (13) of reference (3c), have been used. The computation for 0.0076 m/l argon used similar formulas for all but the first two terms of the sum (86), since these are the only ones seriously affected by that value of [M]. The collision radii quoted in reference (3a) have been adopted.

At 323.7°K, with E_c = 21.0 kcal/mole, we have:

s	m	$\tilde{\nu}$ cm^{-1}	$A'_o(N_2O_5)$ (m/l)$^{-1}$sec^{-1}	E_{act} kcal/mole
15	10	735	1950	20.1
12	14	525	2540	19.5
10	20	369	2550	18.9
9	26	282	2270	18.6
7	∞	0	3300	17.5
Experiment			2250	19.

At 500°K, in argon, the same parameters give:

s	A'_o(argon) (m/l)$^{-1}$sec^{-1}	E_{act} kcal/mole	$A'_{0.007\text{6}}/A'_o$
15	10.6	17.3	
10	7.5	16.3	0.83
9	5.9	16.1	
7	4.6	15.5	
Experiment	3.8 $\pm$ 0.7	$\leq$16.5	0.77 $\pm$ 0.13

Consideration of the values of the rate constants and the observed local activation energies leads to the choice of about ten oscillators with frequencies near 10^{13} sec^{-1} as the best overall description. That was the conclusion reached over the smaller temperature range from the measurements in N_2O_5 plus NO mixtures.[3c] On this basis, the

observed rate constant at 500°K agrees within a factor of two with that calculated solely on the basis of measurements near room temperature. The overall change is a factor of 10^4. In view of the approximate nature of the theory and the uncertainty of the value of the critical energy, this agreement is satisfactory. Closer examination shows that all the values calculated at 500°K are higher than the measured value, and that there is really little to choose between large $\underline{s}$ with large vibrational quanta and small $\underline{s}$ and nearly classical behavior. Also, small changes in the critical energy do not greatly affect the predicted constants at 500° when agreement with those at 324° is maintained. It is not possible to say how much of this inadequacy of the theory lies in the variation of $\underline{f}_{i,M}$ with $\underline{i}$ and M and how much depends on other things.

It is also of interest to compare the room temperature results with the high temperature shock wave results by the simple Arrhenius equation. Comparison of A'_o(argon) between 323.7° and 500°K gives an average activation energy of 17.3 kcal/mole. This value is intermediate between the two measured local activation energies. Direct comparison of the values of A(M) in 0.0076 m/l argon between 300° and 500°K is also possible. The computed average activation energy is 18.6 kcal/mole. The value of A(M) at 300°K used for this comparison was not actually measured in argon, but in other gases.[3d] However, at 0.0076 m/l at 300°K (144 mm), A(M) is closer to its high pressure limit than

to its low pressure limit, and the differences between different inert gases are small. At 500°K, A' at 0.0076 m/l is a much greater fraction of A'_0 than at room temperature, and the distinction between gases is important.

The present experiments near 500°K definitely show that the activation energy of the dissociation of N_2O_5 near the low pressure limit decreases with temperature. They also show that the transition between low pressure and high pressure behavior occurs at higher concentrations as the temperature is increased. Both these facts indicate that the specific rate constants, $\underline{c}_i$, increase with the energy of the molecule. The fact that the low pressure activation energy is less than the high pressure activation energy at 300°K is also a consequence of this property of the $\underline{c}_i$'s.[3d] The present experiments are over too small a range of total pressure and N_2O_5/argon ratio to contribute significantly to our understanding of the activation and deactivation processes. Nor do they reduce the existing uncertainty about the activation energy of the high pressure limiting rate. However, they do confirm the interpretation of the rate measurements made by indirect methods at room temperature by showing that the unimolecular rate of production of NO_3 can be observed directly at suitably high temperatures.

Rate measurements near 300°K on the decomposition of N_2O_5 and on systems containing ozone and N_2O_5 have been combined to yield relationships among the constants

$\underline{e}$, $\underline{g}$, K, and B_∞. In these systems, the NO_3 concentration is determined by the unknown equilibrium constant, K, so that none of the rate constants can be deduced directly. There are enough relationships, however, that knowledge of one of the constants, or of the NO_3 concentration in certain experiments, would permit evaluation of the other constants. These relationships, which have been taken from table II of reference (1), are:

Quantity	Value at 300°K	E_{act} kcal/mole
$\underline{e}K_c$	4.1×10^{-5} sec^{-1}	24.7 ± 0.1
$B_\infty/\underline{e}$	$7. \times 10^{3}$	-4. ± 2.
$\underline{g}^{\frac{1}{2}}K_c$	$1.9 \times 10^{-9}(m/l)^{\frac{1}{2}}sec^{-\frac{1}{2}}$	24. ± 2.

From measurements of the temperature coefficient of the absorption by NO_3 in ozone and N_2O_5 mixtures, the activation energy of reaction (g) has been deduced.[8] This calculation is based on the assumption that the extinction coefficients are independent of temperature and of whatever pressure differences existed. This allows computation of all the energies in the set above, but still none of the constants. The results, taken from table III of reference (1), are:

Quantity	E_{act} kcal/mole	Temperature Coefficients Combined
g	8.1 ± 2.	NO_3 and O_3 decomposition rate
K_c	20. ± 3.	g, h, O_3 decomposition rate
e	5. ± 3.	K_c, N_2O_5 decomposition rate
B_∞	1. ± 4.	K_c, A_∞

This investigation includes direct measurements of values of e, g, and K_c, together with values of their temperature coefficients. Of course, the measurements reported here are at temperatures much higher than the room temperature range. Still good correlation is possible with the two independent sets of activation energies. The raw results of the high temperature work are:

$$e = 2.26 \times 10^8 \, e^{-4.42/RT} \, (m/l)^{-1} sec^{-1} \text{ near } 820^\circ K$$

$$g = 2.63 \times 10^9 \, e^{-7.70/RT} \, (m/l)^{-1} sec^{-1} \text{ near } 820^\circ K$$

$$K_c = 9.26 \times 10^4 \, e^{-20.1/RT} \, (m/l) \quad \text{near } 500^\circ K.$$

R is expressed in kcal/mole degree. The uncertainty in each of these energies is at least one kcal/mole. All of them lie well within the limits set in the room temperature work.

It was pointed out in the concluding remarks of reference (1) that K is a more important and interesting quantity than e or g. Not only is it the most important quantity in this system, it is also the key to other equilibrium controlled reactions involving N_2O_5 and

NO_3.[29][30] From the above tables, it can be seen that the most precisely known quantities are the product, $\underline{e}K$, and the associated sum $(E_e + E_K)$. These come directly from the first order decomposition rate of N_2O_5. (See equation (12).) The evaluation of E_K from E_g involves three other quantities, and introduces some 3. kcal/mole uncertainty, so that the great accuracy of $(E_e + E_K)$ is lost before further use can be made of it. A direct approach to E_K has been recommended.[1]

From the results of the present research, four additional estimates of E_K can be made. E_e and E_g can be adjusted from 820° to 300°K by simple collision theory. Consideration of the factor $T^{\frac{1}{2}}$ in the collision number yields the formula $E_{act} = E_o + \frac{1}{2}RT$. The adjusted values are $E_e = 3.9 \pm 1.$ kcal/mole and $E_g = 7.2 \pm 1.$ kcal/mole at 300°K. The difference between the heat capacities of N_2O_5 and its dissociation products has been estimated in order to adjust the observed value of E_K from 500° to 300°K. Another approach which is probably as accurate as the temperature coefficients measured here is the estimation of the entropy change in the dissociation of N_2O_5. The estimated value $\Delta S^o = 35.5$ e.u. at 300°K has been combined with the estimated small heat capacity difference, $\Delta C_p = -2.$ cal/mole degree to interpret the value of K measured at 460°K. The basis of these estimates is presented in the next section. The five estimates of E_K are assembled below:

E_K kcal/mole	Source
20. ± 3.	reference (1)
20.8 ± 1.	$E_{e(820^\circ)}$, $(E_e + E_K)_{(300^\circ)}$
20.4 ± 2.5	$E_{g(820^\circ)}$, $(\frac{1}{2}E_g + E_K)_{(300^\circ)}$
20.9 ± 1.	$E_{K(500^\circ)}$, ΔC_p
21.9 ± 1.	$K_{(460^\circ)}$, $\Delta S^\circ_{(300^\circ)}$, ΔC_p

The average of these values is taken as 21.0 kcal/mole. The value of $K_c(300^\circ K) = 1.65 \times 10^{-10}$(m/l) is computed from this energy and $\Delta S^\circ(300^\circ) = 33.6$ e.u., which is consistent with the measured value of K at 460°. The two chains of calculations between 300° and 460°K are indicated schematically below.

	Assuming $\Delta S^\circ_{(300^\circ)}$ and $\Delta F^\circ_{(460^\circ)}$		Assuming $\Delta E^\circ_{(300^\circ)}$ and $\Delta F^\circ_{(460^\circ)}$	
T °K	300	460	300	460
ΔS° cal/mole °K	35.5	34.6	33.6	32.7
ΔH° kcal/mole	22.5	22.2	21.6	21.3
ΔE° kcal/mole	21.9	21.3	21.0	
ΔF° kcal/mole	11.9	6.3	11.5	6.3

Examination of these numbers indicates that the standard free energy of dissociation of N_2O_5 at 300°K is probably known to within 0.6 kcal. Accordingly, K is known to within

a factor of three. The other rate constants and activation energies are now evaluated.

Quantity	Value at 300°K	Pre-exponential	Energy kcal/mole
K_c	1.65×10^{-10} m/l	$\Delta S^\circ = 33.6$ e.u.	$21.0 \pm 1.$
$\underline{e}$	2.5×10^{5} $(m/l)^{-1}sec^{-1}$	1.3×10^{8}	$3.7 \pm 1.$
B_∞	1.7×10^{9} $(m/l)^{-1}sec^{-1}$	1.9×10^{9}	$0.0 \pm 2.$
$\underline{g}$	1.3×10^{4} $(m/l)^{-1}sec^{-1}$	3.1×10^{9}	$6.0 \pm 2.$

With the values of $\underline{e}$ and $\underline{g}$ obtained in this way, one can now compute the Arrhenius activation energies E_e and E_g averaged between 300° and 820°K and compare them with the measured local activation energies.

	Local 300°		Local 820°		Average
Reaction	$\log_{10}\underline{k}$	Energy	$\log_{10}\underline{k}$	Energy	Energy
(e)	5.40	3.7 kcal	7.18	4.4 kcal	3.9 kcal
(g)	4.12	6.0 kcal	7.37	7.7 kcal	7.1 kcal

This apparent agreement is probably better than the individual data justify.

One conclusion that can be drawn is that the collision and steric factor in reaction (g) is comparable to the recombination rate, $\sum_i \underline{d}_i = B_\infty$, and is an order of magnitude greater than the corresponding property of reaction (e).

Another approximate check on the values of K_c and $\underline{g}$ at 300°K can be obtained from the optical densities due to NO_3 absorption in the N_2O_5 catalysed decomposition of ozone. Sprenger[8] has reported the product $\epsilon_{NO_3}[NO_3]$ at the

wave length of maximum absorption, 660-664 mμ, together with the other conditions of his experiments. Using the values of the constants proposed here, one can calculate the appropriate extinction coefficient as $1200(m/l)^{-1}cm^{-1}$ near 300°K. The crude estimate derived from the present work is $3000 \pm 1000\ (m/l)^{-1}cm^{-1}$ near 600°K.

Finally, the state of our knowledge of the very fast reaction (f) can be reviewed. Recently values of the ratio $B(M)/\underline{f}$ have been measured in experiments on the oxidation of nitric oxide by N_2O_5 in the presence of excess NO_2.[15] These experiments are at total pressures between 50 and 450 mm and at the temperatures 22°, 30°, and 40°C. The value of $\underline{f}$ at 300°K can be calculated from the values of $B(M)/\underline{f}$ near that temperature and the values of B_∞ and K deduced above. Since the ratio $A(M)/B(M)$ is equal to K at any value of $[M]$ and the ratio $A(M)/A_\infty$ has been measured over the appropriate range of $[M]$, the value of $B_\infty/\underline{f}$ can be computed. At 300°K, this value is about 0.3, and thus $\underline{f} = 6 \times 10^9\ (m/l)^{-1}sec^{-1}$.

This value is a permissible one for a reaction with a very low activation energy. If one formulates $\underline{f}$ as $P\ Z\ e^{-E_f/RT}$ and substitutes the kinetic theory collision number, Z, and the maximum value, unity, for the efficiency factor, P, then the computed maximum value of E_f is 2 kcal/mole. The experimental measurements of $B(M)/\underline{f}$ showed a negative temperature coefficient for that ratio.[15] The present results, combined with the earlier work at room

temperature, indicate that B_∞ has no temperature coefficient and that B(M) decreases with temperature below the high pressure limit. These results lead to the conclusion that $\underline{f}$ has a significant negative temperature coefficient. The computed "deactivation energy" is $E_f = -2 \pm 2$ kcal/mole. Such a negative temperature coefficient is difficult to understand in terms of conventional reaction rate theories. The reaction itself is far too fast to be a complex reaction in which a negative temperature coefficient might be expected. However, the present work on the decomposition of NO_3 at high temperatures does not exclude the possibility that $\underline{f}$ may decrease by a factor of ten or more between 300° and $1000^\circ K$.

Further improvement of our knowledge of the equilibrium constant for N_2O_5 dissociation, and of the rates of the reactions which it controls, may be pursued along several general lines. Quantitative measurements of the visible absorption spectrum of NO_3 are the basis of the present advances. Further work can be done. Throughout the visible region, the absolute absorption coefficients of NO_3 are large compared to those of other simple inorganic molecules. This strong absorption has been both a help and a hindrance in the present work. More important, though, is the strongly banded nature of the spectrum, which makes necessary very careful specification of the wave length, temperature, and chemical environment in quantitative absorption measurements. Preparation of known quantities of gaseous

NO_3 can be achieved at rather high temperatures and for rather short intervals of time. Under similar conditions, the N_2O_5 dissociation equilibrium can be brought into the open and studied directly by photoelectric methods. The shock tube has been very useful for such experiments. Flowing gas experiments in which external heating is used have yielded qualitative observation of the NO_3 absorption spectrum,[31] and it is reported that those experiments are currently being resumed.[32] It will be of interest to compare the results which they provide with those obtained by the shock wave experiments.

The ozone-N_2O_5-oxygen system ought to be reinvestigated spectrophotometrically using a light source, monochromator, and detector combination that can be calibrated directly in high speed experiments over a range of temperatures upward of 500°K. From the standpoint of having a large ratio of $\epsilon_{NO_3}/\epsilon_{O_3}$ combined with unquestionably reproducible monochromatization and adequate intensity for the high speeds required, a d.c. sodium vapor lamp specially adapted for this purpose is recommended.

Another approach to systems involving N_2O_5 and NO_3 lies in better understanding of the properties of the substances themselves. Although N_2O_5 is a fairly common substance, its molecular structure and vibrational frequencies are not yet known in enough detail to permit an accurate calculation of its heat capacity and entropy. Calorimetric measurements to date are likewise inadequate.

Reliable values of these quantities would contribute significantly even to the interpretation of the present results. Surely some of these gaps will be filled in the near future.

NO_3 is a relatively simple molecule, almost certainly a symmetric top. Even now there is enough general information on related substances that reasonable estimates of its thermodynamic properties can be made. Perhaps one day infrared or Raman spectroscopy on liquid or frozen solutions of NO_3 at low temperatures will determine some of the molecular parameters exactly. The heat of formation of gaseous NO_3 from the elements is obtained from knowledge of the heat of dissociation of N_2O_5. The value of $\Delta H^{\circ}_{f_{298.}}$ for NO_3 based on recent work is $17.1 \pm 1.$ kcal/mole, which replaces the value of 13. kcal/mole quoted in the NBS tables.[33]

7. Thermodynamic Properties of N_2O_5 and NO_3.

No experimental information is available on the thermodynamic properties of NO_3, and the information of N_2O_5 is very incomplete. Estimates of the heats of formation, heat capacities, and entropies of these substances have been used in interpreting some of the results of this investigation. The basis of these estimates is presented here.

The heat of formation of $N_2O_5(g)$, $\Delta H_{f_{298}}^{o}$ = +3.6 kcal/mole, is indicated by the heat of formation of the solid, -10.0 kcal/mole, and the heat of sublimation, which is quoted at +13.6 kcal/mole at 31.5°C.[34] These values seem to be known to within 0.5 kcal/mole or less.

The standard entropy of $N_2O_5(g)$, S_{298}^{o} = 82. cal/mole °K, is likewise obtained from data on the solid and the vaporization process.[35] The entropy of sublimation of N_2O_5 derived from vapor pressure data[34][35][36] is 45. e.u. The uncertainty in this value corresponds to the uncertainty in the heat of sublimation, and is about 1.5 e.u. The entropy of one formula weight of the solid is given as 36.6 $\pm$ 2 e.u. from extrapolated calorimetric data.[35] This value is not very well known, and the National Bureau of Standards tables do not include it. An alternative estimate of the entropy of the solid can be made on the basis of its ionic composition, NO_2^+ NO_3^-. The average entropies of nitrite and nitrate ions in crystalline combination with univalent cations are given by Latimer[37] as 17.8 and 21.7 e.u. respectively. Using the idea that

NO_2^+ has about the same entropy as NO_2^- in crystals, one can estimate the standard entropy of solid nitrogen pentoxide as about 39. e.u. (The origin of the value 27.1 e.u. quoted by Latimer[38] is unknown.) Thus the uncertainty in the standard entropy of $N_2O_5(g)$ at 25°C is about 3. e.u.

The heat capacity of N_2O_5 vapor is not known experimentally. Neither the fundamental vibration frequencies nor the details of the molecular structure are known. Still, there is enough general information available that a reasonable estimate of the heat capacity can be made.

N_2O_5 gas is, structurally as well as stoichiometrically, the anhydride of nitric acid. The valence bond structure has been discussed by Pauling and Brockway,[39] who write the formula

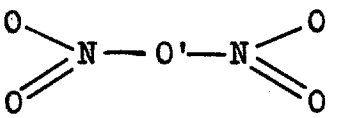

in which double bond resonance is confined to the terminal oxygen atoms in each nitro group. They point out that participation of the central (O') oxygen atom in conjugated structures of the type

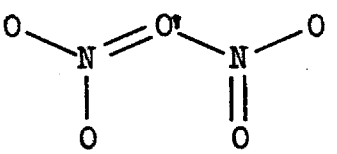

strongly violates the adjacent charge rule. One can also observe that a planar structure with abnormally close contact between oxygen atoms would be required by such a conjugated system of double bonds. Accordingly, a structure

was proposed in which O' lies in the plane of each of the nitro groups and rotation of the nitro groups about the N-O' single bonds is nearly free.

This much information on the structure of N_2O_5 makes possible a classification of the fifteen normal modes of internal motion. Two stretching modes and one bending mode are associated with each nitro group. The bent O_2N-O'-NO_2 skeleton likewise has two stretching modes and one bending mode. The remaining six modes are derivable from rotations of the nitro groups. Four of these are low frequency rocking vibrations normal to the N-O' axes and the other two are the internal rotations about the N-O' axes. All of these but the internal rotations are approximately harmonic vibrations with well defined frequencies. Approximate assignments of these frequencies have been made by using the values generally observed in the simpler nitroalkanes[40] for the rocking, bending, and stretching motions of the nitro groups and substituting the frequencies of Cl_2O[41] for those of the N-O'-N skeleton. The assumed frequencies expressed in cm^{-1}, are as follows: NO_2 symmetric stretches, 1360; NO_2 asymmetric stretches, 1640; NO_2 bends, 630; NO_2 rocks, 450; NO'N symmetric stretch, 680; NO'N asymmetric stretch, 973; and NO'N bend, 330. At 25°C, the calculated contribution of these thirteen vibrations to the heat capacity of N_2O_5 is 5.4 R.

An idea of the height of the barrier hindering the internal rotations can be obtained by examining the entropy of the gas at 25°C. The translational entropy of an ideal gas of molecular weight 108.0 is 40.0 e.u. The estimated entropy of

the thirteen vibrations outlined above is 5.8 e.u. The remainder of the 82 entropy units of N_2O_5 gas must be divided among the internal and total rotations. The moments of inertia have been calculated on the basis of the following assumed structural parameters: $\angle ONO = 128^\circ$, $O-N = 1.22\text{Å}$, $O'-N = 1.45\text{Å}$, $\angle NO'N = 120^\circ$, and molecular symmetry C_{2v} with the planes of the nitro groups perpendicular to each other and to the NO'N plane. The computed rigid rotational entropy of such a structure is 25.9 e.u. This means that the entropy contributed by the internal rotations is about 10 e.u. If one assumes that both nitro groups rotate freely and independently on the rigid NO'N frame, the calculated entropy contribution is 12.7 e.u.[42] This limiting case is not inconsistent with the known facts, but it certainly is not required by them. Harmonic torsional vibrations with frequencies in the neighborhood of 50 cm^{-1} also fit the entropy data. The problem is further complicated by the interaction between the two nitro groups, which form a pair of loosely fitting gears with each other. In the absence of more definitive data, one can only guess that the rotational barriers are at most a few kilocalories, and that the two rotations together contribute about 1.3 R to the heat capacity of N_2O_5 at 25°C. Classical inclusion of rotation, translation, and the PV product in the heat capacity yields the estimate $C_p(N_2O_5)_{300^\circ K} = 10.7$ R.

The only information about the thermodynamic properties of NO_3 is the approximate value of its heat of formation derived from the heat of dissociation of N_2O_5. From the reactions which it exhibits, one is certain that NO_3 is the nitrate free radical, in which all three oxygen atoms are equivalent. Valence bond

formulas involve a three electron bond and two single bonds to oxygen in resonance around a central nitrogen atom. Assumption of a planar structure with symmetry D_{3h}, N - O distances of 1.33 Å, a doublet electronic ground state, and vibration frequencies somewhat lower than those of the nitrate ion [43] leads to the heat capacity and entropy values calculated below. An alternative basis for the estimation of these properties is provided by the known properties of NO_2 [44] and the differences between the known properties of SO_3 and SO_2. [45] The computations of S° and C_p/R at 25°C for NO_3 are summarized below:

Estimated Molecular Properties	S° e.u.	C_p/R
Translation: Molecular weight = 62.01	38.05	1.50
Rotation: N - O = 1.33 Å, D_{3h}	19.96	1.50
$I_a I_{bc}^2 = 1.532 \times 10^5$ amu Å^2		
Vibration: $\tilde{\nu}_1 = 1000$; $\tilde{\nu}_2 = 800$; $\tilde{\nu}_3 = 1200$; $\tilde{\nu}_4 = 600$ cm^{-1}	1.29	1.76
Electronic: One unpaired electron	1.38	-
	-	1.00
	60.68	5.76
Analogous Compounds		
NO_2	57.47	4.47
SO_3 - SO_2	1.91	1.30
	59.38	5.77
Average	60.0	5.77

C. DETAILS OF THE METHOD

1. Reagents.

NO_2-N_2O_4 was condensed from a cylinder (Matheson) into a bubbling trap at -10°C. Oxygen (Linde), purified by passage through a U-tube packed with glass wool and cooled in dry ice, was bubbled through the liquid N_2O_4. The effluent oxygen stream, saturated with nitrogen dioxide vapor, was directed through a 35 ml column of P_2O_5 coated glass beads into a storage trap on the vacuum line. After the liquid N_2O_4 had become pale yellow, solid N_2O_4 was condensed from the stream by application of dry ice to the storage trap. When the liquid was exhausted to the point that its composition was formally 95% N_2O_4 and 5% HNO_3, as indicated by the appearance of a nitric acid rich phase, the flow was stopped and the oxygen was pumped from the solid preparation. In one instance the product was surrounded by an ice-salt bath in a Dewar flask at about -15°C and allowed to stand five hours. On examination, the N_2O_4 was partially melted and the temperature of the bath was -11°C. The melting point reported by Giauque and Kemp is -11.26°C.(46)

N_2O_5 was prepared from N_2O_4 by oxidation with ozone in a flowing system in the glassware described above. The oxygen stream was divided after passage through the dry ice-glass wool trap and the major portion was passed

through a P_2O_5 column into an ozonizer.* The effluent stream, which was about five percent ozone, was fed into the NO_2-N_2O_4 stream immediately after the latter had passed its P_2O_5 chamber. The flow rates were adjusted so that the stream was colorless after the junction. (The glass was warm to the touch for a few cm after the junction.) The O_3-N_2O_5-O_2 mixture flowed through about a foot of tubing, which could be examined lengthwise for color, before it reached the collecting trap at -80°C. After each preparation, the nitronium nitrate crystals were warmed to 0°C and the vapor was examined for color.

Two points of caution should be made about this preparation. First, in using the batch process described by Nightingale, et al.,[47] one should NOT concentrate the ozone and then admit it to a bulb containing N_2O_4 or N_2O_5, for in the absence of diluent gas, the N_2O_5 catalyzed decomposition of ozone is dangerously explosive. Second, if the flow method described above is used to prepare large quantities of N_2O_5 in a small vessel, care should be taken to avoid condensing too thick a layer of N_2O_5 on the inside of the trap. This is because solid N_2O_5 has a significantly higher coefficient of thermal expansion than Pyrex and is a hard ionic solid even at room temperature, so that it is

---

*This ozonizer, a 1 meter tall, water cooled discharge chamber, was generously loaned by Professor L. Zechmeister and his colleagues.

not possible to warm the preparation up without cracking the container.

Argon (Linde, 99.92% pure, principal impurity N_2) was passed through a dry ice-glass wool trap and admitted to the vacuum line through a phosphoric anhydride column.

N_2O_5 - Argon mixtures were prepared individually for each shock wave experiment because of the instability of N_2O_5 vapor. The mixtures were made up in a five liter flask immersed in an ice water bath. The flask was evacuated to a pressure of 10^{-4}mm of Hg or less. The N_2O_5 storage trap was warmed to 0°C and a charge of vapor was withdrawn. The pressure of N_2O_5 in the mixing bulb was measured with a dibutyl phthalate manometer whose reference arm was connected to the diffusion pump while the measurement was being made. The balance of the mixture was made up with argon, and the total pressure, which was usually near one atmosphere, was measured on a mercury manometer. A cold finger in the mixing bulb was then filled with an ice and salt mixture at about -15°C to promote convective stirring. The reagents were allowed two hours to mix in this fashion. The 1/e time for the first order decomposition of N_2O_5 at 0°C is 350 hours,[48] so that the decomposition during the mixing period was always less than one percent. The shock tube was routinely evacuated to 2×10^{-3} mm of Hg or less. In the later experiments it was purged of water by a five minute exposure to a few millimeters pressure of N_2O_5 vapor and re-evacuated before the

experimental mixture was admitted. In order to avoid a pressure measurement after the charge was admitted to the warm shock tube, the concentration ratio involved in the expansion from the mixing bulb into the shock tube and connecting manifold was determined accurately in separate experiments. At the end of the mixing period, the ice-salt mixture was removed from the cold finger. When the stopcock was opened admitting the charge to the shock tube, one minute was allowed for the attainment of thermal equilibrium, and then the shock tube was isolated and the experiment was initiated as soon thereafter as possible. Thus the N_2O_5 was at room temperature for no more than two minutes before the gas was shocked. Eighty-five seconds at 25°C is equivalent to an hour at 0°C, from the standpoint of N_2O_5 decomposition. Thus the total decomposition in the handling of a charge of N_2O_5 was not more than one percent.

NO_2 - N_2O_4 - N_2O_5 - Argon mixtures. In those experiments in which extra NO_2 was included in the charge of N_2O_5, the latter was admitted to the mixing bulb at 0°C first. NO_2 - N_2O_4 was admitted second, the total pressure was again measured on the dibutyl phthalate manometer, and finally argon was added. Calculation of the formal mole fraction of NO_2 in these mixtures was carried out using the value $K = p^2_{NO_2} p^{-1}_{N_2O_4} = 0.016$ atmospheres at 0°C. This value is an average of extrapolated data of Verhoek and Daniels[49] and Bodenstein and Boes[50] and measurements

at $0^{o}C$ by Wourtzel.[51]

2. Instrumentation.

An Osram HBO-200 high pressure d.c. mercury arc provided an intense monochromatic source of light for one of the spectrophotometric records in each experiment. The light output of this lamp was satisfactorily free of 120 cycle ripple when it was operated from a 150 volt generator stabilized by a choke input filter with L = 1 henry and C = 1.5 x 10^3 μf. The prominent lines in the mercury spectrum were isolated from the beam incident on the photomultiplier with the filter combinations listed below.

Wave Length	Interference Filter Bausch & Lomb	Cutoff Filter Corning #	Cutoff Filter Laboratory #
366 mμ	360 mμ	5562	15
405	405	3060	48
436	436	3060	48
546	546	3384	54

RCA 931-A photomultipliers were used to detect this radiation.

For the spectrophotometric measurements with red light, a 500 watt tungsten projection bulb, operated at 120 volts d.c., served as source. An RCA 6217 photomultiplier was the detector. This photomultiplier tube has the S-10 spectral response, with maximum sensitivity at 540 mμ and 34% of that sensitivity at 650 mμ. A wave length band of triangular profile and 3.3 mμ half width centered at 650 mμ was isolated by means of a Bausch & Lomb 500 mm reflection grating monochromator with slits 1.0 mm wide. The experiments in which the center of the band was moved to

648 and 652 mμ were done with this monochromator.

Most of the experiments, however, were done using a similar wave length band isolated by means of a two prism glass spectrograph* with an exit slit mounted in the focal plane. This monochromator was about three times as fast as the grating in this application. The dispersion and the position of the spectrum in the focal plane were determined from a plate of the mercury arc emission. A pair of parallel slits was constructed with the principal slit 0.40 mm wide and displaced 15.0 mm from a narrow auxiliary slit. This slit system was mounted in the focal plane of the spectrograph so that the 5461Å line of mercury emerged through the auxiliary slit, which was then taped shut. By measurement of the plate it was determined that the band thus isolated was centered at 652 mμ and was 3.6 mμ wide. The entrance slit was adjusted to subtend the same angle on the prism as the exit slit, thus giving the optical band its triangular profile.(52) In the earlier experiments, the exit slit was positioned differently, and the band was centered at 650 mμ.

The optical bench is described in part II.

---

*This spectrograph was built at the California Institute for use in Raman spectroscopic work and is described briefly in papers by the late Professor R. G. Dickinson.(53) Professor R. M. Badger has generously made available this instrument and instruction in its use.

The flash tube used to photograph NO_3 in absorption was a G.E. FT-126 lamp. The lines in its output are those of xenon. The lamp was operated with a 1 μf capacitor charged to 12 kv., and the flash had a mean duration of about 30 microseconds. The beam included a 1.7 cm length of the shock tube which in a typical experiment contained a linearly inhomogeneous region of gas whose times of shock arrival spanned some sixty microseconds. The spectrograph that was used is the one referred to above. The plate was exposed at f/8, and figure 1 is a contact print.

Measurement of the shock velocity was accomplished by timing the wave over a 30.00 cm or a 40.00 cm course with a 1.6 megacycle counter chronograph, Potter model 456. The photoelectric signals which were amplified to start and stop the chronograph were generated in the absence of colored material in the shock tube by the large refractive index gradient in the shock front. This was observed by the schlieren optical method as a decrease in light passing onto the photomultiplier when the light beam emerging from the shock tube was deflected to the upstream side of the final slit. Care was taken to align the light beams so that they missed the unremovable downstream slit edges. Light filters were used in these beams, but only as convenient attenuators. No failure of this triggering system was ever observed. The smallest density increments in any of the experiments involved compression of 0.04 atmospheres of

of argon by a factor of two. (The width of the shock tube is 15.0 cm.)

Triggering of the oscilloscopes was initiated by the same device that started the chronograph. The signal was sent to the oscilloscope via a thyratron in order to lock out subsequent trigger pulses from later disturbances of the light beam by reflected waves, bits of membrane, and the like.

The voltage developed by the photomultiplier anode current across 10^4 ohms was introduced at the vertical amplifier input of the oscilloscope. With coaxial leads, this circuit presents nearly 100 $\mu\mu$f of capacitance, so that the rise time of the detection apparatus was about one microsecond. To obtain signals of the order of a volt, currents of 100 microamperes were drawn from the photomultiplier, and the voltage divider on the dynodes was stabilized for the duration of the experiments with suitable capacitors.

The oscillographic records of the photomultiplier outputs were photographed on 35 mm film (Eastman Linagraph Pan.) and were measured from tracings of enlarged projections.

The time scale was provided by a 100 kc. crystal controlled oscillator circuit. This was connected to an intensifying electrode in the cathode ray tube so as to blank the trace once every 10n μsec, where n could be selected from the set of integers 1, 3, 4, 5, or 6.

The duration of the blanking was about $\underline{n}$ μsec. This disturbance of ten percent of the trace necessarily interfered slightly with the observation of the passage of the shock wave in some of the experiments, but this interference was tolerable.

Calibration of the photoelectric measurements was achieved by using the d.c. difference amplifier of the oscilloscope (Tektronix model 512) to display on the experimental trace the difference between the photomultiplier output voltage and a reference potential from a dry cell. Auxiliary traces displayed fractions of the reference potential selected by a Helipot precision potentiometer. (When these traces were recorded, the photomultiplier output was replaced by ground; it is not sufficient to simply remove the photomultiplier and allow the unused input grid to float.) This calibration procedure is valid provided that the reference potential and the reference position of the oscilloscope trace are constant for the few minutes between the experiment and the introduction of the calibrations, and provided that the reference position of the trace is independent of the magnitude and duration of the signal which deflects it. When the oscilloscope is warm, the former condition is satisfied, but the latter is not. However, the behavior of the so called "d.c. shift" is known, and correction for this inadequacy of the instrument has been made in interpreting the data.

3. Calculation of Shock Wave Parameters.

Temperatures and concentrations are not measured directly in the shock wave experiments. They are calculated from measurements of the conditions before the arrival of the shock wave, the velocity of the wave, and the progress of chemical changes induced by the shock. The equations that govern the shock wave behavior are expressions of the conservation of mass, momentum, and energy as gas flows normally across a plane shock front. The velocities that appear in equations (87) through (89) represent motion relative to the shock front.

(87) $\rho_1 \underset{\sim}{u}_1 = \rho_2 \underset{\sim}{u}_2$ = density x velocity

(88) $\rho_1 \underset{\sim}{u}_1^2 + P_1 = \rho_2 \underset{\sim}{u}_2^2 + P_2$ = density x (velocity)^2 + pressure

(89) $h_1 + \frac{1}{2}\underset{\sim}{u}_1^2 = h_2 + \frac{1}{2}\underset{\sim}{u}_2^2$ = specific enthalpy + $\frac{1}{2}$(velocity)^2

Subscripts 1 and 2 refer to conditions in the unshocked and shocked gases, respectively. The adaptation of these equations to the laboratory situation of a shock wave moving through stationary gas with velocity $\underset{\sim}{s}$ and imparting the flow velocity $\underset{\sim}{v}$ involves the Galilean transformation $\underset{\sim}{s} = -\underset{\sim}{u}_1$, $\underset{\sim}{v} = \underset{\sim}{s} + \underset{\sim}{u}_2$. Elimination of the velocities from (89) by (87) and (88) leaves:

(90) $h_2 - h_1 = \frac{1}{2}(P_2 - P_1)(1/\rho_1 + 1/\rho_2)$

Expression of the initial conditions for W_1 grams = one mole of ideal gas and introduction of the compression ratios $\pi = P_2/P_1$, $\Delta = \rho_2/\rho_1$, and $\Theta = T_2/T_1$ yields:

(91) $(h_2 - h_1)W_1 = RT_1/2\,(\pi - 1)(1 - 1/\Delta) = \overline{\Delta H}$

Solving (87) and (88) for the transformed velocities yields:

$$(92) \qquad \underset{\sim}{s}^2 = \rho_2/\rho_1 \ (P_2 - P_1)(\rho_2 - \rho_1)^{-1}$$

or

$$(93) \qquad \underset{\sim}{s}^2 = RT/W_1 \ (\pi - 1)(1 - 1/\Delta)^{-1}$$

and

$$(94) \qquad \underset{\sim}{v} = \underset{\sim}{s} \ (1 - 1/\Delta)$$

For a given one-dimensional shock wave with fixed $\underset{\sim}{s}$, these equations relate the initial conditions to the shocked conditions in any plane behind the shock front. For the chemical changes in which we are interested, the specific enthalpy, h_2, adjusts with the progress of the reaction, so that π, Δ, Θ, and $\underset{\sim}{v}$ also vary with time and distance behind the shock. In general the molar composition of a reacting mixture changes too. With the assumption of ideal gas behavior, h_2 can be formulated in terms of the molar composition and the temperature for a selected extent of reaction.

The procedure that has been used to obtain numerical solutions of the shock wave equations in individual experiments is guided by three considerations. First, T_1 for all experiments is room temperature, which is never far from 25°C. Second, tables of enthalpies are available at convenient temperatures throughout the range of T_2 of the experiments. Third, the shock parameters in all the experiments are essentially determined by the carrier gas, whose behavior can be calculated easily and precisely. The effect of the reacting component is treated as a small perturbation

which is proportional to the percentage of reactant in the mixture and linear in the fractional extent of reaction. Accordingly, $\underset{\sim}{s}$ and Δ are calculated at selected shock temperatures, T_2, and fixed $T_1 = 298.16^{\circ}K$ for the pure carrier gas and for mixtures containing one percent of the reactant, with and without reaction. Large plots of $\underset{\sim}{s}$ and Δ versus T_2 are constructed for the carrier gas. The adjustments of $\underset{\sim}{s}$ appropriate for one percent of the reacting component are tabulated over the temperature range of the experiments and plotted against $\underset{\sim}{s}$. The corresponding adjustments in Δ are likewise determined and plotted against T_2.

The form in which equation (91) is used for these calculations is given first for the pure carrier gas. The perfect gas law implies: $\pi = \Delta\Theta$, since the molecular weight is fixed. The left side of equation (91) is

$$\overline{\Delta H} = \int_{298.16}^{T_2} C_p \, dT$$

$$(95)\quad \Delta = \left[\frac{2\,\overline{\Delta H}/RT_1 + 1}{\Theta} - 1\right] + \frac{1}{\Delta\Theta}$$

This quadratic equation is easily solved for a series of values of Θ by tabulating the function in brackets and solving for Δ by iteration, since $1/\Delta\Theta = 1/\pi$ is small for most of the cases of interest. For the special cases in which the heat capacity of the gas is satisfactorily constant between T_2 and T_1, the term in brackets in (95) becomes $(2C_p/R - 1)(1 - 1/\Theta)$. This is certainly the case

with argon, and one may use:

(96) $$\Delta = 4(1 - 1/\Theta) + 1/\Pi$$

Calculations for vibrationally unexcited gases are made similarly, using only the heat capacity for the active degrees of freedom. The values of Δ and Π thus obtained are substituted into equations (93) and (94) to obtain the corresponding shock velocities.

The inclusion of two or more components in the initial mixture introduces the following changes which must be substituted in equations (91) and (93). W_1 is the mass, in grams, of that quantity of gas that contains Avogadro's number of molecules before the arrival of the shock wave. In terms of the individual substances of molecular weight W_i present in that gas in mole fractions ϕ_i, $\overline{W_1}$ is the mean molecular weight:

(97) $$\overline{W_1} = \sum_i \phi_i W_i$$

In this case, the mechanical equation, (93), becomes:

(98) $$\underset{\sim}{s}^2 = \frac{RT \quad (\Pi - 1)}{\sum_i \phi_i W_i \quad (1 - 1/\Delta)}$$

It should be observed that this equation is valid whether or not the molar composition changes behind the shock front.

The enthalpy increase for $\overline{W_1}$ grams of material now becomes the sum:

(99) $$\overline{\Delta H} = \sum_i \phi_i (H_2^o - H_1^o)_i$$

so that (95) becomes:

$$(100) \qquad \Delta = \frac{2/RT_1 \sum_i \phi_i (H_2 - H_1)_i + 1}{\Theta} - 1 + \frac{1}{\Delta\Theta}$$

Reaction of one of the components according to a process in which ($\underline{n}$+1) moles of products are formed for each mole that reacts further complicates the expression for $\overline{\Delta H}$ and also affects the gas law. Suppose for simplicity that there is only one reacting species, $\underline{r}$, in the carrier gas, $\underline{c}$. Let α represent the fractional extent of the reaction that results in the disappearance of $\underline{r}$ to form the products, $\underline{p}$. Then:

$$(101) \qquad \overline{\Pi} = (1 + \phi_r \underline{n} \alpha) \Delta \Theta$$

and

$$(102) \qquad \overline{\Delta H} = \phi_c (H_2^o - H_1^o)_c + \phi_r (1 - \alpha)(H_2^o - H_1^o)_r + \phi_r \alpha (H_2^o - H_1^o)_p + \phi_r \alpha (\Delta H_1)_{reaction}$$

The extension to two or more reactants or products is straightforward. With these substitutions, equation (95) becomes:

$$(103) \qquad \Delta = \frac{2\ \overline{\Delta H}/RT_1 + 1}{(1 + \phi_r \underline{n} \alpha)\ \Theta} - 1 + \frac{1}{(1 + \phi_r \underline{n} \alpha) \Delta \Theta}$$

The specific form of the expression used to compute $\overline{w_1}(h_2 - h_1) = \overline{\Delta H}$ is governed by convenience. The heat of the reaction may be introduced at any reference temperature, and the enthalpies of the products and reactants are accounted for accordingly. Equation (102) chooses the initial temperature of the experiment, T_1, as this reference temperature.

The sets of calculated shock wave parameters that have been used in this investigation are recorded in table 6. In the calculation of these tables, thermal and thermochemical data on gaseous A, O_2, NO, NO_2, N_2O_5, and NO_3 have been used. Reliable data for A, O_2, and NO have been taken from Series III of the NBS Tables.[45] Data on NO_2 have been taken from Series I of these tables[33] and from the NBS-NACA tables.[44] The other data are less accurately known. Their sources have been discussed in a previous section. The only reservation on the validity of the calculations for mixtures of argon and NO_2 is that they apply to initial conditions in which the association of NO_2 to N_2O_4 is negligible.

D. TABLES

1. Extinction Coefficients of NO_2 Measured in the Shock Tube.

$\lambda = 366$ mμ $\epsilon_{(300^\circ K)} = 150$ $(m/l)^{-1}cm^{-1}$

N#	T_2 °K	D'	D	ϵ_{NO_2}
58	730	.0545	.1062	120
59	703	.0632	.1203	126
60	718	.0609	.1185	122
61	737	.0400	.0758	123
62	723	.0454	.0864	124
63	733	.0902	.1768	119
64	768	.0210	.0408	117
66	782	.0851	.1566	123
67	722	.0953	.1810	124
68	818	.0581	.1073	120
69	988	.0788	.1438	113
70	965	.0460	.0849	113
71	888	.0600	.1134	113
98	846	.229	.388	127
99	905	.0380	.0690	118

$\lambda = 405$ mμ $\epsilon_{(300^\circ K)} = 160$ $(m/l)^{-1}cm^{-1}$

N#	T_2 °K	D'	D	ϵ_{NO_2}
58	730	.0580	.1131	128
59	703	.0665	.1275	133
60	718	.0680	.1295	133
61	737	.0430	.0812	132
62	723	.0510	.0947	136
63	733	.0976	.1900	128
64	768	.0223	.0434	125
65	956	.0591	.1028	130
66	782	.1000	.1763	139
67	722	.1032	.1947	134
68	818	.0639	.1164	130
70	965	.0530	.0945	125

Table 1 (continued)

λ = 436 mμ $\epsilon_{(300°K)}$ = 150 $(m/l)^{-1}cm^{-1}$

N#	T_2 °K	D'	D	ϵ_{NO_2}
1	616	.1035	.2198	123
2	643	.0800	.1728	118
		.0879	.1807	123
3	722	.0638	.1233	122
		.0630	.1225	121
4	739	.0602	.1161	121
		.0535	.1094	124
23	713	.0598	.1102	130
24	727	.0680	.1267	126
25	709	.0670	.1246	129
26	713	.0633	.1159	131

λ = 546 mμ $\epsilon_{(300°K)}$ = 37 $(m/l)^{-1}cm^{-1}$

N#	T_2 °K	D'	D	ϵ_{NO_2}
23	713	.0240	.0364	43
24	727	.0289	.0434	43
25	709	.0263	.0405	42
131	708	.102	.148	45

λ = 652 mμ $\epsilon_{(300°K)}$ = 5 $(m/l)^{-1}cm^{-1}$

N#	T_2 °K	D'	D	ϵ_{NO_2}
98	846	.038	.043	14

2. Absorption by the Initial Dissociation Products of N_2O_5: Calculated Extinction Coefficients of NO_3.

Experiments near 650 mμ with initially pure N_2O_5.

N#	T_2 °K	$c_o\Delta$ (m/l) x 10^3	$c_o\phi\Delta$ (m/l) x 10^5	λ mμ	$\epsilon_{NO_2}+\epsilon_{NO_3}$ $(m/l)^{-1}$ cm^{-1}	ϵ_{NO_3}
54	586	8.75	4.80	650	260	251
55	642	9.35	5.24	650	262	252
56	686	9.72	5.44	650	276	266
57	684	5.20	6.17	650	268	258
72	818	10.8	6.01	650	298	285
73	826	10.4	5.91	648	270	257
74	824	10.6	5.95	648	284	271
75	820	10.6	5.50	652	292	279
76	820	10.6	5.72	652	283	270
77	820	10.5	5.72	650	311	298
78	813	10.6	6.45	650	280	267
81	998	4.55	2.83	650	308	291
82	997	4.72	3.57	650	292	275
83	1014	13.6	2.60	650	325	308
84	1022	13.6	2.54	650	319	302
91	786	13.4	12.2	652	303	291
93	801	13.5	12.1	652	304	291
94	825	10.1	2.46	652	296	283
95	832	10.1	2.35	652	295	282
96	779	3.94	3.50	652	280	267
100	860	10.4	3.07	652	302	288
102	832	10.3	2.96	652	305	292
103	830	10.5	3.48	652	312	299
108	972	9.20	5.91	652	342	326
109	1048	7.56	5.01	652	329	311
110	1154	9.54	5.40	652	331	311
111	1216	9.41	2.60	652	318	297
112	1064	11.2	3.50	652	340	322
35	517	7.65	4.18	615	1260	1250

Table 2 (continued)

Experiments at 652 mμ with mixtures containing NO_2 and N_2O_5.

N#	T_2 °K	$C_o\Delta$ m/l x 10^3	$[NO_2]/[N_2O_5]$ in initial mixture	D total	D NO_3	ϵ_{NO_3}
113	1090	11.9	3.54	.245	.193	314
115	893	13.4	2.18	.275	.239	309
116	1122	14.8	3.16	.345	.274	308
117	934	14.1	4.78	.360	.283	326
119	750	12.5	3.08	.260	.228	342
120	751	12.8	9.12	.261	.185	297
124	643	10.0	4.46	.273	.231	302
126	661	11.4	3.48	.205	.179	303
127	582	10.8	3.04	.231	.204	282

Experiments at 546 mμ with initially pure N_2O_5.

N#	T_2 °K	$C_o\Delta$ m/l x 10^3	$C_o\phi\Delta$ m/l x 10^5	$\epsilon_{NO_2}+\epsilon_{NO_3}$ $(m/l)^{-1}cm^{-1}$	ϵ_{NO_3}
17	640	8.58	4.14	500	457
18	627	8.30	3.66	550	507
19	614	8.30	3.38	596	554
20	570	7.97	3.66	610	569
21	739	8.91	3.24	590	545
22	786	6.75	2.11	562	516
132	686	11.2	4.00	710	666

Experiments at 436 mμ with initially pure N_2O_5.

N#	T_2 °K	$C_o\Delta$ m/l x 10^3	$C_o\phi\Delta$ m/l x 10^5	$\epsilon_{NO_2}+\epsilon_{NO_3}$ $(m/l)^{-1}cm^{-1}$	ϵ_{NO_3}
17	640	8.58	4.14	203	75
18	627	8.30	3.66	218	89
19	614	8.30	3.38	242	112
20	570	7.97	3.66	233	100
21	739	8.91	3.24	261	149
22	786	6.75	2.11	262	143

Table 2 (continued)

Experiments at 405 mμ with initially pure N_2O_5.

N#	T_2 °K	$C_o\Delta$ m/l x 10^3	$C_o\phi\Delta$ m/l x 10^5	$\epsilon_{NO_2}+\epsilon_{NO_3}$ $(m/l)^{-1}cm^{-1}$	ϵ_{NO_3}
33	585	8.73	4.65	204	64
34	714	8.40	10.6	232	100

Experiments at 366 mμ with initially pure N_2O_5.

N#	T_2 °K	$C_o\Delta$ m/l x 10^3	$C_o\phi\Delta$ m/l x 10^5	$\epsilon_{NO_2}+\epsilon_{NO_3}$ $(m/l)^{-1}cm^{-1}$	ϵ_{NO_3}
33	585	8.73	4.65	143	13
34	714	8.40	10.6	159	35
54	586	8.75	4.80	149	19
55	642	9.35	5.24	144	17
56	686	9.72	5.44	151	26
57	684	5.20	6.17	147	22
72	818	10.8	6.01	185	66
73	826	10.4	5.91	174	55
74	824	10.6	5.95	149	30
75	820	10.6	5.50	147	28
76	820	10.6	5.72	152	33
77	820	10.5	5.72	156	37
78	813	10.6	6.45	158	39
83	1014	4.55	2.60	151	39
84	1022	4.72	2.54	134	23
86	972	14.6	12.8	153	40
87	972	14.3	12.8	141	28
90	1005	14.6	13.1	162	50
91	786	13.4	12.2	173	52
92	796	13.5	11.9	164	44
93	801	13.5	12.1	165	45
94	825	10.1	2.46	145	26
95	832	10.1	2.35	145	26
96	779	3.94	3.50	146	25
103	830	10.5	3.48	149	30
109	1048	7.56	5.01	157	47
110	1154	9.54	5.40	181	74
111	1216	9.41	2.60	182	76
112	1064	11.2	3.50	158	48

3. Absorption by the Final Decomposition Products of N_2O_5. Calculated Extinction Coefficients of NO_2.

Experiments at 366 mμ with initially pure N_2O_5.

N#	T_2 °K	$2C_o\phi\Delta$ m/l x 10^5	D_∞	ϵ_{NO_2} $(m/l)^{-1}cm^{-1}$
33	575	9.05	.148	109
34	726	20.3	.362	119
86	981	24.8	.398	107
87	981	24.8	.401	108
90	1018	25.5	.420	110
91	797	23.5	.407	115
92	806	23.2	.391	112
93	811	23.6	.402	113
103	835	6.87	.115	112
109	1054	9.81	.164	112
110	1162	10.6	.190	119
111	1220	5.16	.085	110

Experiments at 366 mμ with mixtures containing NO_2 and N_2O_5.

N#	T_2 °K	$C_o\phi_{NO_2}\Delta$ m/l x 10^5	$2C_o\phi_{N_2O_5}\Delta$ m/l x 10^5	D_∞	ϵ_{NO_2} $(m/l)^{-1}cm^{-1}$
113	1095	14.3	8.16	.364	108
114	680	11.3	7.10	.317	121
115	898	11.1	10.2	.370	116
116	1127	18.6	11.7	.526	116
117	939	27.1	11.4	.649	112
118	830	11.5	11.0	.403	119
119	754	13.6	8.80	.402	125
120	754	37.4	8.20	.853	125
121	754	18.4	9.06	.506	123
122	690	15.0	10.8	.469	121
123	713	22.1	9.93	.553	115
124	649	22.4	10.0	.609	125
126	664	13.5	7.80	.411	129

Table 3 (continued)

Experiments at 405 mμ with initially pure N_2O_5.

N#	T_2 °K	$2C_o\phi\Delta$ m/l x 10^5	D_∞	ϵ_{NO_2} $(m/l)^{-1}cm^{-1}$
33	575	9.06	.172	127
34	726	20.3	.403	132

Experiments at 436 mμ with initially pure N_2O_5.

N#	T_2 °K	$2C_o\phi\Delta$ m/l x 10^5	D_∞	ϵ_{NO_2} $(m/l)^{-1}cm^{-1}$
17	645	8.15	.126	103
18	633	7.25	.120	111
19	620	6.65	.123	123
20	574	7.16	.128	119
21	742	6.40	.113	118
22	790	4.20	.068	108

Experiments at 652 mμ with initially pure N_2O_5.

N#	T_2 °K	$2C_o\phi\Delta$ m/l x 10^5	D_∞	ϵ_{NO_2} $(m/l)^{-1}cm^{-1}$
78	819	12.6	.017	9
84	1024	5.05	.013	17
87	981	24.8	.065	17
90	1018	25.4	.067	18
110	1162	10.6	.034	21
111	1220	5.16	.018	23

Experiments at 652 mμ with mixtures containing NO_2 and N_2O_5.

N#	T_2 °K	$C_o\phi_{NO_2}\Delta$ m/l x 10^5	$2C_o\phi_{N_2O_5}\Delta$ m/l x 10^5	D_∞	ϵ_{NO_2} $(m/l)^{-1}cm^{-1}$
113	1095	14.3	8.16	.065	19
116	1127	18.6	11.7	.083	18
120	754	37.4	8.20	.076	11

4. Measurements of the Initial Rate of Dissociation of N_2O_5.

N#	T_2 °K	ø %	$C_o\triangle = M$ m/l x 10^3	A(M) sec^{-1} x 10^{-4}	A'_M $(m/l)^{-1}sec^{-1}$ x 10^{-6}
41	543	.92	3.22	3.81	11.8
42	533	1.05	3.18	3.37	10.6
43	527	1.05	3.18	2.51	7.90
44	528	1.13	3.12	2.52	8.07
45	516	1.12	3.11	2.24	7.20
37	511	1.12	7.62	3.30	4.32
38	511	.89	7.55	3.46	4.59
39	512	.81	7.50	3.81	5.08
40	524	.42	7.60	4.05	5.33
46	481	.65	7.79	1.25	1.61
47	471	.67	7.79	.682	.878
48	473	.66	7.75	.704	.909
49	469	.66	7.79	.820	1.05
50	465	.68	7.70	.567	.736
51	462	.67	7.69	.643	.836
52	469	.40	7.70	.820	1.07
53	462	.94	7.75	.751	.970
104	483	.36	8.75	1.34	1.53
106	468	.41	8.60	.98	1.14
107	546	.41	9.85	9.02	9.16

5. Equilibrium Constants in the Dissociation of N_2O_5 Measured at the Time of Maximum Absorption by NO_3.

Experiments with pure N_2O_5.

$$K_c = \frac{[NO_2][NO_3]}{[N_2O_5]} \approx C_o \phi \Delta \frac{(\alpha^2 - \beta^2)}{(1 - \alpha)}$$

N#	T_2 °K	$C_o\phi\Delta$ m/l x 10^5	α apparent	β apparent	K_c m/l x 10^4
47	463	5.4	.52	.04	.30
48	465	5.4	.51	.06	.29
49	461	5.3	.52	.04	.28
50	458	5.4	.50	.04	.26
51	456	5.4	.47	.04	.22
52	464	3.2	.62	.05	.31
53	453	7.7	.42	.03	.22
104	477	3.2	.79	.01	.97
106	462	3.6	.64	.01	.42
43	505	3.7	.80	.07	1.11
44	506	3.8	.80	.04	1.17
45	495	3.9	.75	.02	.86
36	514	4.8	.76	.04	1.15
37	492	9.2	.67	.06	1.24
38	495	7.1	.77	.08	1.85
39	494	6.5	.79	.03	1.92
40	515	3.3	.89	.07	2.34

Experiments in mixtures of NO_2 and N_2O_5.

N#	T_2 °K	$C_o\phi_{N_2O_5}\Delta$ m/l x 10^5	$[NO_2]/[N_2O_5]$ in original mixture	α apparent	K_c m/l x 10^4
128	548	4.3	3.86	.90	18.7
129	547	4.7	6.50	.78	12.2
130	519	4.4	1.57	.73	2.7

6. Shock Parameters Calculated for Argon and Mixtures Containing Oxides of Nitrogen.

$T_1 = 298.16^{\circ}K$

Argon $C_p = 4.9680$ cal/mole $^{\circ}K$ $W = 39.944$ grams/mole

T_2 $^{\circ}K$	Π	Δ	$\underset{\sim}{s}^2$ $(cm/sec)^2 \times 10^{-8}$	$\underset{\sim}{s}$ cm/msec	$\underset{\sim}{v}$ cm/msec
298.16	1.000	1.000	10.344	32.16	0.000
400	2.028	1.512	18.85	43.42	14.70
500	3.227	1.924	28.78	53.65	25.77
600	4.497	2.235	39.28	62.67	34.63
700	5.796	2.469	50.03	70.73	42.08
800	7.110	2.650	60.90	78.04	48.59
900	8.430	2.793	71.82	84.75	54.41
1000	9.759	2.910	82.82	91.01	59.73
1100	11.090	3.006	93.84	96.87	64.64
1200	12.422	3.087	104.87	102.41	69.23
1300	13.757	3.155	115.91	107.66	73.54
1400	15.089	3.213	126.94	112.67	77.61
1500	16.429	3.266	138.02	117.48	81.50
1600	17.767	3.311	149.09	122.10	85.22
1700	19.105	3.351	160.16	126.55	88.78
1800	20.444	3.386	171.24	130.86	92.22
1900	21.783	3.418	182.32	135.03	95.53
2000	23.120	3.447	193.39	139.06	98.72

Mixture 99% argon, 1% NO_2 $\overline{W}_1 = 40.005$ grams/mole

T_2 $^{\circ}K$	$(H_2^{\circ} - H_1^{\circ})^*_{NO_2}$ kcal/mole	Δ	$\frac{\Delta}{\Delta(\text{mixture}) - \Delta(\text{argon})}$	$\underset{\sim}{s}$ cm/msec	$\frac{\delta s}{\underset{\sim}{s}(\text{mixture}) - \underset{\sim}{s}(\text{argon})}$
400	.944	1.520	.007	43.39	-.03
500	1.949	1.941	.017	53.69	+.04
600	3.023	2.258	.023	62.78	+.12
700	4.156	2.498	.029	70.90	+.17
800	5.335	2.684	.034	78.26	+.22
900	6.551	2.831	.038	85.03	+.28
1000	7.800	2.951	.041	91.33	+.32
1100	9.070	3.051	.045	97.23	+.36
1200	10.362	3.135	.049	102.82	+.41

* From reference (44).

Table 6 (continued)

Mixture 99% argon, 1% N_2O_5 $\overline{W_1}$ = 40.625 grams/mole

No Reaction

Approximation: $(H_2^\circ - H_1^\circ)_{N_2O_5} = 2(H_2^\circ - H_1^\circ)_{NO_2} + (H_2^\circ - H_1^\circ)_{O_2}$

T_2 °K	$(H_2^\circ - H_1^\circ)_{N_2O_5}$ kcal/mole	Δ	$\delta\Delta$	$\underset{\sim}{s}$ cm/msec	$\delta\underset{\sim}{s}$ cm/msec
400	2.61	1.551	.04	43.09	-.33
450	3.96	1.797	.06	48.54	-.16
500	5.35	2.000	.08	53.60	-.05
600	8.25	2.338	.11	62.86	.19
700	11.30	2.594	.12	71.10	.37
800	14.45	2.793	.14	78.57	.53
900	17.70	2.951	.16	85.43	.68
1000	21.03	3.081	.17	91.82	.81

Reaction: $N_2O_5 \longrightarrow 2NO_2 + \frac{1}{2}O_2$, ΔH°_{298} = +12.6 kcal/mole

T_2 °K	$H_2^\circ(2NO_2 + \frac{1}{2}O_2) - H^\circ_{298}(N_2O_5)$ kcal/mole	Δ	$\delta\Delta$	$\underset{\sim}{s}$ cm/msec	$\delta\underset{\sim}{s}$ cm/msec
400	14.8	1.760	.25	44.43	1.01
500	17.2	2.168	.25	55.20	1.55
600	19.8	2.468	.24	64.38	1.71
700	22.4	2.692	.22	72.51	1.78
800	25.2	2.867	.22	79.87	1.83
900	28.0	3.005	.21	86.64	1.89
1000	30.9	3.117	.21	92.92	1.91
1100	33.9	3.231	.22	98.77	1.90
1200	36.8	3.309	.22	104.34	1.93

Table 6 (continued)

Reaction: $N_2O_5 \longrightarrow NO_2 + NO_3$, $\Delta H^\circ_{298} = +20.5$ kcal/mole

Approximation: $(H^\circ_2 - H^\circ_1)_{NO_3} = (H^\circ_2 - H^\circ_1)_{NO_2} + \frac{1}{2}(H^\circ_2 - H^\circ_1)_{O_2}$

T_2 °K	$H^\circ_2(NO_2 + NO_3) - H^\circ_2(N_2O_5)$ kcal/mole	Δ	$\delta\Delta$	$\underset{\sim}{s}$ cm/msec	$\delta\underset{\sim}{s}$ cm/msec
400	22.7	1.933	.42	45.24	1.82
450	23.9	2.150	.41	50.97	2.27
500	25.1	2.323	.40	56.08	2.43
600	27.7	2.607	.38	65.22	2.55
700	30.3	2.816	.35	73.30	2.57
800	33.1	2.979	.33	80.60	2.56
900	35.9	3.108	.32	87.32	2.57
1000	38.8	3.213	.30	93.56	2.55
1100	41.8	3.301	.30	99.47	2.60
1200	44.8	3.374	.28	105.0	2.6

E. REFERENCES

1.) H. S. Johnston, J. Am. Chem. Soc., 73, 4542 (1951).

2.) J. H. Smith and F. Daniels, J. Am. Chem. Soc., 69, 1735 (1947).

3a.) D. J. Wilson and H. S. Johnston, J. Am. Chem. Soc., 75, 5763 (1953) is paper IV of a series. The earlier papers are:

3b.) H. S. Johnston, ibid., 75, 1567 (1953).

3c.) H. S. Johnston and R. L. Perrine, ibid., 73, 4782 (1951).

3d.) R. L. Mills and H. S. Johnston, ibid., 73, 938 (1951).

4.) R. A. Ogg, Jr., J. Chem. Phys., 15, 613 (1947).

5.) R. A. Ogg, Jr., W. S. Richardson, and M. K. Wilson, J. Chem. Phys., 18, 573 (1950).

6.) A. R. Amell and F. Daniels, J. Am. Chem. Soc., 74, 6209 (1952).

7.) R. A. Ogg, Jr., J. Chem. Phys., 15, 337 (1947).

8.) G. Sprenger, Z. Elektrochem., 37, 674 (1931).

9.) T. Carrington and N. Davidson, J. Phys. Chem., 57, 418 (1953).

10.) D. Britton, N. Davidson, and G. Schott, Discussions Faraday Soc., No. 17, 58 (1954).

11.) D. Britton and N. Davidson, J. Chem. Phys., 23, 2461 (1955).

12.) D. Britton, Thesis, California Institute of Technology, 1955.

13.) R. G. W. Norrish and G. Porter, Discussions Faraday Soc., No. 17, 40 (1954).

14.) R. Courant and K. O. Friedrichs, "Supersonic Flow and Shock Waves," Interscience Publishers, Inc., New York, 1948, Chapter III C.

15.) I. C. Hisatsune, A. P. McHale, R. E. Nightingale, D. L. Rotenberg, and B. L. Crawford, Jr., J. Chem. Phys., 23, 2467 (1955).

16.) L. S. Kassel, "The Kinetics of Homogeneous Gas Reactions," Chemical Catalog Co., New York, 1932, pp. 181-192.

17.) E. J. Jones and O. R. Wulf, J. Chem. Phys., 5, 873 (1937).

18.) J. K. Dixon, J. Chem. Phys., 8, 157 (1940).

19.) T. C. Hall, Jr., and F. E. Blacet, J. Chem. Phys., 20, 1745 (1952).

20.) H. H. Holmes and F. Daniels, J. Am. Chem. Soc., 56, 630 (1934).

21.) W. A. Rosser, Jr., and H. Wise, J. Chem. Phys., 24, 493 (1956).

22.) W. R. Gilkerson, unpublished research in this laboratory.

23.) A. A. Frost and R. G. Pearson, "Kinetics and Mechanism," John Wiley & Sons, Inc., New York, 1953, pp. 63-72.

24.) R. A. Ogg, Jr., J. Chem. Phys., 21, 2079 (1953).

25.) H. S. Johnston and D. M. Yost, J. Chem. Phys., 17, 386 (1949).

26.) E. F. Linhorst and J. H. Hodges, J. Am. Chem. Soc., 56,836 (1934).

27.) R. A. Ogg, Jr., J. Chem. Phys., 18, 572 (1950) has analyzed the data of (26) in terms of recent findings.

28.) L. S. Kassel, op. cit., pp. 93-105.

29.) H. S. Johnston and F. Leighton, Jr., J. Am. Chem. Soc., 75, 3612 (1953).

30.) J. C. D. Brand, J. Am. Chem. Soc., 77, 2703 (1955).

31.) R. Weston, Thesis, Stanford University, 1950.

32.) R. A. Ogg, Jr., private communication to Professor N. Davidson.

33.) "Selected Values of Chemical Thermodynamic Properties," Nat'l. Bur. Standards (U.S.), Circ. 500, Series I, Table 18-2 (1952).

34.) id., Series II, Table 18-1.

35.) K. K. Kelley, "Entropies of Inorganic Substances. Revision (1948) of Data and Methods of Calculation," U. S. Bur. Mines Bull. No. 477, (1950).

36.) F. Daniels and A. C. Bright, J. Am. Chem. Soc., 42, 1131 (1920).

37.) W. M. Latimer, "The Oxidation States of the Elements and their Potentials in Aqueous Solutions," Prentice-Hall, Inc., New York, 2nd. ed., 1952, p. 363.

38.) W. M. Latimer, id., p. 91.

39.) L. Pauling and L. O. Brockway, J. Am. Chem. Soc., 59, 18 (1937).

40.) D. C. Smith, C.-Y. Pan, and J. R. Nielsen, J. Chem. Phys., 18, 706 (1950).

41.) G. Herzberg, "Infrared and Raman Spectra of Polyatomic Molecules," D. Van Nostrand Company, Inc., New York, 1945, p. 161.

42.) K. S. Pitzer, "Quantum Chemistry," Prentice-Hall, Inc., New York, 1953, Appendix 18.

43.) G. Herzberg, op. cit., p. 178.

44.) H. W. Wooley, "The NBS-NACA Tables of Thermal Properties of Gases," National Bureau of Standards, Washington, D. C., Table 15.10, 1950.

45.) "Selected Values of Chemical Thermodynamic Properties," National Bureau of Standards, Washington, D. C., Series III, 1954.

46.) W. F. Giauque and J. D. Kemp, J. Chem. Phys., 6, 40 (1938).

47.) R. E. Nightingale, A. R. Downie, D. L. Rotenberg, B. L. Crawford, Jr., and R. A. Ogg, Jr., J. Phys. Chem., 58, 1047 (1954).

48.) F. Daniels and R. A. Alberty, "Physical Chemistry," John Wiley & Sons, Inc., New York, 1955, p. 342.

49.) F. H. Verhoek and F. Daniels, J. Am. Chem. Soc., 53, 1250 (1931).

50.) M. Bodenstein and F. Boës, Z. phyzik. Chem., A 100, 75 (1922).

51.) E. Wourtzel, Compt. rend., 169, 1397 (1919).

52.) W. A. Noyes, Jr., and P. A. Leighton, "The Photochemistry of Gases," Reinhold Publishing Corp., New York, 1941, p. 64.

53.) R. G. Dickinson and R. T. Dillon, Proc. Nat'l. Acad. Sci. U.S., 15, 695 (1929).

II THE RATE OF DISSOCIATION OF MOLECULAR IODINE

This section consists of two papers describing measurements of the rate of dissociation of molecular iodine in the shock tube. The first of these is reprinted from "The Study of Fast Reactions," a general discussion of the Faraday Society held in Birmingham, England, in April of 1954. The second is copied from a manuscript accepted for publication by the Journal of Chemical Physics on February 20, 1956. The investigation includes experiments in several inert gases and combines the work of the authors indicated in each paper. The present author has contributed only the measurements in argon, helium, and oxygen.

SHOCK WAVES IN CHEMICAL KINETICS

THE RATE OF DISSOCIATION OF MOLECULAR IODINE

By Doyle Britton, Norman Davidson and Garry Schott
Gates and Crellin Laboratories of Chemistry, California Institute of Technology, Pasadena, California

Received 18th February, 1954

Inert gas + *ca.* 1 % I_2 mixtures have been rapidly heated to temperatures of 1060°-1860° K by passage of a shock wave and the rate of the dissociation reaction,

$$M + I_2 \underset{k_R}{\overset{k_D}{\rightleftharpoons}} M + I + I,$$

measured photoelectrically. The reaction times were of the order of 30-300 μsec. The experimental results for the rate constants for recombination are given by $\log_{10} k_R$ (mole^{-2} l.^{2} sec^{-1}) $= 8{\cdot}87 - 1{\cdot}90\ (\pm\ 0{\cdot}14) \log_{10} (T/1000)$, (argon); $\log_{10} k_R = 8{\cdot}85 - 1{\cdot}91\ (\pm\ 0{\cdot}29) \log_{10} (T/1000)$, ($N_2$, assumed to be vibrationally unexcited); $\log_{10} k_R = 9{\cdot}01 - 1{\cdot}44\ (\pm\ 0{\cdot}32) \log_{10} (T/1000)$, ($N_2$ assumed to be vibrationally excited). Comparison of the average high temperature results with those obtained at room temperature by flash photolysis confirms the negative temperature coefficient for k_R but suggests the relation, $k_R = A/T^{1{\cdot}5}$. *The high temperature values for* k_D *for argon fit the equation,* $k_D = 1{\cdot}5 \times 10^7 T^{\frac{1}{2}}(U/RT)^{2{\cdot}8} \exp(-U/RT)$ mole^{-1} l. sec^{-1}, where U = molal energy of dissociation of I_2 at 0° K. The extinction coefficients of I_2 at 490 mμ and 436 mμ were measured as a function of temperature; as expected, the former decreased with temperature and the latter increased. The rate data do not reveal whether the nitrogen is vibrationally unexcited or excited during the time period of the experiments; the extinction coefficient data favour the former possibility.

A shock wave is a positive pressure wave with the shape of a step-function which moves through a gas with a velocity which is greater than the velocity of sound in the unshocked gas, and therefore which is of the order of, or for strong shocks somewhat greater than, the mean molecular velocity. The shock front is a few mean free paths thick, so that, as the shock passes through a particular molecule, the translational and rotational energy of the latter is increased in a time of the order of a few collision times. A shock wave is, therefore, the most rapid method of directly transmitting translational energy to an element of a gas. The number of collisions required to readjust the vibrational energy varies with the nature of the gas.

The rates of chemical reactions in the heated gases behind a shock can be most conveniently studied with the plane, uniform waves generated in a shock tube.[1, 2] Fig. 1 illustrates the basic features of this instrument. The left-hand chamber contains a " driving " gas B at a high pressure; the right-hand chamber contains the gas which is to be shocked, A, at a lower pressure. When the diaphragm D breaks, the gas A is subjected to a compressional pressure wave. The propagation of the various pressure disturbances in the tube is represented in the sequence of pressure profiles in the lower half of the figure. Irregularities caused by the breaking process are smoothed out by the time the pressure wave has propagated downstream a few (3-20) tube diameters and a shock wave S is formed. The uniform pressure behind the shock front characterizes the case in which gas A undergoes no chemical reaction after being shocked. At the same time, B expands

and pushes on A, so that an expansion wave propagates to the left through B. D′ is the boundary between expanded cold B and heated compressed A. In practice the shock front S is well formed but the boundary D′ is not.

For a given initial pressure ratio between chambers B and A the greater the velocity of sound or the molecular velocity of the driving gas B, the greater is the shock strength. It is therefore advantageous for the generation of strong shocks to use hydrogen or helium as B. It is easy to compute that the limiting enthalpy increase per mole (W_A g) of gas A in a shock tube configuration for infinite bursting pressure ratio is $2(W_A/W_B)\gamma_B RT_B/(\gamma_B - 1)^2$, where W refers to molecular weight, γ_B is the heat capacity ratio, and T_B is the initial temperature of gas B.[3]

A light beam and a photomultiplier-oscilloscope combination can be used to observe the initial compression and any subsequent chemical changes provided a reacting component of gas A is coloured. The temperature and density changes across the shock can be computed from the velocity of the shock wave using the quantitative relations described subsequently.

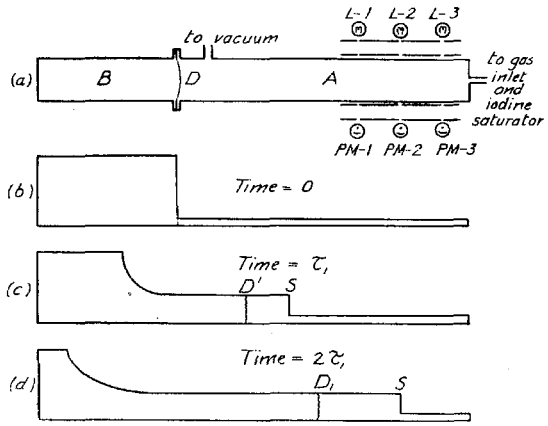

FIG. 1.—(*a*) Schematic diagram of apparatus. B, driving gas; D, diaphragm; A, driven gas (inert gas + iodine mixture); L, lights; PM, photomultipliers. (*b*) initial pressure configuration in the tube. (*c*) and (*d*) pressure configurations after diaphragm bursts. S, shock front; D′, boundary between expanded, cold B, and compressed, hot A.

The time resolution in this method is related to the time for the shock wave to move through the light beam. For a 1 mm beam and a shock of velocity 10^5 cm/sec (typical of the experiments reported here), this is 1μ sec. The gas behind the shock wave is flowing downstream (to the right in fig. 1) so that at a time τ after the shock wave passes the observer at PM-2, the gas at PM-2 has come from farther upstream and has therefore been heated for a time considerably longer than τ. Because of this feature, the true time resolution is that computed above multiplied by a factor equal to the compression ratio across the shock and is 3-7 μsec for our typical experiments.

The measurement, in this laboratory, of the rate of dissociation of N_2O_4 behind a (weak) shock wave at final temperatures of — 20° to 28° C has previously been described.[4] We report here a study of the rate of dissociation of iodine, $M + I_2 \rightarrow M + I + I$, where M is an inert gas (nitrogen or argon), in the temperature range 1060-1860° K. This reaction is of kinetic interest because it is a simple dissociation process and because its rate is known at room temperature from the flash photolysis measurements of the reverse process.[5] Because of its kinetic and experimental simplicity it is well suited for an initial investigation of the use of strong shock waves in high temperature kinetic studies. A problem of interest in the nitrogen investigations was whether the vibrational degree of

freedom of N_2 became excited during the short time of the experiment (*ca.* 4×10^5 collision times) or whether the N_2 behaved as a rigid dumbbell.

Other investigations of elementary processes by means of shock waves include the study of the structure of the shock front itself and the rate of equilibration between translational and rotational energy,[6] and the measurement of vibrational equilibration times.[7]

METHODS

EXPERIMENTATION.—The driving section of the shock tube was a 180 cm length of 15 cm diameter steel pipe. The shock wave section consisted of a 140 cm length of 15 cm aluminium pipe and a 150 cm length of 15 cm Pyrex pipe. Cellulose acetate diaphragms were clamped between the steel and the aluminium sections. The shock wave chamber could be evacuated to 1 μ pressure and degassed or leaked at a rate less than 0·1 μ/min.

The spontaneous bursting pressures of the membranes are not very reproducible ($\pm$ 20 %). Some typical values are: 0·005 in., 1·7 atm; 0·0075 in, 2·2 atm; 0·010 in., 2·1-2·7 atm; 0·015 in., 3·5-4·1 atm. Depending on the experiment, the membranes were allowed to break spontaneously or were induced to break at a slightly lower pressure with a needle. Good shocks were obtained even when the membranes were broken at one-half their spontaneous breaking pressures.

The inert gases used were Linde Air Products Co. argon, stated by the supplier to be better than 99·8 % pure (with the principal impurity nitrogen), and Linde pure dry nitrogen, stated to be 99·90 % pure. In many of the experiments, the N_2 was passed through a 150 cm column of Drierite; within the rather large experimental error, this did not affect the results. These gases were allowed to flow from the cylinder at a regulated pressure of a few psi and at a rate of *ca.* 500 cm^3/min through a flowmeter and then a needle valve across which the pressure dropped to that of the experiment, and then through a 1 cm diameter U-tube packed with a 30 cm length of C.P. iodine. The gas mixture entered the shock tube at the downstream end, flowed through the tube, and then out via a needle valve to a trap at $-$ 80° and a pump. The only significant constrictions were the needle valves; and the flowing gas between them was at a constant pressure. The total pressure was measured with a dibutyl phthalate manometer and the iodine partial pressure computed from the temperature of the saturator (measured to 0·10°) and vapour pressure data.[8] The shock tube was isolated just before breaking the membrane, by closing wide-bore stopcocks lubricated with Silicone grease.

Observations were made with light beams defined by 2·5 cm by 1 mm slits on both sides of the shock tube. The light sources were 500 W tungsten projection lamps operated from a d.c. generator. Observations with $\lambda = 436$ mμ were made with a Hanovia medium pressure d.c. mercury arc, Sc 5031. *Schlieren* and total internal reflection at the shock front can bend a light ray several degrees. It is therefore necessary to use a well-collimated sheet of light if the sharp change in density at the shock front is to be observed. The four slit system indicated in fig. 1 achieved this end.

The transmitted light was passed through suitable filters and the intensity changes measured with RCA 931 photomultipliers and a Tektronix 512 oscilloscope. Typical operating conditions were 80 V/dynode, 100 μA output current, and electronics rise time about 1 μsec. The signal/noise ratio is limited by the intensity of the light sources and was about 50. Three or four light beams were used, each one being 10·0 or 20·0 cm downstream from the preceding one, and the first one being 240 cm (16 tube diameters) from the membrane.

Several slightly different systems for obtaining data were used. The one used for most of the experiments is illustrated in fig. 2. The amplified signal from the first photomultiplier, PM—1, triggers a univibrator trigger circuit when the shock wave passes this station. This triggers two delay circuits. The delayed output of one of these triggers a single horizontal sweep of the oscilloscope at a suitable time (30-150 μsec) later. The delay time of the second circuit is accurately known from careful calibrations ($\pm$ 1 μsec) and this output pulse is mixed into the vertical amplifier system. Its position on the trace essentially gives the time that the shock wave passes PM—1. The particular oscilloscope used is provided with a difference amplifier and the difference in photocurrent between PM—2 and PM—3 is recorded as the vertical deflection. Until the shock wave reaches station 3, this is essentially the photoelectric record of the change in iodine concentration at station 2. From the record one can measure the average velocity between stations 1 and 2 and between 2 and 3. The pictures also contain vertical calibration

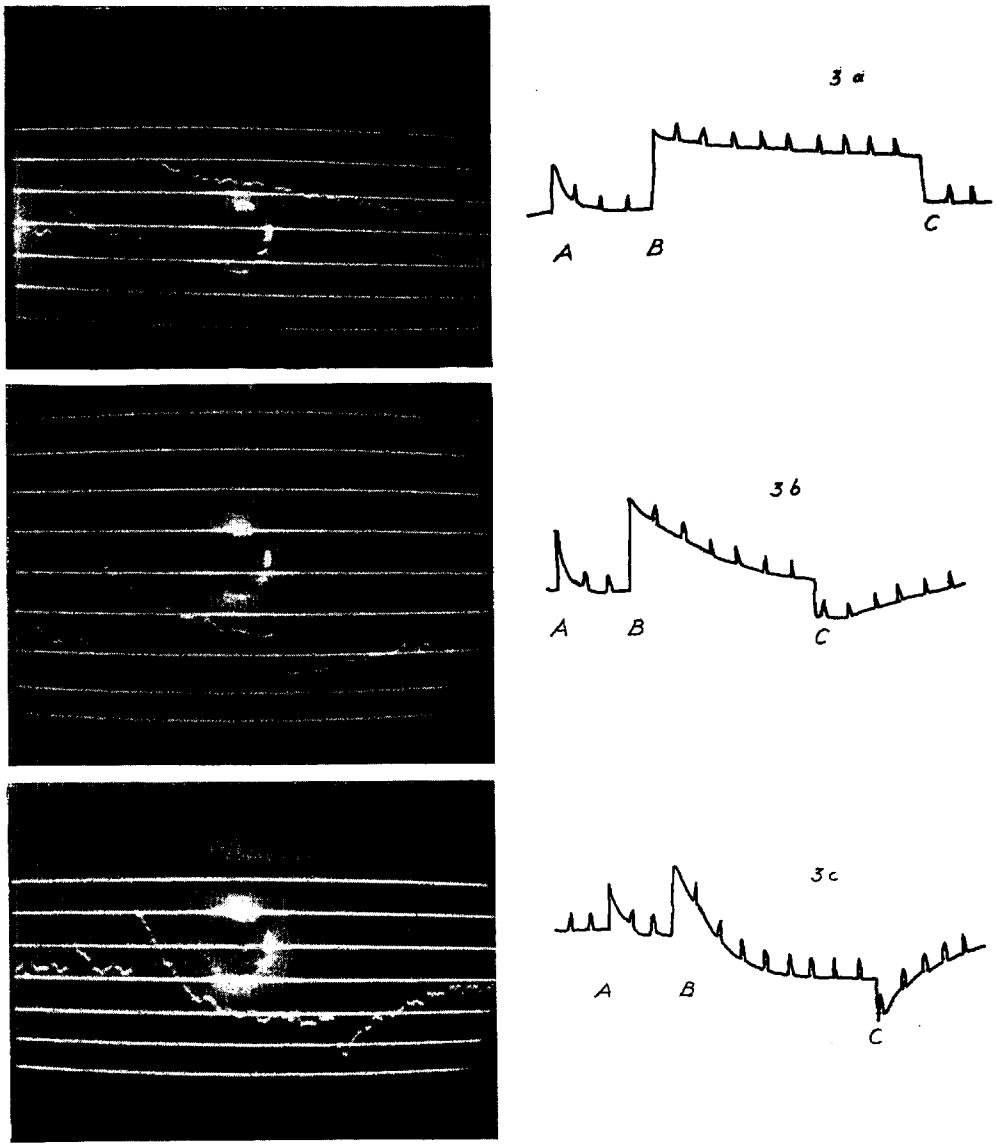

FIG. 3.—Oscillograph records of photocurrent for typical experiments. A, signal from delay circuit 2, related to arrival of shock wave at PM—1; B, compression as shock front passes PM—2 (increasing photocurrent from this station deflects the trace down); C, compression as shock front passes PM—3 (end of experiment). The small pips are 10μ sec timing markers. The smooth horizontal traces are evenly spaced voltage calibrations.

Photograph	*a*		*b*		*c*
	argon		nitrogen		argon
c_1	$2{\cdot}27 \times 10^{-3}$ mole/l.		1·65		1·75
ϕ	$0{\cdot}484 \times 10^{-2}$		0·524		0·623
s	$1{\cdot}000 \times 10^{5}$ cm/sec		1·429		1·136
		*		†	
Δ_0	3·10	4·65		4·97	3·26
T_0	1195° K	1276		1216	1455
α_∞	0·79	0·90		0·82	0·97
Δ_∞	3·27	4·73		5·03	3·46
T_∞	1172° K	1253		1195	1422

Subscripts zero refer to conditions immediately behind the shock front. Subscripts ∞ refer to equilibrium with respect to iodine dissociation.

* calculations made assuming N_2 to be not vibrationally excited.

† calculations made assuming N_2 to be vibrationally excited.

[*To face page* 60

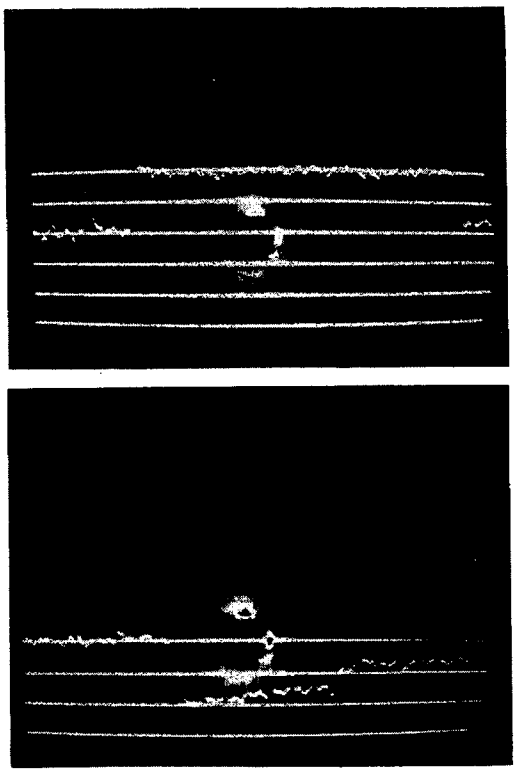

FIG. 4.—(*a*) Shock wave heating an argon + iodine mixture to 953° K, where the rate of dissociation is negligible; (*b*) shock wave heating an argon + iodine mixture to 2100° K, where the dissociation is complete and rapid. The subsequent decrease in photocurrent is attributed to cooling at the walls.

[*To face page* 61

marks applied with a precision potentiometer (Helipot) and time markers on the sweep from a 100 kc crystal controlled oscillator.

An improved procedure has been to measure the time for the shock to travel between stations 1 and 3 or 4 with a Potter Model 456 1·6 Megacycle Counter Chronograph which is a time interval meter that can be triggered on and off by univibrator voltage pulses from the photoelectric stations. Two oscilloscopes are available and two independent photoelectric records can be made from PM—2 and PM—3. The time scales of the two sweeps can be interrelated so that the average velocities between all the successive stations are known.

CALCULATIONS.—Fig. 3 and 4 show some typical oscilloscope records for shock waves heating inert gas + iodine mixtures (*ca.* 1 % I_2). When the shock passes through the light beam, the light transmission abruptly decreases because of the compression and then gradually increases as the iodine molecules dissociate into an equilibrium mixture of atoms and molecules.

Quantitative interpretation requires a knowledge of the conditions of the heated gas, specifically of its temperature and density and of the extinction coefficient of molecular iodine at the high temperature. As the endothermic dissociation reaction occurs, the gas mixture cools and compresses somewhat. The photoelectric curve of light transmission as a function of time, after the initial step due to the shock compression, results

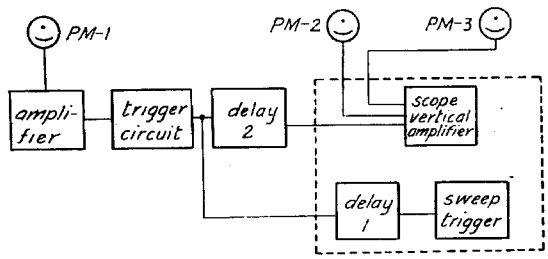

FIG. 2.—Block diagram of the recording system. Circuits enclosed by the dotted line are part of the oscilloscope.

from a combination of (*a*) a decrease in iodine molecule concentration due to dissociation, (*b*) an increase in iodine molecule concentration due to compression, and (*c*) a change in extinction coefficient due to the change in temperature. Fortunately, effect (*a*) is much larger than (*b*) or (*c*). The kinetics are complicated by the following factors. As the molecular iodine dissociates, the reverse recombination reaction $I + I + M \rightarrow I_2 + M$ must also be considered. Since the gas behind the shock is flowing downstream, a transformation from laboratory time to the time that molecules in the light beam have been heated is introduced. The rate constant for dissociation is a function of temperature and therefore changes as the reaction proceeds. It is the object of this section to outline the calculational procedure for making all these corrections. Because the iodine is highly diluted with inert gas (*ca.* 1 : 100) the changes in density, temperature, and extinction coefficient are small and the corrections are readily made. The legends to fig. 3 give typical examples of the changes.

For a perfect gas of constant heat capacity, the temperature and density of the gas just behind the shock can be expressed as simple closed functions of the initial conditions and the velocity of the shock wave.[9] For a general fluid, a numerical solution of the following equations is required:

$$\frac{H_2 - H_1}{W} = \frac{1}{2}(P_2 - P_1)\left(\frac{1}{D_1} + \frac{1}{D_2}\right), \tag{1}$$

$$s^2 = \frac{D_2}{D_1}\frac{P_2 - P_1}{D_2 - D_1} \tag{2}$$

where subscripts 1 and 2 refer to conditions in the unshocked and shocked gas, respectively, W = mean molecular weight of the unshocked gas, H = enthalpy per W g of gas, P = pressure, D = density, and s = shock velocity. The enthalpy is a function of P_2 and D_2 (for a perfect gas with variable heat capacity it is a function of P_2/D_2, that is,

of the temperature). For a given s the above equations can be solved. For a shock wave propagating at a constant velocity down a tube of uniform cross-section, these equations apply to the properties of the fluid at any point behind the shock. In particular, for a reacting gas, the enthalpy can be expressed as a function of temperature and of a reaction variable (which in the present instance is α, the degree of dissociation). For a given shock (fixed s), the pressure, density and temperature can therefore be determined as functions of α.

Let $\pi = (P_2/P_1)$, $\theta = (T_2/T_1)$, $\Delta = (D_2/D_1)$, U = molal energy of dissociation of I_2 gas at 0° K, $\beta = 2[(H - H_0)/RT] - 1$, ϕ = mole fraction I_2 in the initial gas. The quantity β is related to an effective heat capacity for the gas. Superscripts M, I_2, and I refer to inert gas, iodine molecules, and iodine atoms. The perfect gas law is,

$$\pi = (1 + \phi\alpha)\Delta\theta.$$

Eqn. (1) and (2) become:

$$\begin{aligned}\pi = {} & (1 - \phi)(\beta_2^{\mathrm{M}}\phi - \beta_1^{\mathrm{M}}) \\ & + \phi\{[(1 - \alpha)\beta_2^{\mathrm{I}_2} + 2\alpha\beta_2^{\mathrm{I}}]\theta - \beta_1^{\mathrm{I}_2} + 2\alpha(U/RT_1)\} \\ & + (1 + \phi\alpha)(\theta/\pi), \end{aligned} \tag{3}$$

$$s^2 = \frac{RT_1}{W}\,\frac{(\pi - 1)}{(1 - (1/\Delta)}. \tag{4}$$

With these equations and thermodynamic tables,[10] numerical values for π, Δ and s as functions of θ and α can be calculated for an assumed value of ϕ. These can be graphed so as to show the variation of Δ and θ with α at particular values of s. The characteristics of the shock wave were computed for $\phi = 0$ and, as a function of α, for $\phi = 0{\cdot}01$, and it was shown by a few additional calculations that for the range of ϕ used ($\phi < 0{\cdot}025$), a linear extrapolation or interpolation was satisfactory. Two separate sets of calculations for nitrogen were made assuming: (*a*) that $H_2^{\mathrm{M}} - H_1^{\mathrm{M}} = (7/2)R(T_2 - T_1)$, i.e. that during the time of the experiment the N_2 remained vibrationally unexcited, and (*b*) using the thermal equilibrium values for H_2^{M}.

If the velocity of the flowing gas behind the shock is v, conservation of mass in steady-state flow requires $\Delta = s/(s - v)$. The transformation between "molecule" time t and laboratory time τ is then readily shown to be $\mathrm{d}t = \Delta\mathrm{d}\tau$. For the chemical reaction, $\mathrm{M} + \mathrm{I}_2 \rightleftharpoons \mathrm{M} + \mathrm{I} + \mathrm{I}$, the rate equation is $-[\partial(\mathrm{I}_2)/\partial t]_\Delta = k_{\mathrm{D}}(\mathrm{M})(\mathrm{I}_2) - k_{\mathrm{R}}(\mathrm{M})(\mathrm{I})^2$; $k_{\mathrm{R}} = k_{\mathrm{D}}/K$, where K is the equilibrium constant (dimensions, moles/l.) for the chemical equation above. The rate equation can be transformed to

$$\mathrm{d}\alpha/\mathrm{d}\tau = k_{\mathrm{R}}\Delta^3[(c_1K(1 - \alpha)/\Delta) - 4\phi c_1^2\alpha^2], \tag{5}$$

where c_1 = total concentration of unshocked gas (mole/l.). The quantity Δ changed at most by 10 % from $\alpha = 0$ to $\alpha = 1$, whereas K changed typically by 50 %, but both Δ^3 and K/Δ were, to a satisfactory approximation, linear functions of α. This makes t possible to integrate eqn. (5).

$$\begin{aligned}\frac{-1}{K_0\Delta_0^2c_1}\Bigg\{ & \left[1 + \frac{4(\xi + \eta)}{(1 - \eta)^2}\right]^{-\frac{1}{2}}\left[\frac{2(\xi + \eta) - \zeta(1 - \eta)}{2(1 - \eta)[(\xi + \eta) - \zeta^2 - \zeta(1 - \eta)]}\right] \\ & \times \ln\left[\frac{\alpha_\infty - \alpha}{(1 - \eta) - (\xi + \eta)(\alpha_\infty - \alpha)}\right] - \left[\frac{\zeta/2}{(\xi + \eta) - \zeta^2 - \zeta(1 - \eta)}\right] \\ & \times \ln\left[\frac{(\alpha_\infty - \alpha)[(1 - \eta) + (\xi + \eta)(\alpha_\infty + \alpha)]}{(1 + \zeta\alpha)^2}\right]\Bigg\} = k_{\mathrm{R}}\tau + \text{constant}, \end{aligned} \tag{6}$$

where

$$\xi = \frac{4\phi c_1\Delta_0}{K_0},$$

$$\eta = \frac{\mathrm{d}\ln K}{\mathrm{d}\alpha} - \frac{\mathrm{d}\ln\Delta}{\mathrm{d}\alpha} - \frac{3}{4}\,\frac{\mathrm{d}\ln k}{\mathrm{d}\alpha}\,\frac{\mathrm{d}\ln\Delta}{\mathrm{d}\alpha},$$

$$\zeta = \frac{3\mathrm{d}\ln\Delta}{\mathrm{d}\alpha}.$$

Subscript zero refers to conditions just behind the shock wave at $\alpha = 0$.

On the oscilloscope records one determines α at various points in time behind the shock. This involves knowing the density as a function of α (from measured velocity), the initial concentration, and the extinction coefficient of I_2 as a function of temperature (i.e. α). These values of α at times τ are inserted in eqn. (6) and the indicated function plotted against τ. The slope of this plot gives k_R and $k_D = k_R K$. The basic assumption here is that k_R is temperature independent and k_D has the same temperature dependence as K. The results of the experiments show this is not so but correcting for this effect would change the individual k_D's by less than 5 % and the temperature dependence not at all. It may be mentioned that for cases where at equilibrium $\alpha > 95$ %, the effect of the back reaction can be neglected and a simpler integrated rate equation used.

RESULTS AND DISCUSSION

DISSIPATIVE EFFECTS

Other workers have observed, by means of flash interferograms or *Schlieren* pictures, that the shock waves generated in shock tubes are planar and normal to the tube walls.[2] In most of our experiments when the light beam was properly aligned and collimated, the abrupt decrease in photocurrent as the shock wave passed the light beam occurred in 1-2 μsec, indicating that the shock front was well formed, plane, and perpendicular to the tube axis.

Fig. 4*a* shows a shock wave heating an argon + iodine mixture to 953° K where the rate of dissociation is negligible. The photocurrent is constant to $\pm$ 1 % for 220 μsec of laboratory time (600 μsec molecule time) indicating that there is no appreciable cooling and compression at the walls.

Fig. 4*b* shows a shock wave heating an argon + iodine mixture to 2100° K where the dissociation occurs in about 20μ sec. The photocurrent then corresponds to 100 % transmission. There is a subsequent slow decrease in photocurrent which, we surmise, is due to re-association in a cooled layer next to the walls. In this case there is a decrease in transmission of about 5 % over a period of about 70 μsec (laboratory time), which means that a layer of gas about 1/40 the diameter of the tube (i.e., 0·4 cm) has cooled to below 1100° K where the re-association becomes large. It was noted that, as expected, this cooling effect was greater at low gas densities. A rough estimate of the rate of cooling may be made as follows. The thermal conductivity [11] of argon at 1500° is about $1{\cdot}1 \times 10^{-4}$ cal cm^{-1} sec^{-1} and the heat diffusivity at a concentration of 3×10^{-6} moles/cm^3 (the concentration of the shocked gas for fig. 4*b*) is about 12 cm^2 sec^{-1}. Therefore in 240 μsec (molecule time for this experiment), the mean diffusion distance $(2\,Dt)^{\frac{1}{2}}$, is calculated as 0·08 cm, compared to the 0·40 cm which is the crude observation. If gas in a cylinder is uniformly heated to a temperature above that of the wall and if a concentric ring of gas at the wall, dr thick, cools by conduction so completely that it effectively contracts to a much smaller volume, the gas in the middle of the cylinder will expand outward adiabatically and therefore cool. The magnitude of this cooling effect is $(dT/T) = 2(\gamma - 1)\,(dr/r)$. Taking $dr = 0{\cdot}20$ cm as a compromise between the experimental and theoretical values for the thickness of the cooled layer, the computed value dT/T for the main body of gas is 0·03.

Experiments at the higher temperatures were done at low gas densities to increase the reaction time; nevertheless, the rate of dissociation was so fast that a slope like that of fig. 4*b* and a cooling like that computed above are not serious. In experiments at lower temperature, the gas density was higher and cooling less important. The kinetic results did not show any anomalies or variations with pressure that could be attributed to cooling effects. The evidence is, therefore, that cooling effects due to the walls were not large enough seriously to affect the kinetic results of this investigation. It should be emphasized that there is no satisfactory experimental or theoretical treatment of dissipative phenomena in a shock tube; the problem is quite complicated because it involves both heat conductivity and viscosity effects. It is probable that these dissipative effects will be

limiting factors in the quantitative study of reaction rates at still higher temperatures by the shock tube method.

In almost all of the experiments, the two average velocities measured with three photoelectric stations at 10 or 20 cm intervals agreed to 1½ %. The apparent accceleration was sometimes positive and sometimes negative. It is not known to what extent this change in velocity is due to experimental error in measuring the oscilloscope records or to a lack of reproducibility in the delay time of the calibrated delay circuit, rather than to a real change in strength of the shock wave. A few experiments were discarded because the velocity change between successive stations was as high as 4 % The temperature of the reacting gas is calculated from the shock velocity and is approximately proportional to the square of the velocity, so that a 1 % uncertainty in velocity corresponds to a 2 % uncertainty in temperature. At 1500° K, the corresponding uncertainty in the rate constant for dissociation is $\pm$ 26 %, which is about the same as the mean deviation of the results.

EXTINCTION COEFFICIENTS

Most of the observations were made with the light from a 500-W tungsten filament projection bulb with the colour temperature defined by operation at 120 V. The light filters were a Bausch and Lomb interference filter with a measured maximum transmission of 36 % at 487 mμ, a half width of 8 mμ and a transmission of the order of ½-1 % through the rest of the spectrum, and a Corning no. 3385 sharp cut filter with a transmission of 50 % at 487 mμ, of 37 % at 481 mμ, and which was opaque to bluer light. The detector was an RCA 931 photomultiplier. The molar extinction coefficient of I_2 at room temperature, $\epsilon = \log_{10} (I_0/I)/cl$ mole^{-1} l. cm^{-1}, for this particular optical system, was found to be 450 $\pm$ 20, by measuring the photocurrent in front of and behind shocks of sufficient strength to dissociate more than 99 % of the I_2 present in an argon 1 % I_2 mixture, as in fig 4*b*. This value is the same as that at 490 mμ as measured in a Beckman spectrophotometer [12] and we take 490 mμ as the effective wave length of the light. In previous experiments using the interference filter without the cut-off filter, lower values of ϵ were observed because of a greater contribution from blue light.[5c] For some shocks in nitrogen, ϵ at 436 mμ was measured using a mercury arc, a 436 mμ interference filter, and a Corning no. 3389 sharp cut filter which was down to 37 % transmission at 436 mμ. The value of 30 for ϵ at room temperature was taken from spectrophotometer experiments.

The high temperature extinction coefficients were found by extrapolating the photocurrent records back to zero time visually, and computing the concentration of I_2 just behind the shock from the compression ratio which is calculated from the shock velocity.

Curve A of fig. 5 displays the results in argon for 490 mμ and fig. 6 gives the results in N_2 at 436 mμ. As expected in view of the potential curves and by analogy with the other halogens,[13] the extinction coefficient at 490 mμ falls with temperature because the extinction coefficient of the zeroth vibrational state is greater than that of the higher vibrational states at this wavelength, and the extinction coefficient at 436 mμ rises with temperature, because the reverse is the case.

Fig. 5 also shows the absorption coefficients at 490 mμ measured in nitrogen experiments and computed assuming that the nitrogen behind the shock is not vibrationally excited (curve B) and is vibrationally excited (curve C). The experimental points are shown for curve B and the scatter of the points is about the same for the other curves. The wave length 490 mμ is beyond the convergence limit of the discrete spectrum of I_2, and the absorption coefficient should be independent of inert gas. Curves A and B coincide within the limit of experimental error but curves A and C (vibrationally excited N_2) do not. This suggests that

the nitrogen is not vibrationally excited for at least 25 μsec (typically 4×10^4 nitrogen-nitrogen collisions) after being shocked, but, in view of the rather large experimental error, this conclusion is only a tentative one.

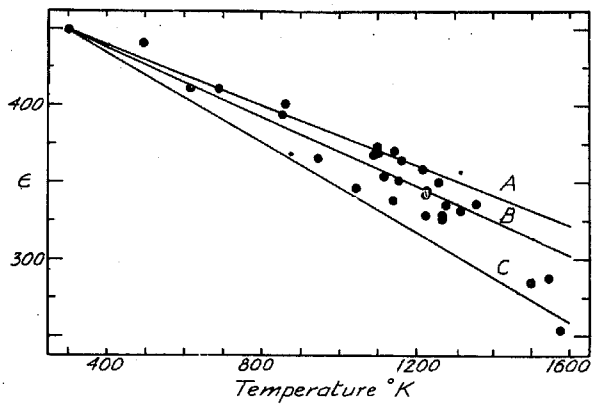

FIG. 5.—Extinction coefficients for I_2 at 490 mμ. A, argon; B, N_2 assumed vibrationally unexcited; C, N_2 assumed vibrationally excited. The experimental points for curve B only are shown.

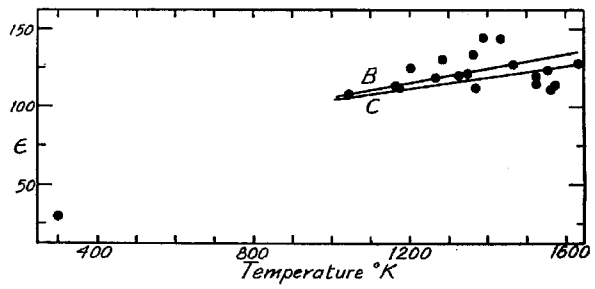

FIG. 6.—Extinction coefficients for I_2 at 436 mμ in N_2. B, assumed unexcited, points shown; C assumed excited.

KINETICS

Fig. 7 shows the results of this investigation plotted as $\log_{10} k_R$ against $\log_{10} T$ for argon, nitrogen assumed to be vibrationally unexcited, and nitrogen assumed excited. Parameters for straight line plots of the results have been found by least squares (using for convenience the erroneous assumption that the temperatures are known with certainty):

$\log_{10} k_R$ (moles^{-2} l.^{2} sec^{-2}) $= -1{\cdot}90\ (\pm 0{\cdot}14) \log_{10} (T/1000) + 8{\cdot}87$ (argon),
$\log_{10} k_R = -1{\cdot}91\ (\pm 0{\cdot}29) \log_{10} (T/1000) + 8{\cdot}85$ (N_2 unexcited),
$\log_{10} k_R = -1{\cdot}44\ (\pm 0{\cdot}32) \log_{10} (T/1000) + 9{\cdot}01$ (N_2 excited),

where the indicated uncertainties are probable errors. The mean deviations of the experimental rate constants from the calculated curves are $\pm$ 11 % (argon), $\pm$ 22 % (nitrogen-excited or unexcited). We cannot at present evaluate all the sources of experimental error. As noted previously, there is an uncertainty of the order of 26 % in the rate constants due to possible errors in the measurement of shock velocity. It appears that there are also significant errors in reading the oscillograph records and in making the elaborate calculations involved in interpreting the data. We do not know why the nitrogen results show greater scatter than the argon results. Over a threefold variation in total pressure at a fixed

temperature, the rate showed the expected first-order dependence on inert gas concentration.

Fig. 8 shows the results of this investigation at 1060-1860° K and of the various flash photolysis measurements of k_R, mainly at room temperature,[5] as a $\log_{10} k$

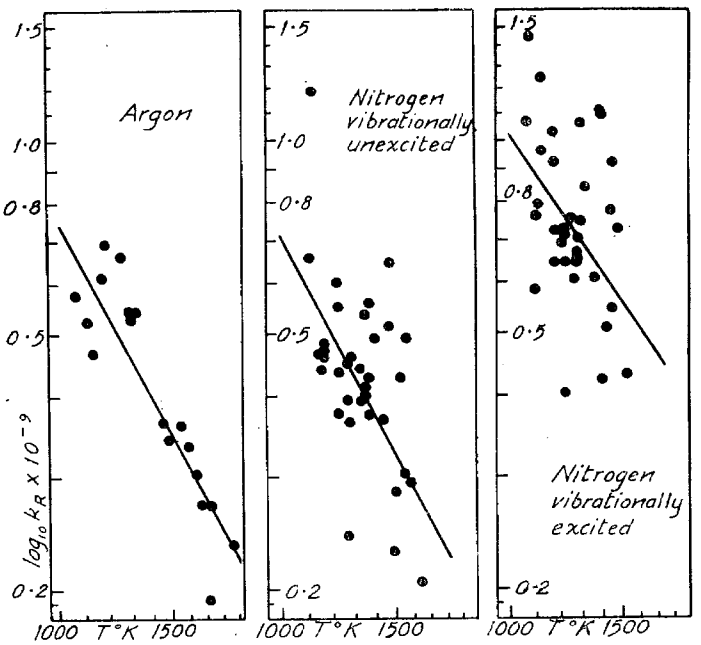

FIG. 7.—Recombination rate constants.

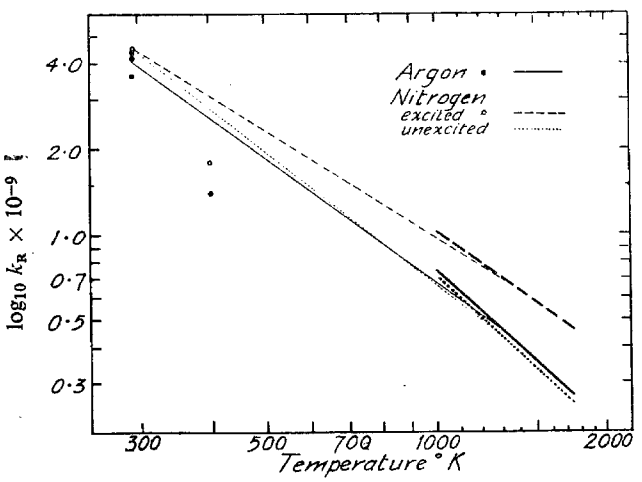

FIG. 8.—Recombination rate constants. Points are the low-temperature flash-photolysis results. Heavy lines are the results of this research. The light lines go through the average room temperature results and the average high temperature results.

against $\log_{10} T$ plot. In spite of the present experimental uncertainties both at high and low temperatures, it is clear that k_R decreases quite significantly with

temperature. The slope of a straight line through the average of the room temperature argon results and an average high temperature argon result is 1·49 i.e., $k_R = A/T^{1.49}$, as compared to a slope of 1·90 for the high temperature results above. It is possible but by no means certain that this change in slope is real. The slopes of the $\log_{10} k$ against $\log_{10} T$ plots through the room temperature and the average high temperature results for nitrogen are 1·59 (unexcited), 1·26 (excited).

The temperature coefficients of k_R obtained at Manchester by flash photolysis [5b] at 293° and 400° K are larger than those reported here and correspond to $n = 3{\cdot}0$ for an assumed power law dependence, $k_R = A/T^n$. It is most probable that the conflicting result obtained in Pasadena [5c] by flash lamp experiments that k_R for *neo*pentane is constant from 298° to 473° K is wrong. A curve going through both the Manchester and the shock wave points is irregular and bumpy in an implausible way; probably one set of data or the other are wrong in so far as the temperature coefficients are concerned. The shock wave experiments cannot be extended to lower temperatures because the rate of dissociation is too slow; further careful flash lamp experiments over a range of temperatures will be of great interest.

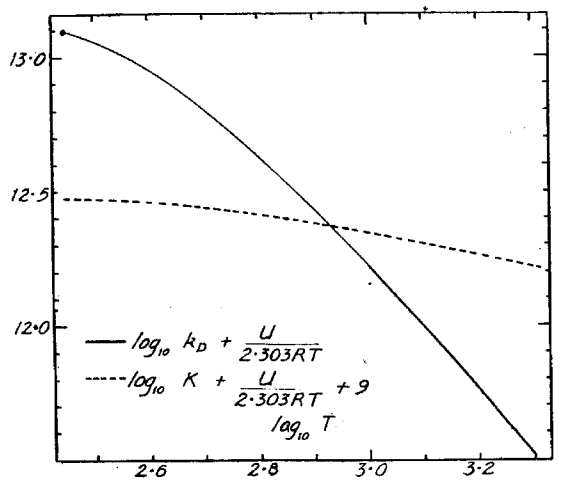

FIG. 9.—Temperature dependence of the rate constant (inert gas, argon) and the equilibrium constant for I_2 dissociation.

It is of interest to consider the temperature coefficient of k_D, the rate constant for dissociation. Fig. 9 displays the temperature dependence of $\log k_D + U/2{\cdot}303\,RT$ for argon and $\log K + U/2{\cdot}303\,RT$, where $U = 35{,}544$ cal. The former, of course, decreases more rapidly with temperature; the high temperature data fit the equation

$$k_D = (A/T^{2.3}) \exp(-U/RT),$$

although the room temperature results fall considerably below this.

In conclusion then, the main results of the present investigation is to provide additional evidence that k_R decreases with temperature, and that this dependence can be approximated by $k_R = A/T^{1.5}$. The physical significance of this result is that the average kinetic energy in a system undergoing a recombining three-body collision is less than the average kinetic energy of all three-body collisions. By microscopic reversibility, in a dissociating collision between an inert gas molecule and an iodine molecule, the resulting iodine atoms and inert gas molecule have less than the average kinetic energy as they fly apart. The rate constant for dissociation can be described by the equation,

$$k_D = 1{\cdot}50 \times 10^7\, T^{\frac{1}{2}}\, (U/RT)^{2.83} \exp(-U/RT) \text{ moles}^{-1}\text{ l. sec}^{-1}.$$

The " collision theory " interpretation of this kind of a rate expression is that several degrees of freedom other than translation along the line of centres contribute energy to the dissociation process.

It is to be noted that in the rate constants which have been used for making calculations about $H_2 + Br_2$ flames, it has been assumed that the rate constant for recombination is a constant and that the pre-exponential factor for k_D increases with temperature.[14]

The kinetic results for nitrogen do not reveal whether or not it remains vibrationally unexcited during the time of an experiment (typically, about 4×10^5 nitrogen-nitrogen collisions and 4×10^3 nitrogen-iodine collisions). The extinction coefficient measurements make it appear probable, but not certain, that for the first 10^4 collisions the nitrogen remains unexcited. It is of course conceivable that the nitrogen relaxed vibrationally during the course of the iodine dissociation reaction. This would make the measured values of k_R too low. With the present limited experimental accuracy there is no possibility of recognizing such a phenomenon. It may be recalled that impact tube measurements [15] indicate that vibrational equilibration requires at least 10^7 nitrogen-nitrogen collisions at 600°-700° K, whereas *ca.* 3×10^4 collisions between N_2 and H_2O are required for vibrational adjustment of the N_2.

We are grateful to the O.N.R. for its support of this research. One of us (D. B.) is the recipient of a fellowship from Du Pont, Co.

[1] Payman and Shepherd, *Proc. Roy. Soc. A*, 1949, **186**, 293.
[2] Bleakney, Weimer and Fletcher, *Rev. Sci. Instr.*, 1949, **20**, 807.
[3] Resler, Lin and Kantrowitz, *J. Appl. Physics*, 1952, **23**, 1390.
[4] Carrington and Davidson, *J. Physic. Chem.*, 1953, **57**, 418.
[5] (*a*) Christie, Norrish and Porter, *Proc. Roy. Soc. A*, 1953, **216**, 152. (*b*) Russell and Simons, *Proc. Roy. Soc. A*, 1953, **217**, 271. (*c*) Marshall and Davidson, *J. Chem. Physics*, 1953, **21**, 659.
[6] Greene and Hornig, *J. Chem. Physics*, 1953, **21**, 617.
[7] Schwartz, Slawsky and Herzfeld, *J. Chem. Physics*, 1952, **20**, 1591.
[8] Giauque, *J. Amer. Chem. Soc.*, 1931, **53**, 510.
[9] ref. 1, p. 313 or any standard treatise on gas dynamics.
[10] *Selected Values of Chemical Thermodynamic Properties* (National Bureau of Standards, Washington, series III, 1947).
[11] *Tables of Thermal Properties of Gases* (National Bureau of Standards, Washington, 1951), table 19.42.
[12] DeMore and Davidson, private communication.
[13] (*a*) Acton, Aickin and Bayliss, *J. Chem. Physics*, 1936, **4**, 476. (*b*) Gibson, Rice and Bayliss, *Physic. Rev.*, 1933, **44**, 193.
[14] Cooley and Anderson, *Ind. Eng. Chem.*, 1952, **44**, 1402.
[15] Huber and Kantrowitz, *J. Chem. Physics*, 1947, **15**, 275.

PRINTED IN GREAT BRITAIN AT
THE UNIVERSITY PRESS
ABERDEEN

Shock Waves in Chemical Kinetics: Further Studies on the Rate of Dissociation of Molecular Iodine.

Doyle Britton, Norman Davidson, William Gehman, and Garry Schott

Gates and Crellin Laboratories of Chemistry
California Institute of Technology

Abstract

The rate of the dissociation reaction,

$$M + I_2 \underset{\underline{k}_R}{\overset{\underline{k}_D}{\rightleftharpoons}} M + I + I,$$

has been measured by the shock tube method for argon, helium, nitrogen, oxygen, and carbon dioxide as inert gases, M, in the temperature range 1000°-1600°K. The shock wave results by themselves and the comparison of the shock wave measurements with the room temperature measurements of $\underline{k}_R$ by flash photolysis both show that $\underline{k}_R$ has a negative temperature coefficient. The absolute value of this negative temperature coefficient derived from the shock wave measurements is greater than the value derived from comparison of the average high temperature result with the room temperature result for any particular gas. This may be due to experimental error in the determination of $d\underline{k}_R/d\underline{T}$ at the high temperatures, but it is believed that the values of $\underline{k}_R$

determined in the middle of the temperature range studied (Table I) are reliable.

The experimental evidence indicates that, for the measurements with CO_2, the rate of vibrational equilibration is so fast that the observations made here pertain entirely to vibrationally equilibrated CO_2. Evidence from other experiments indicates that the rate of vibrational relaxation in oxygen is such that most of the dissociation reaction occurs in relaxed O_2, but that nitrogen remains vibrationally unexcited under the conditions of the dissociation reactions studied here.

The ratio, $\underline{k}_{R,I_2}/\underline{k}_{R,A}$, of the efficiencies of iodine and argon as third bodies is not greater than 30 at 1300°K whereas it is 250-600 at room temperature. The hypothesis is proposed that in general the ratio $\underline{k}_{R,gas}/\underline{k}_{R,A}$ for complex gases will decrease with increasing temperature.

* * * * * * * * *

In a previous communication[1] the application of the shock wave method to the study of the rate of dissociation of molecular iodine was reported. The kinetic results were computed as rate constants for the reverse recombination process

(1) $\quad I + I + M \longrightarrow I_2 + M,\ d(I_2)/d\underline{t} = \underline{k}_R(I)^2(M)$

M represents a "third body" gas molecule. Values of $\underline{k}_R$ at room temperature for a number of gases as M were first measured by the photostationary state method.[2] More

recently, measurements of k_R at room temperature (and a few at 127°C) have been made by the flash photolysis method.[3] (4)(5)(6)(7)(8)

Neither the flash lamp results nor the shock wave results are as yet satisfactorily accurate or precise. However, several significant conclusions are already apparent and further problems are suggested.

The present set of measurements which consists in part of the repetition of our previous experiments and in part of measurements with different gases and with different ratios of iodine to inert gas, were performed in order to extend our knowledge of reaction (1) and to test the accuracy and limitations of the shock wave method of measuring reaction rates.

Experimental. - The technique was essentially as described previously. An improved system for aligning and collimating the light beams was used in the spectrophotometric measurements. Each light beam from a 500 watt projection lamp was defined by a set of three slits, each 2.5 cm by 1.00 mm. Light from a lamp 17 cm from the tube passed through the first slit 1 cm from the tube, then through the 15 cm tube, through another slit 1 cm from the tube, through the third slit 16 cm from the tube, through some filters, and onto the photomultiplier, 9 cm further on. There were four light beams and slit systems, 10.000 $\pm$ .005 cm apart. The slit systems were perpendicular to the tube axis to within an angle of 1.4×10^{-3} radian. The plane containing the

successive first slits was parallel to the tube axis to 3 x 10^{-3} radian, as were the planes for the second slits and the third slits. The 6 inch (15 cm) Pyrex pipe used for the shock tube was of uniform wall thickness and the diameter varied by 0.1 cm over a 100 cm length of the pipe in such a way that the maximum angular variation of the walls from parallel was 4 x 10^{-3} radian.

The collimation systems were such that, for a shock wave requiring 1 μsec to actually traverse the 1 mm width of the slits, schlieren and reflection effects at the shock front would cause a rise time of 3 μsec or less for the step function change in photocurrent as the shock passed by the light beam. Most of the shock waves showed rise times within this limit. In some cases, rise times of 5 to 7 μsec were observed, indicating that the shocks were, to a small degree, curved or not normal to the tube axis.

Extinction coefficients at high temperatures were measured by extrapolating the oscilloscope traces back to zero time to obtain the initial change in photocurrent. The effective wave length obtained from the tungsten lamp with a Bausch and Lomb interference filter and a Corning no. 3385 sharp cut filter was 487 mμ. In experiments on helium and oxygen, the same interference filter and a Corning no. 3389 sharp cut filter were used, and the effective wave length was 484 mμ. The 436 mμ mercury line was isolated with a Bausch and Lomb interference filter and a Corning no. 3389 sharp cut filter.

Dissipative Effects. - It was noted in a set of special experiments using two electronic timers that the shock waves were of uniform velocity to ± 1% over two 10.0 cm intervals starting at 245 cm and 265 cm from the membrane. Spectrophotometric rate measurements were normally made at the 255 cm and 265 cm stations. The curves of photocurrent vs. time in shocked compressed gases at temperatures below 900°K, where dissociation is negligible, were constant to 1% or better over periods of time of 100-200 μsec on the oscilloscope trace, under conditions of 50% light absorption.

The facts cited above support the belief that, in accordance with ideal shock tube theory, the temperatures and densities behind the shock waves in nonreacting gases were satisfactorily constant under the conditions of our experiments. The effects of heat and momentum transfer from the walls and of pressure disturbances radiated from the contact surface were therefore thought to be unimportant.

Some special difficulties encountered in the high temperature carbon dioxide experiments are mentioned separately.

RESULTS

Smoothed curves of the measured extinction coefficient of I_2 for all the gases used are displayed in Fig. 1. The average deviation of the experimental points from a smoothed curve was 5%. Special features of the experiments with different gases are discussed below.

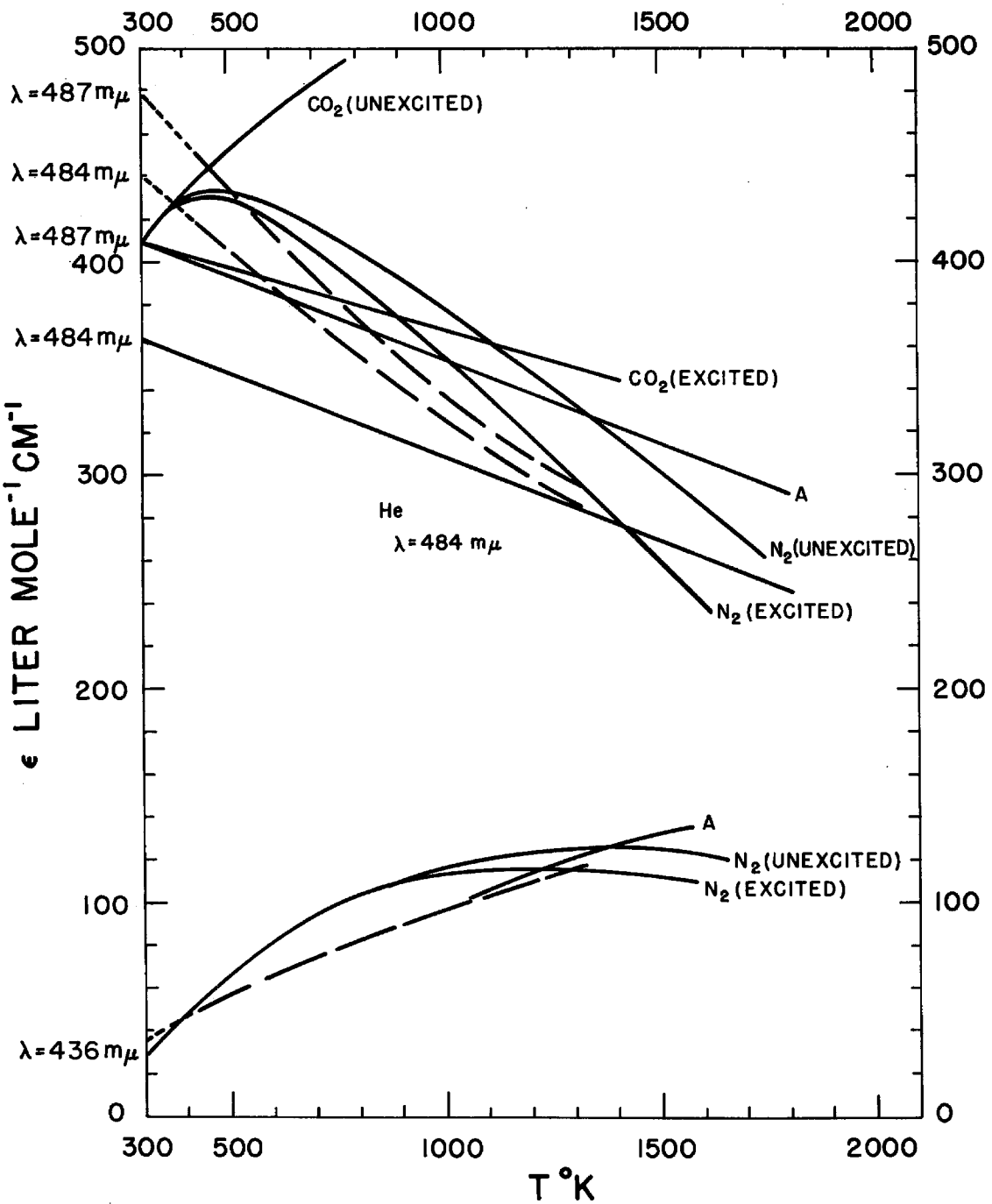

Fig. 1. Extinction coefficients of I_2 in various gases as measured in the present shock wave experiments. The dotted lines show data from ref. 14 for the temperature range 423 - 1323°K, and our extrapolation of these data to 300°K.

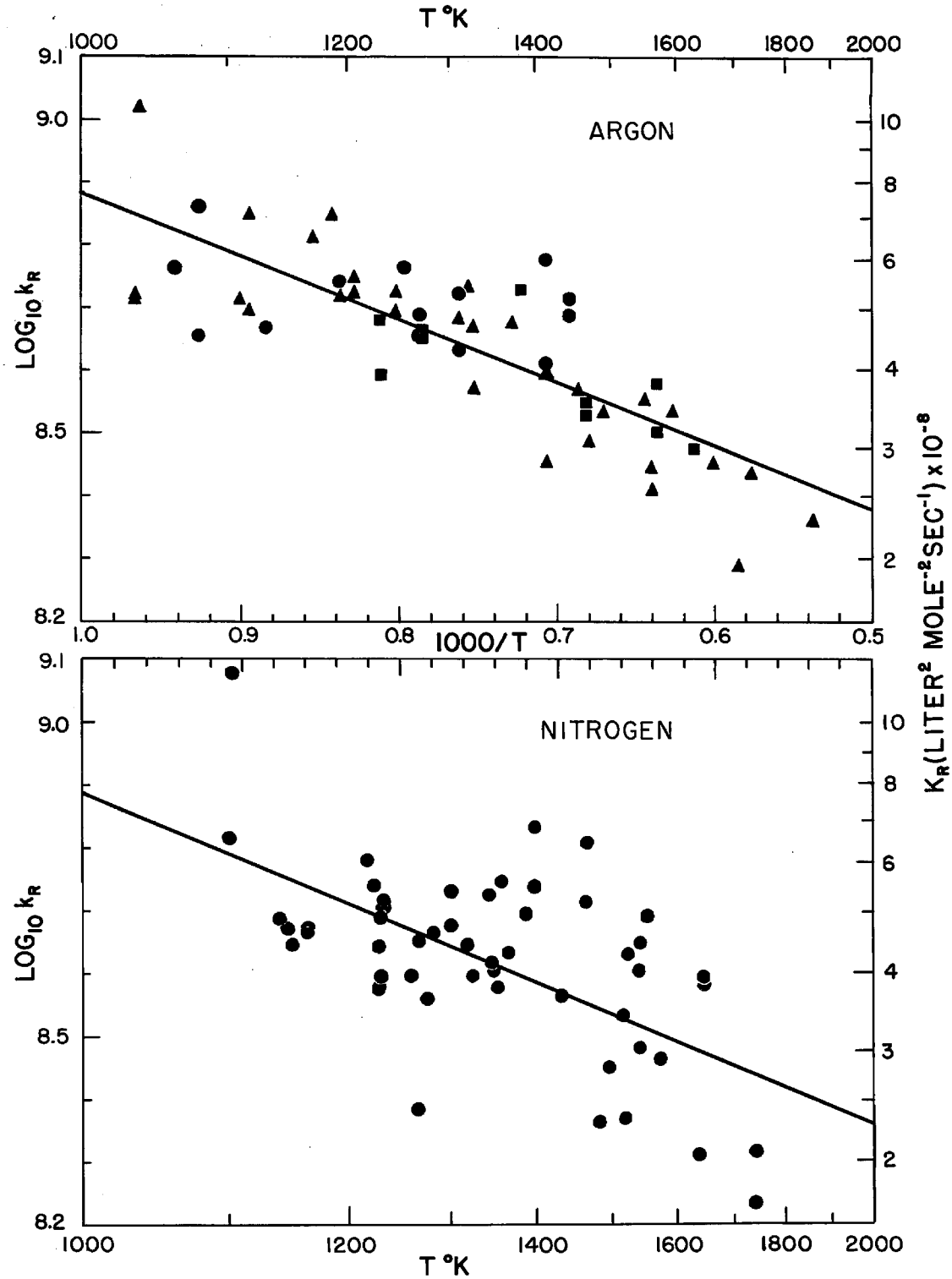

Fig. 2. Measured values of $\underline{k}_R$ in argon and nitrogen. In the top figure, ●, $(I_2/A) \leq 0.002$; ▲, $0.003 \leq (I_2/A) \leq 0.0125$; ■, $0.015 \leq (I_2/A)$. For the bottom figure, the I_2/N_2 ratio is not shown.

A summary of the kinetic results is presented in Table I. The way in which $\underline{k}_R$ should vary with temperature is not understood theoretically. Therefore the experimental results for $\underline{k}_R$ as a function of temperature are represented by the two alternative equations, $\underline{k}_R = \underline{A} \exp(\underline{U}/\underline{RT})$ and $\underline{k}_R = \underline{B}(\underline{T}/1000)^{\underline{n}}$. Values of $\underline{k}_R$ are listed for the middle of the temperature range studied, where we believe that the results are most reliable. This value of $\underline{k}_R$ is compared to the value for argon at the same temperature computed from the equation $\underline{k}_{R,A} = 0.76 \times 10^8 \exp(4560/\underline{RT})$.

Argon. - A set of 37 new experiments was performed with initial argon pressures ranging from 0.025 to 0.075 atm, with I_2/A ratios of 0.002 to 0.018, and with initial shock temperatures between 1080 and 1570°K. The results are displayed in Fig. 2. They are in complete agreement with those obtained previously over a narrower range of conditions. As can be seen in Fig. 2 there is no systematic variation of $\underline{k}_R$ when the I_2/A ratio is varied from 0.002 to 0.018. Using $\pm$ 50% as the safe limits of error for $\underline{k}_R$ we deduce that the ratio $\underline{k}_{R,I_2}/\underline{k}_{R,A}$, the relative efficiency of iodine compared to argon as M in reaction (1), is less than 30.

Helium. - A set of 19 experiments was performed with initial pressures ranging from 0.015 to 0.030 atm, I_2/A ratios of 0.007 to 0.011, and initial shock temperatures between 1100 and 1800°.

Nitrogen. - The interpretation of these experiments is

Table I

Shock Wave Measurement of $\underline{k}_R$*

Gas	A** $\text{liter}^2\ \text{mole}^{-2}\ \text{sec}^{-1}$ x 10^{-8}	U** cal	B*** $\text{liter}^2\ \text{mole}^{-2}\ \text{sec}^{-1}$ x 10^{-8}	n***	average $\underline{k}_R$ $\text{liter}^2\ \text{mole}^{-2}\ \text{sec}^{-1}$ x 10^{-8}	ratio to $\underline{k}_R$ for argon at same temp.	ratio $\underline{k}_{R,\text{gas}}$ to $\underline{k}_{R,A}$ at room temp.
A	0.76	4560(±320)	7.3	1.77(±.12)	4.5(1300°)	1	1
He	0.104	7960(±1000)	5.3	2.85(±.80)	1.8(1400°)	0.5	0.36
N_2 (unrelaxed)	0.68	4830(±650)	6.8	1.65(±.24)	4.4(1300°)	1.0	1.25
N_2 (relaxed)	1.37	4240(±790)	1.03	1.38(±.27)	7.1(1300°)	1.6	
O_2					5.3(1275°)	1.2	1.8
CO_2	1.3	9460	1.6	4.74	9.3(1120°)	1.6	3.7

*Equilibrium constants were taken or extrapolated from "Selected Values of Chemical Thermodynamic Properties" (National Bureau of Standards, Washington, Series III, 1954). Representative values are 1.84×10^{-4}, 2.10×10^{-3}, and 1.24×10^{-2} mole liter^{-1} at 1100°, 1300°, and 1500°.

**Representation of $\underline{k}_R$ by $\underline{k}_R = \underline{A} \exp(\underline{U}/\underline{RT})$

***Representation of $\underline{k}_R$ by $\underline{k}_R = \underline{B}(1000/\underline{T})^{\underline{n}}$

complicated by the interesting question as to whether or not the vibrational degree of freedom of N_2 becomes excited during the short time of the experiments. This makes a small but significant difference in the calculated temperature and density ratio ($\underline{\triangle}$) behind a shock wave of given velocity, especially for stronger shocks. This is illustrated in Table II.

Table II

Calculated Conditions behind Shocks of Given Velocity in N_2 with and without Vibrational Relaxation.

Velocity ($\times 10^{-5}$) cm sec^{-1}	Relaxed		Unrelaxed	
	T° K	$\underline{\triangle}$	T° K	$\underline{\triangle}$
1.30	1040	4.70	1073	4.38
1.50	1190	5.08	1336	4.70
1.70	1541	5.44	1634	4.93

The results in Fig. 1 and Table I have been calculated assuming vibrational relaxation and again assuming no relaxation. Fig. 2 shows the data for rate constants, to illustrate the experimental scatter.

Rate measurements were made for a set of forty experiments over a temperature range from 1100 to 1740°K (N_2 assumed unrelaxed). The total initial pressure of gas varied from 0.01 to 0.05 atm, and the mole fraction of I_2 from 0.004 to

0.02. The results agree quite well with those obtained previously. There is no evidence that the ratio of iodine to nitrogen affects the rate, indicating $k_{R,I_2}/k_{R,N_2} < 35$.

It is not possible to decide on the basis of the present results whether vibrational relaxation is occurring. However, Blackman[9] has recently reported a set of direct density measurements with an interferometer on the rate of vibrational relaxation in nitrogen behind a shock wave, for shock temperatures varying from 3500°K to 6000°K. Extrapolation predicts relaxation times at 1/2 atm pressure as follows: 3600 μsec (1100°K), 1700 μsec (1300°K), 480 μsec (1740°K). At the same temperatures and pressures, reaction times were 1200 μsec, 75 μsec, and 15 μsec respectively. The theory of vibrational relaxation indicates that collisions with fast moving light atoms are effective in inducing vibrational transitions; therefore it is not to be expected that iodine molecules or atoms would affect the vibrational relaxation time of nitrogen. Thus Blackman's results indicate that the present experiments measure the rate of dissociation or recombination of iodine in vibrationally unexcited nitrogen.

Oxygen. - A set of 12 oscilloscope traces for 6 shock waves in oxygen-iodine mixtures (driven with helium, not hydrogen) were analyzed. In all six experiments the calculated final temperature was within 25° of the average of the group. The initial pressures were about 0.03 atm, and the I_2/O_2 ratios about 0.007. For a shock of velocity 1.45×10^5 cm sec^{-1} in such a mixture, the calculated temperature and

compression ratio are: (a) assuming no vibrational relaxation of O_2, 1400°K and 4.80; (b) assuming vibrational relaxation, 1275°K and 5.40. Blackman's[9] measurements of relaxation times in oxygen from 1300° to 2500° give a relaxation time of 16 μsec at 1300-1400°K at 1 atm pressure, and therefore of 29 μsec at the pressure used in our experiments. The observed (1/e) dissociation time was about 160 μsec. Therefore it is probable that the dissociation reactions occurred principally in vibrationally relaxed oxygen.

Rate data were computed from the photocurrent traces for the last part of the reaction when, according to the above hypothesis, the vibrational relaxation was complete. The result is: $\underline{k}_R = 5.3 \times 10^8$ at 1275° in vibrationally relaxed oxygen. In performing this calculation, I_2 concentrations were computed using the value of the extinction coefficient, $\underline{\epsilon}$, measured in the helium experiments.

Assuming unrelaxed O_2, interpretation of the data leads to a rate constant for recombination at 1400° of 1.55×10^8 liter^2 mole^{-2} sec^{-1}, which is less than the argon value of 3.9×10^8 at this temperature. In view of the room temperature ratio $\underline{k}_{R,O_2}/\underline{k}_{R,A}$ of 1.8, it is expected that O_2 is more effective than argon as a third body at 1400°. The kinetics data therefore support the hypothesis that the O_2 was vibrationally relaxed during most of the dissociation reaction.

It should be noted that it would be difficult to recognize the occurrence of vibrational relaxation in a time of the order of magnitude of the iodine dissociation time from the

shapes of the iodine concentration versus time curves. In the unrelaxed gas, the translational temperature is high and the value of $d(I_2)/dt$ due to reaction is more negative than that in the relaxed gas. The gas compresses, however, as relaxation occurs, and this contributes a positive term to the value of $d(I_2)/dt$. The resultant $d(I_2)/dt$ is not very different from that for the dissociation reaction in the relaxed gas.

It should have been possible to have determined whether conditions immediately behind the shock wave corresponded to vibrationally relaxed or unrelaxed oxygen by measuring the apparent extinction coefficients of I_2. However, there was an unfortunate error in the use of the oscilloscopes in this particular series of experiments such that the abrupt change in photocurrent when the shock wave passed the light beam was not correctly measured, although the subsequent slow changes in photocurrent were not significantly affected.*

Carbon Dioxide. - The photoelectric curves for the high temperature shock waves in carbon dioxide were rougher and

---

*This error (sob) consisted of failure to provide a low impedance connection to ground of the unused grid in the input circuit of the difference amplifier (input B of Tektronix 512 oscilloscopes). A step function applied to the A input is thereby converted to a step function of 0.85 times the input magnitude followed by a slow ($\sim$ 100 μsec) rise of the signal by the remaining 15 percent.

much less regular than for the experiments in any of the other gases. This is illustrated in Fig. 3. Below about 900°, the shocks in CO_2 were very smooth and flat. We believe that the difference between CO_2 and the other gases used is due to the much larger density ratios for shock waves in CO_2. The observations were made at a station 255 cm from the membrane. For a typical compression factor of 8, when the shock front is at this station, the contact surface between the hot compressed CO_2 and the cold expanded driving gas is only 32 cm behind the shock front, The contact surface does not possess the self-sharpening feature that the shock front does, and it may be assumed that there is a turbulent zone of mixed driving gas (H_2) and shocked gas (CO_2) with dimensions of the order of magnitude of the diameter of the tube (15 cm). Thus it is not surprising that conditions behind the shock are not entirely steady. The compression factors for experiments in argon and nitrogen are all less than 4 and 5 respectively. It has been impractical, at the present time, to test this hypothesis by construction of a longer tube.

A set of 24 shock wave experiments with final temperatures ranging from 1000° to 1400°K were analyzed to obtain kinetic data. Some lower temperature shocks were used for extinction coefficient measurements. Initial pressures were varied in the range 0.01 to 0.05 atm, and I_2/CO_2 ratios were between 0.005 and 0.02.

There is a tremendous difference between calculated temperatures and densities behind a shock wave for vibration-

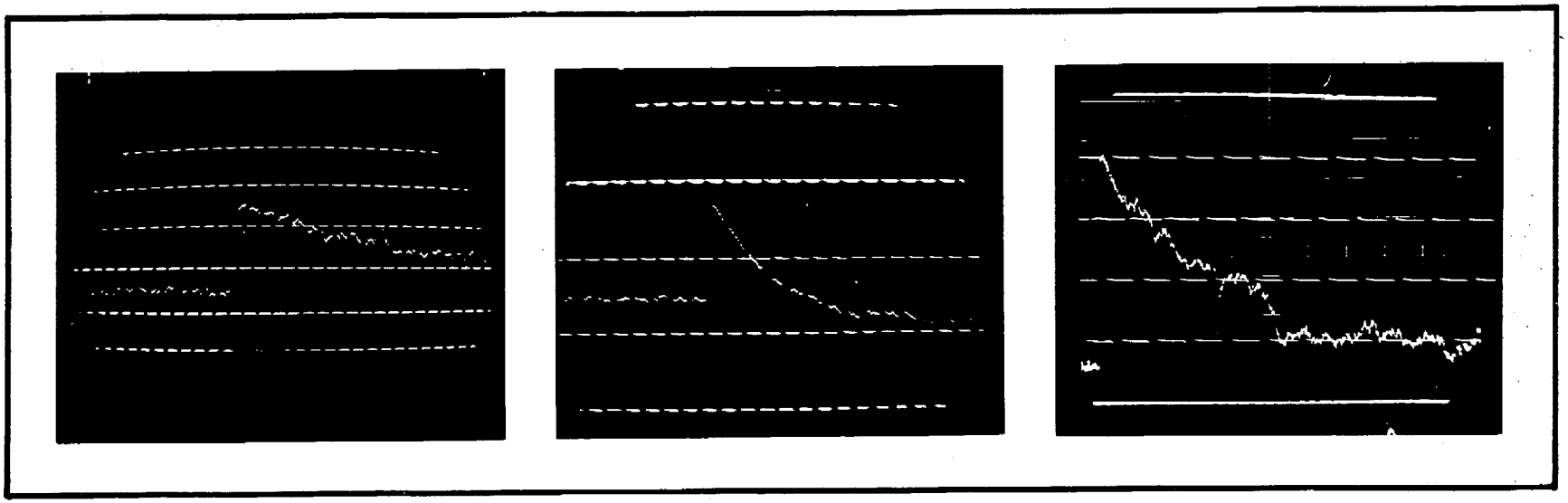

Fig. 3. Shock waves in argon (left), oxygen (middle), and carbon dioxide (right) showing the rate of dissociation of iodine. 10 μsec timing markers are shown. The shock velocities, shock temperatures, compression ratios, I_2/A ratios, and initial gas concentrations were: (argon) 1.001 x 10^5 cm sec^{-1}, 1232°, 3.16, 0.0161, 0.00111 mole $liter^{-1}$; (oxygen) 1.423 x 10^5 cm sec^{-1}, 1400°, 4.80 (unrelaxed), 0.0067, 0.00124 mole $liter^{-1}$; (CO_2) 1.266 x 10^5 cm sec^{-1}, 1047°, 7.57, 0.0069, 0.00112 mole $liter^{-1}$. A vertical spike used for velocity measurement is present on the argon picture about 3/4 of the way across the trace.

ally relaxed and unrelaxed carbon dioxide. Thus, for example, for a shock of velocity 1.34×10^5 cm sec^{-1} in CO_2 initially at 300°K, the calculated temperatures and density ratios are: 1100°K, 7.78 (relaxed); 1604°K, 4.92 (unrelaxed). The extinction coefficient data (Fig. 1) are reasonably consistent with the argon results assuming relaxed CO_2, and are very different for unrelaxed CO_2. The rate constants are of a reasonable order of magnitude assuming relaxed CO_2, but would have been about a hundred times smaller if calculated on the basis of unrelaxed CO_2. Therefore, the evidence is clear that under the conditions of our experiments, the carbon dioxide was vibrationally relaxed. This is in agreement with direct measurements of the relaxation time in CO_2 of about[11] [12] 0.5 μsec at 1 atm. pressure at 1000°K and less at higher temperatures.

Our measurements are not sufficiently accurate to test the proposal by Griffith that the relaxation time for the stretching modes of CO_2 is much larger than the relaxation time for the doubly degenerate bending mode.[12] The effect of assuming that the stretching modes are frozen in would be to decrease the extinction coefficients somewhat, bringing them closer to the values measured in argon, and to decrease the calculated value of $\underline{k}_R$ by about 30%.

We have briefly considered the following problem. Consider a shock wave of velocity 1.34×10^5 cm sec^{-1} in CO_2 at an initial pressure of 0.010 atm at 300°K. The temperature, density ratio, and pressure just behind the shock and

before vibrational relaxation are 1604°, 4.92, 0.263 atm; after vibrational relaxation, these quantities are 1100°, 7.78 and 0.286 atm. The vibrational relaxation time is estimated as 1.6 μsec.[11][12] This time is too short to be resolved in our experiments. The question is how much iodine dissociation occurs while the gas is relaxing from 1604° to 1100°.

The 1/e reaction times for iodine dissociation at the given concentrations of CO_2 are 40 μsec at 1100°. An approximate numerical integration for the amount of reaction in each temperature interval as the gas undergoes vibrational relaxation in 1.6 μsec gives an upper limit of 0.02 for the degree of dissociation by the time ($\sim$ 4.8 μsec) the gas has cooled to 1120°. This amount of dissociation is too small to be detected by the measurement of the apparent extinction coefficients of iodine, and it is concluded that the amount of reaction during the vibrational relaxation time is negligible.

DISCUSSION

The experiments reported here are to be considered in part as a study of the iodine dissociation and recombination process and in part as an evaluation of the shock wave spectrophotometric method of studying reaction rates.

Rate Constants. - It is clear from the experiments performed so far that the rate constants for the process $I + I + M \longrightarrow I_2 + M$ decrease with increasing temperature.

The exact functional form of the temperature dependence and its variation with the nature of the inert gas, M, are not yet well known.

Measurements of the values of $\underline{k}_R$ for the common gases at room temperature made by the flash photolysis method in different laboratories are not yet in satisfactory agreement. One of the sources of difficulty has been recognized by the discovery[3b] that I_2 itself is a remarkably efficient third body for the recombination of I atoms. Thus, in many previous measurements, the contribution of I_2 to the recombination rate was quite significant. The Cambridge group have recently reported,

$\underline{k}_{R,A} = 3.3 \times 10^9$ liter^2 mole^{-2} sec^{-1}, $\underline{k}_{R,I_2} =$

850×10^9, $\underline{k}_{R,He} = 1.2 \times 10^9$.

Unpublished work in our laboratory gives

$$\underline{k}_{R,A} = 2.2 \times 10^9, \quad \underline{k}_{R,I_2} = 1300 \times 10^9.$$

The value $\underline{k}_{R,A} = 2.5 \times 10^9$ has been selected for purposes of discussion here and for the calculations in Table I. (This selection was made prior to the appearance of the most recent Cambridge paper and no implication as to our assessment of the relative accuracy of the conflicting values noted above is intended.) The values reported by Christie *et al.* for argon and helium agree fairly well with earlier measurements by Russell and Simons. The values of $\underline{k}_R$ for O_2, N_2, and CO_2 determined by the latter investigators have been used in

Table I.

There is of course no assurance that the dependence of $\underline{k}_R$ on $\underline{T}$ fits any simple relation such as $\underline{k}_R = \underline{B}/\underline{T}^{\underline{n}}$ or $\underline{k}_R = \underline{A} \exp(\underline{U}/\underline{RT})$. The former relation is suggested by the equation for $\underline{k}_D$, the rate constant for dissociation,

$\underline{k}_D = \underline{Z} \left[(\underline{E}/\underline{RT})^{\underline{n}}/\underline{n}\,!\right] \exp(-\underline{E}/\underline{RT})$. This equation is obtained in the collision theory of chemical kinetics when it is said that 2n classical degrees of freedom in addition to translation along the line of centers contribute to the energy of dissociation, $\underline{E}$. The exponential representation for $\underline{k}_R$ is suggested by the following formulation of the recombination process.

$$M + I \rightleftharpoons MI$$

$$MI + I \longrightarrow M + I_2$$

The quantity $\underline{U}$ is the energy of dissociation of the complex MI, which would normally be held together by Van der Waals forces.

The scatter in the shock wave points is too great and the temperature range that can be studied is too small to permit a choice between the two suggested representations of $\underline{k}_R$ *vs.* $\underline{T}$. Furthermore, the average high temperature value of $\underline{k}_R$ for argon at 1300°K of 4.5×10^8 in conjunction with the room temperature value of 2.5×10^9 leads to the equations: $\underline{k}_R = 2.7 \times 10^8 \exp(1330/\underline{RT})$ or $6.1 \times 10^8 (\underline{T}/1000)^{-1.17}$. Thus, we see that the temperature coefficient of $\underline{k}_R$ obtained by comparison of the average high temperature result with

the room temperature result (and uncertainty about the latter does not qualitatively affect the conclusion) is less than the temperature coefficient for $\underline{k}_R$ obtained from the shock wave results alone (Table I).

As noted before, there is no assurance that one simple representation for $\underline{k}_R$ vs. $\underline{T}$ will hold from 300°K to 1500°K. However we suspect that there are unknown systematic sources of error in the shock wave experiments causing $d\underline{k}_R/d\underline{T}$ to be too negative. The largest temperature coefficients were obtained for CO_2 and He, for which evidence of experimental irregularities has already been cited.

It should be realized that in effect the quantity experimentally measured is $\underline{k}_D$, the rate constant for dissociation, and the activation energy for $\underline{k}_R$ is obtained from the small difference in temperature coefficients of $\underline{k}_D$ and $\underline{K}$, the equilibrium constant for dissociation. The discrepancy between the shock wave negative activation energy of 4500 cal and the average shock wave-flash lamp value of 1500 for $\underline{k}_R$ for argon is 3000 cal. This uncertainty in the activation energy of 33 - 36 kcal for $\underline{k}_D$ would arise from a systematic error in temperature determinations that was 50° greater at one end of the temperature range (1080° - 1570°) than at the other or from a systematic error by a factor of 1.55 in the ratio of rate constants at the extremes of this temperature range. The estimated random uncertainties in temperature and rate constant are of the order of 25° and 25%.

The rate constant for iodine as a third body is about

10^{12} liter^2 mole^{-2} sec^{-1} at room temperature and less than 1.3×10^{10} at 1300°K, corresponding to a minimum value of U of 3400 cal. The large difference between the temperature coefficients of k_{R,I_2} and $k_{R,A}$ seems to us to favor the representation of k_R by the function $A \exp(U/RT)$ over the B/T^n representation. This view leads to the prediction that the temperature coefficient of k_R will be greater for complex gases as third bodies and that the large differences in the values of k_R for different substances at room temperature will decrease as the temperature is raised.[2][4] The available experimental data presented in Table I is in agreement with this hypothesis but is not adequate as a critical test.

Extinction Coefficients. - The wave lengths 487 mμ and 436 mμ are in the region of continuous absorption by I_2 beyond the dissociation limit at 499 mμ. It is expected theoretically and it has been observed in previous experiments that the extinction coefficients of iodine in this region are independent of the nature or amount of inert gas present,[13] and that ϵ_{487} decreases with increasing temperature, whereas ϵ_{436} increases as the temperature is raised.[14] The results obtained in this investigation and presented in Fig. 1 are in general agreement with these expectations. Thus the extinction coefficient data completely exclude the possibility that CO_2 was vibrationally unrelaxed in the high temperature experiments. The nitrogen results, unlike any of the other results, show a maximum in the ϵ vs. T curves at 487 mμ in the neighborhood of 500°K. This is

probably due to experimental errors in this particular set of measurements. Under these circumstances, the extinction coefficient data at higher temperatures cannot be used to decide between the nitrogen relaxed and nitrogen unrelaxed assumptions.

In general shape, our $\underline{\epsilon}$ vs. $\underline{T}$ curves agree with those of Sulzer and Wieland for iodine in the absence of inert gas, but in quantitative detail, there is considerable disagreement. Our value at room temperature is based on careful static measurements by Mr. W. DeMore in this laboratory. We believe that this value is correct. The measured values at higher temperatures depend upon the assumed room temperature absorption of the sample prior to its compression by the shock wave.

ACKNOWLEDGMENTS

We are indebted to the ONR for its support of this research, to the NSF for fellowships (DB and GS) and to the du Pont Company for a fellowship (DB).

REFERENCES

(1) Britton, Davidson, and Schott, Discussions Faraday Soc., 17, 58 (1954).

(2) E. Rabinowitch and W. C. Wood, J. Chem. Phys., 4, 497 (1936).

(3) Christie, Norrish, and Porter, (a) Proc. Roy. Soc. A216, 152 (1953); (b) Discussions Faraday Soc., 17, 107 (1954).

(4) K. E. Russel and J. Simons, Proc. Roy. Soc. A217, 271 (1953).

(5) R. Marshall and N. Davidson, J. Chem. Phys., 21, 659 (1953).

(6) R. L. Strong and J. E. Willard, Abstracts, American Chemical Society Meeting, New York, Sept. 1954, p. 26 R.

(7) Christie, Harrison, Norrish, and Porter, Proc. Roy. Soc. A231, 446 (1955).

(8) D. Bunker and N. Davidson, private communication.

(9) V. Blackman, ONR Technical Report II 20, NR 061-020, Princeton University, Dept. of Physics, May, 1955.

(11) A. Kantrowitz, J. Chem. Phys., 14, 150 (1946).

(12) W. Griffith, to be published.

(13) E. Rabinowitch and W. C. Wood, Trans. Faraday Soc., 32, 540 (1936).

(14) P. Sulzer and K. Wieland, Helvetica Physica Acta, 25, 653 (1952).

III PROPOSITIONS

1. An investigation of the kinetics of oxidation of carbon monoxide by ozone in the presence of nitrogen pentoxide is proposed. This system may provide another example of the catalysis through NO_3 that has been observed in the oxidation of nitrosyl chloride.(1) Such an investigation would also serve as another check on the unimportance of oxides of nitrogen in the recent study of the oxidation of CO by pure ozone.(2)

(1) H. S. Johnston and F. Leighton, J. Am. Chem. Soc., 75, 3612 (1953).

(2) D. Garvin, ibid., 76, 1523 (1954).

2. It is proposed to study the kinetics of the partial hydrolysis of thioamides to the ordinary amides in alkaline solutions, where thioamides exist predominantly in an anionic form. The effects of metallic ions, such as those of Sn^{IV} and Zn^{II} on these systems are also of interest, both from the standpoint of catalysis of the hydrolysis and of the formation of stable mono- or bidentate complexes with thioamide anions.

3. The results of Nathan(1) suggest that the unstable crystal structure determined for 1-methyl-7-ethyl-3-azaphenanthrene is dictated by the spatial requirements of the 7-isopropyl impurity. Synthesis of the pure 7-isopropyl compound might distinguish this possibility from the

alternative one that the unstable 7-ethyl structure is stable at some lower temperature of crystallization.

(1) R. Nathan, Thesis, California Institute of Technology, Pasadena, 1956.

4. A reinterpretation is proposed for the rate constants deduced from the polarographic kinetic currents due to the liberation of formaldehyde from its hydrate in alkaline solutions. Also, the explanation offered for the maximum at pH = 13.15 by the original investigators[1] and copied by Kolthoff and Lingane[2] is conceptually misleading.

(1) K. Vesely and R. Brdicka, Collection Czechoslov. Chem. Communs., 12, 313 (1947).

(2) I. M. Kolthoff and J. J. Lingane, "Polarography," Interscience Publishers, Inc., New York, 1952, 2nd ed., Vol. I, pp. 278-281.

5. An acetamidomethionic ester synthesis of α-aminosulfonic acids analogous to the one used for α-aminocarboxylic acids is proposed. These compounds are of interest for their acid strengths and for their detergent properties, as well as for their physiological effects.

6. Enough information is now available that the decomposition flames in mixtures of ozone and nitrogen pentoxide can be profitably reinvestigated.[1] Emission and absorption spectroscopy on the flame, the possibility of ignition by injection of oxidizable impurities, and theoretical examination

of the flame velocities and ignition limits are of interest.

(1) T. M. Lowry and R. V. Seddon, J. Chem. Soc., 1937, 1461.

7. A spectrophotometric reinvestigation of the slow decomposition of ozone in the presence of N_2O_5 is proposed, using a sodium vapor lamp that can be adapted for high temperature experiments in which the NO_3 concentrations can be known. It may be possible to discover a contribution to the rate by the process: $NO_3 + O_3 \longrightarrow NO_2 + 2O_2$

8. The research described in part I of this thesis was proposed by the author in 1954. Suggested extensions are: (1) a quartz apparatus for the examination of NO_3 in the ultraviolet, and (2) low concentration experiments near 1300°K to determine the nature of the unimolecular decomposition of NO_3. See pages 47-50 of this thesis.

9. The flow filling method described on page 120 of this thesis for use with iodine can be adapted easily to the preparation of large volumes of accurately humidified gases for shock wave experiments with the aid of Glauber's salt.

10. A tax on radio and television advertisements is proposed as a valuable source of revenue for the federal government and as a deterrent to the obnoxious advertising currently being broadcast. A tax structure is recommended that is hardest on the transcribed commercials employing singing and other

affectations of voice, and on station break commercials, and easier on the advertising portions that are essential in the support of the longer programs.